Muscle and soft tissue monitoring via smart compression garments

A thesis submitted in fulfilment of the requirements for the degree of Doctor of Philosophy

Aaron Belbasis
B.Eng, B.Bus
RMIT University

School of Engineering
College of Science, Technology, Engineering and Maths
RMIT University

January 2021

Declaration

I certify that except where due acknowledgement has been made, the work is that of the author alone; the work has not been submitted previously, in whole or in part, to qualify for any other academic award; the content of the project is the result of work which has been carried out since the official commencement date of the approved research program; any editorial work, paid or unpaid, carried out by a third party is acknowledged; and, ethics procedures and guidelines have been followed.

I acknowledge the support I have received for my research through the provision of an Australian Government Research Training Program Scholarship.

Aaron Belbasis
January 13th, 2021

Acknowledgments

Firstly, this work would not have been possible without the wealth of knowledge and guiding support of Prof. Franz 'Tino' Fuss, he has my gratitude and sincere thanks. I have his supervision to primarily thank for the journey that my research career has undergone, both in its development, and my own. His skill in exploring both direct and lateral research approaches, his mathematical acumen and keen commercialisation drive all fostered learnings I will take throughout my career.

In addition I would also like to thank both my secondary supervisors; Prof. Aleksandar Subic for his early support and guidance in my research from whom I have learnt much from on multidisciplinary engineering, and Prof. Simon Watkins for his continued support throughout my candidature, his mentorship and insights have proven invaluable to my academic career.

Importantly I would like to thank Prof. Florian 'Floyd' Mueller who opened his research lab, team and supporting equipment to my research as a second-home and in doing so taught me much about the generosity and importance of multidisciplinary research.

A special acknowledgement to my fellow researchers; Jesper Sidhu, Dr. Adin Tan and Dr. Udi Weisman. Your support and camaraderie was well appreciated as we pursued our unique research pathways. To all my friends, colleagues and research participants, you have all been fundamental in support, assistance and motivation in seeing this work completed, thank you.

I would like to acknowledge the support of the Skins Compression company for their donation to the research lab of a number of compression apparel products which aided in the foundational exploration of the work.

Lastly and most importantly, my heartfelt appreciation and gratitude to both Hannah my amazing wife, and Lulu the most faithful of research companions. Both have seen me through the journey of completing this work, counselled me in times of need, joined me on my successes and above all acted as a steadfast pillar of support and motivation, I love you both.

Contents

List of Figures

List of Tables

Summary

This research follows a multi-disciplinary pathway which begins with the development of a novel measurement technique via the application of custom piezoresistive sensor arrays, continues through to integration within compression apparel as a validated biomechanical analysis system, finishing at the exploration of a system capable of providing detailed feedback to a wearer on their muscle activity and fatigue performance, with the scope to identify impending higher-risk injury conditions.

The aim of this work was the development of a wearable system that focuses on near real-time muscle performance analysis through the measurement of muscle activity induced surface pressure variations. It further explores ligament loading and muscle fatigue condition parameters through the use of the developed system. In doing so the research methodology questions whether pressure could be used to measure muscle activity at varying levels of muscle exertion, whether additional performance metrics could be extracted in real-time, and how these metrics reflected changing performance over sustained activity.

The research serves to demonstrate that an alternative measurement system for muscle performance monitoring is possible through the use of surface pressure changes. Further demonstrating that advantages of such a system can be used to extend beyond measuring just the direct muscle performance, but also the performance and loading on other soft tissues connected in the biomechanical chain, and lastly present an alternative to the gold standard of muscle fatigue measurement that alternatively measures the instability present within the measured signal of a fatiguing muscle as a valid fatigue index.

Through the completion of this exploration three main contributions to the knowledge gap are made. New evidence and methodology is presented on the viability of measuring muscle performance (activity, load and fatigue) through pressure-based Force Myography using a compression garment and pressure sensors. A new technique for fast estimation of Cruciate Ligament loading for early warning and injury prevention detailed, and lastly a determination of a new muscle fatigue index that uses Fractal Dimension analysis to calculate level of muscular fatigue and muscle interdependence.

Research Development

1. Introduction

1.1 Overview

The level of enjoyment and participation in physical activity at all levels will always be contingent on a need to consider and address the associated dangers and risks of injury, and therefore its implications to our ongoing participation. Unlike a significant portion of medical injuries, almost 50% of all sports-related injuries are deemed preventable [Sports Medicine Australia *et al.* 1997].

Early efforts in addressing injuries in sport led to the deployment of various defensive equipment to reduce injuries through predominantly impact-related events. Glasses shielded the eyes, padding and armour protected the body, braces supported the joints and helmets cushioned the brain. These solutions, and their ongoing developments, have had a profound effect on reducing the frequency and severity of injuries sustained through broken bones, concussions and soft-tissue impact damage. They represent a form of protection which encourages active injury-prevention by wearing 'passive' protection equipment for preventing time-dependent accidents and impact events.

More recent efforts toward injury prevention have seen the focus extend toward the design of equipment that actively retrains participant behaviours to avoid injury. A form of 'active' protection equipment, this approach largely focuses on addressing the consequences of longer-duration behaviours which lead to injuries through excessive overloading and overuse of muscles and the soft-tissues of the body. Of particular focus are the upper and lower limbs which have demonstrated a higher prevalence to injuries as a result of muscle and ligament overloading and straining.

This thesis explores the foundational development and viability of such a system for active injury prevention. The system focuses upon monitoring muscle and soft tissue loading conditions through the instrumentation of compression apparel for direct monitoring and feedback of muscle and soft tissue loads to aid in the early warning of high-risk conditions and the prevention of sport-related injuries. The novel application of Force Myography and material-based sensors is utilised to detect pressure changes at the skin surface due to muscle contraction activity, allowing for analytical insights into how muscles and soft tissues perform under various loading and fatigue conditions.

The long-term direction of the research is toward development of an innovative solution for wearable sports technology, aiding in the improvement of training, assessment of performance and physical welfare of participants in exercise activities. With current high-end compression apparel still limited to only providing passive muscular and vascular exercise response the additional intelligence from a pressure mapping system enhances a compression garment, from a standard piece of clothing to a wearable biomechanical performance analysis system providing data analytics and biofeedback. The anticipated benefits realised from this research extend beyond the traditionally elite domain of professional athletes, encompassing multi-discipline enrichments to broader fields of sport participation, healthcare and injury rehabilitation.

1.1.1 Research Field: Where the research gap exists

Significant literature and developments exist within the scope of muscle activity and performance measurement, largely due to its fundamental role across biomechanical and medical fields. Commonly applied gold-standard techniques are:

- Coaching and Feedback, the traditional method of utilising a third-party or visual recording to observe behaviour, and relay insights and feedback based on experience and knowledge.
- Electromyography (EMG), a system measuring the electrical activity of the muscles and correlating this behaviour to a muscle's activity and loading.
- Motion Tracking with Force Plates, an approach which tracks biomechanical markers and ground forces to define muscle loads from external loading and movement conditions

Whilst being go-to industry standards, these techniques are not without their limitations; coaching lacks numerical accuracy and repeatability, EMG suffers from high costs, and motion tracking systems are not readily portable. A new technique is growing in capability with potential to address some of these limitations, Force Myography (FMG) measures mechanical changes at the skin surface as a result of muscular activity. A sensor measures the force (or its distribution as pressure) between the muscle and a constraining compression device. With greater commercial availability and consumer demand for compression garments in sport, this has opened up a strong research opportunity to pursue this FMG technique as a means of integrated muscle analytics within a compression garment.

To date very little FMG research has been undertaken to explore the biomechanical evaluation of muscle performance (and subsequent soft-tissue) through surface pressure variation. The vast body of literature primarily focuses upon detecting only muscle activation, and is popularly used in prosthetics control for robotic hands and devices. Additional research has demonstrated the further use of pressure-based FMG to measure varying levels of healthy muscle output, but again do not explore the muscle performance itself, rather the focus lends toward the signal output as a means of controlling another device through human interaction. As such there exists a lack of established literature in the use of FMG for introspective exploration of the efficiency in muscular activity and execution behaviour. This work endeavours to explore this niche, and compare and contrast the performance of pressure-based FMG against the industry gold-standards.

1.2 Research Scope and Objectives

The research focuses on the development of a novel system and methodology capable of muscle and injury diagnostics using an instrumented compression garment. Current (passive) compression garments provide little to no feedback on a wearer's performance, wherein functioning mainly as a proprioceptive aid. By monitoring select muscle groups and joints, a smart garment ultimately provides a system that allows the wearer to eliminate the restrictions of lab-based analysis, and place them free to perform in their natural physical environment with similar analytical monitoring. This however by no means is restricted to the sporting fields, and is directly, if not more applicable within rehabilitation, medical and aged care pathways.

Presently there is no single portable system capable of assessing in realtime the Active muscle loading of an athlete in the lower limbs, Cruciate Ligament strains within the knee joint, and co-contraction and fatigue of paired lower limb muscles. This research endeavours to explore the development of such a methodology system. Where the research presented demonstrates the necessary analytics and engineering considerations required to capture, process, analyse and extract insights relevant to human performance in uncertain and realtime environments.

1.2.1 Research Questions

The scope of the research is framed around the empirical observation of the behaviour of the muscles, and thus testing of these assumptions, being that:

- Muscle activity under the surface of the skin should correlate to localised pressure changes directly above the muscle when wearing a garment that applies sufficient compressive pressure to the muscle and dermis.
- A muscle undergoing a consistently repetitive, medium to high exertion action will experience an increase in fatigue. This should be reflective in an increasing level of chaotic instability when measuring the muscle activity.

In an effort to better define, analyse and ultimately better the knowledge gap within the field, the following research questions formed the guiding framework of the research:

Question 1 How can deformation changes in the physical surface of a limb during activity be utilised for quantification of muscular activity levels?

- This question explores the following key research pursuits:
  - Does muscle deformation correlate to the performed muscle activity?
  - What sensor considerations are needed for measurement of deformation?
  - How does this compare and correlate to the current gold standards of measurement?

Question 2 With an understanding of the muscle loads associated with a set activity, how can we further determine the non-measurable loads (i.e. knee ligament loads, fatigue), that otherwise cannot, or have not been measured before within a real-time measurement capacity?

- This question explores the following key research pursuits:
  - How does the proposed methodology compare to the currently implemented measure-

ment systems, such as surface Electromyography?

- What comparative advantages or weaknesses exist?

Question 3 What insight can the analysis of temporal loading conditions on the muscle surface provide?

○ This question explores the following key research pursuits:

- How does the onset of a muscle fatigue condition affect the changes in the resultant measured signal?
- What insight is provided through the analysis of the muscles behaviour over time with respect to fatigue?

1.3 Research Significance and Contribution

Listed below is a summary of the impact the completed research has made through the pursuit of the research questions stated above. Impact within the field is separated as to the Novelty, the Contribution toward a knowledge gap, and the relevant Breadth and Depth entailed.

1.3.1 Novelty and Innovation

- The measurement of muscle activity through surface pressure changes for the purpose of calculating soft-tissue performance parameters, including; muscular loading force, co-contraction behaviour, ligament force, and muscular fatigue. (Chapters 4-7)
- Novel development of a cruciate ligament load monitoring methodology for fast alerting of dangerous behaviour, as highlighted within an International PCT Patent filed, which the author of this thesis is a co-inventor. (Chapter 5)
- Peer-recognised research innovation as recipient of the APCST-ASICS International Innovation Award (2015) for research conducted (Chapters 3-4)
- The discovery and demonstration of visualising antagonistic muscle co-dependent mechanical fatigue behaviours through the use of Fractal Dimension Analysis. (Chapter 7)

1.3.2 Breadth and Depth

Breadth across the developmental research:

- Design and development of calibrated material-based soft piezoresistive pressure sensors
- Development of a wearable system (Smart Compression Garment) capable of realtime data capture across numerous activities
- Correlation of inverse dynamic muscle force to forward dynamic EMG and FMG sensors
- Development of a biomechanical model for the fast calculation of Cruciate ligament forces
- Analysis of athlete cycling performance using motion tracking and muscular monitoring
- Fatigue analysis through advanced signal processing and analytics

Depth into the development of muscle fatigue analysis:

- Application and comparison of standard technique for fatigue analysis to alternative methods
- Development of an automated Fractal Dimension analysis program
- Completion of over 65 tests in the development and refinement of the test procedure and analysis of athletes
- Full testing methodology applied to seven cyclists in assessment of fatigue through measurement of surface EMG and FMG using both gold-standard and novel methodologies
- Thorough analysis of alternating recovery and fatigue of antagonistic muscle groups using both the gold standard and developed novel technique
- Analysis of muscle activation behaviour and fatigue patterns over peak crank angle activation

Depth into benchmarking pressure sensors to the gold-standard:

- Application of a 5-point EMG signal analysis for correct sensor positioning and alignment
- Peak pressure determination of muscle belly for centre of pressure positioning of sensors
- Novel pressure material-based sensor development and calibration to gold standard equipment

1.3.3 Main Findings and Contribution to the Knowledge Gap

The completed works focused upon the development of a smart compression apparel device that utilised pressure and EMG sensors to detect muscle and soft tissue performance parameters.

The main findings and contributions of the work are discussed below.

1. **Development of material-based sensors for Force Myography in a smart garment**
   For the successful application of Force Myography using pressure sensors underneath a compression garment it was necessary to utilise pliant sensors that conformed to the changing shape of the muscle's surface. Early investigations of the research were supported by the use of commercially available sensors that were not adequately compliant to the measurement task, and as such integration into a smart garment was completed. Therefore as a critical component of the research, design and development of soft material-based sensors tailored for FMG application within a garment. This involved the selection of materials whose properties met the electrical, mechanical and environmental requirements, the construction and selection of the best sensor form, and lastly the calibration of these sensors using gold-standard equipment.

2. **Demonstration that Force Myography can be extended beyond activation detection to include muscle loading and fatigue conditions**
   The work demonstrates through multiple tests that muscle activity and loading can be measured by pressure changes to the muscle surface. This extends the knowledge from existing literature works beyond simply detecting muscle activation for binary switch control, to include an understanding into the correlation of surface pressure to that of muscle loading conditions. Whilst somewhat confirmation of what we already know empirically (contraction of muscles exert larger deformation changes with increasing contractile force), the work quantifies this change through set activity from seated, standing and cycling positions for multiple participants. Validating this against both a biomechanical model, and the gold-standard technique of monitoring electrical behaviour of the muscles.
   Through the comparison of the cyclist muscle behaviour at the beginning and end of a fatigue-inducing exercise, FMG was shown to demonstrate changes in the muscle activation timing and levels due to the onset of fatigue. Subsequently, radial shift of the peak activation tended toward earlier activation for all participants, but was more prevalent within the cycling dominant power generation muscles (quadriceps) and with participants more conditioned to fatigue-based cycling exertion.

3. **Development of a methodology for fast calculation of Cruciate Ligament forces**

The body of literature providing detailed analysis of the knee's cruciate ligaments is extensive. The majority of this however focuses understanding on the detailed failure mechanism of the ligaments, largely post-injury or within controlled laboratory conditions. The thesis work undertaken presents a novel, lateral contribution, which focuses on the fast detection of cruciate ligament loading conditions for in-situ, near real-time analysis and alerting of dangerous activity to a wearer. The solution prioritises a biofeedback loop to prevent injury invoking behaviours, rather than fully discretising the ligament failure mechanisms.

4. **Highlighting weaknesses in Electromyography when measuring high-speed activity**
   Whilst considered the gold-standard for monitoring muscle performance, it was presented that Electromyography suffers from significant inaccuracies in measuring the timing of muscle power generation during high speed cycling activity. This was identified as a consequence of the inherent electromechanical delay in the muscle engagement, compounded by the high speed activity when mapped across the circular pedalling path of the bicycle crank. The work identifies this and makes recommendations to consider alternate measurement techniques such as pressure-based FMG which does not suffer from the same electromechanical delay as it measures the direct mechanical response muscles during high speed activity.

5. **Fractal Dimension analysis as an alternate method for measuring muscle fatigue**
   The measurement of muscle degradation in performance due to fatigue most commonly is done through the established gold-standard, a combination of EMG measurement and calculation of changes in the resultant median value of an FFT analysis. The research enforced a fatigue condition within participants and demonstrated the confirmation of fatigue using this established methodology. This was furthered through exploration of a new technique using Fractal Dimension Analysis to correlate muscle signal instability with fatigue. The increasing presence of muscle fatigue, confirmed by both a test known to enforce fatigue conditions and the gold standard, is directly correlated in the increasing level of chaotic signal instability of the measured signal through fractal dimension analysis. Where the use of fractals demonstrates the detection of electrical and mechanical fatigue for both EMG and pressure-based FMG signals respectively across the tests.

6. **Fractal Dimension analysis as a method for measuring muscle interdependent behaviour during fatigue conditions**
   Further to confirmation in the detection of fatigue, the Fractal-based fatigue measurement yielded a discovery that was not clearly evident through the measurement of fatigue using traditional means. The analysis method highlights interdependent load-sharing behaviour of antagonistically-paired muscles that extends activity duration whilst maintaining required output power. This is observed through cyclic accelerated fatigue-recovery patterns between the two muscles, which allows for one of the muscle to reduce power delivery (recover) whilst the other muscle balances the activity's power demand. This behaviour slows the longer-term rate of fatigue, as measured through the fractal dimension value.

1.4 Published Research Output

As a result of the research undertaken, portions of the material in this thesis have been published or represented within the following publications.

Journal Articles:

- Belbasis, A. & Fuss, F. K. Muscle performance investigated with a novel smart compression garment based on pressure sensor force myography and its validation against emg. *Frontiers in Physiology* **9** [2018]
- Belbasis, A., Fuss, F. K. & Sidhu, J. Estimation of cruciate ligament forces via smart compression garments. *Procedia Engineering* **112,** 169–174. ISSN: 18777058 [2015]
- Belbasis, A., Fuss, F. K. & Sidhu, J. Muscle activity analysis with a smart compression garment. *Procedia Engineering* **112,** 163–168. ISSN: 18777058 [2015]
- Belbasis, A. & Fuss, F. K. Development of Next-generation Compression Apparel. *Procedia Technology* **20,** 85–90. ISSN: 22120173. `http://linkinghub.elsevier.com/retrieve/pii/S2212017315001929` [2015]
- Fuss, F. K., Belbasis, A., van den Hazel, B., *et al.* Design Strategy For Selecting Appropriate Energy Absorbing Materials and Structures: Data Library and Customised Selection Criteria. *Procedia Technology* **20,** 98–103. ISSN: 22120173. `http://linkinghub.elsevier.com/retrieve/pii/S2212017315001942` [2015]

Conference Proceedings:

- Fuss, F. K., Belbasis, A., Sidhu, J., *et al. Fractal dimension analysis of muscle fatigue with muscle surface pressure measured via compression garments* in *Proceedings of ICSST 2016, 2nd International Conference in Sports Science and Technology* [Nanyang Technological University, Singapore, 2016]
- Salim, F. *et al. Design and evaluation of smart wearable undergarment for monitoring physiological extremes in firefighting* in *Proceedings of the 2014 ACM International Symposium on Wearable Computers Adjunct Program - ISWC '14 Adjunct* [2014], 249–254. ISBN: 9781450330480

Patents:

- Fuss, F. K. & Belbasis, A. Soft tissue management method and system. *WIPO PCT Patent (filed)* **WO2016065404A1** [May 2016]

Awards:

- Asia-Pacific Conference on Sports Technology 2015, APCST-ASICS International Innovation Award (2015) for research presented within:
  - Muscle activity analysis with a smart compression garment
  - Estimation of cruciate ligament forces via a smart compression garment

1.5 Thesis Structure

The thesis is divided into two main parts; Research Development, and Research Implementation. The first part encompasses chapters 1-3, and provides an introduction into the thesis and the research gap within the literature, and a documentation of the development of the foundational capture systems and methodology used throughout the work. The second part of the thesis covers chapter 4-8 and focuses upon the implementation of the developed research, with each chapter focusing on addressing the research questions.

The thesis chapter breakdown is as follows:

Chapter 1 Thesis overview and scope of research performed (this chapter).

Chapter 2 Literature review of the current state of works surrounding the research of performance monitoring through wearable technologies.

Chapter 3 The design of a wearable data collection system. The design of soft pressure sensors and the installation within a compression garment to read dynamic pressure changes during an activity. Necessary considerations in the measurement of limb angles using a motion capture system, and the utilisation of a Surface Electromyography system for gold-standard validation.

Chapter 4 The measurement of muscle activity through the use of a controlled leg extension and flexion activity to determine muscle activation and load criterion. Testing methodology explores increases in limb loading, therefore required muscle force, to determine whether this reflects changes in the measured surface pressure exerted by the muscle.

Chapter 5 Resolution of the biomechanical forces in the upper leg to the forces present in the Cruciate ligaments in the knee. A theoretical model based upon muscle exertion levels, limb angle, and understood soft tissue parameters from literature is developed to increase speed of in-situ warnings over overloading and strain to the ligaments.

Chapter 6 The testing of fatigue performance of the lower leg by using an established fatigue-inducing test methodology for cycling activity. Analysis of the results explores how muscle performance changes were evident between the start and end of the test, as measured by the surface pressure and EMG, that reflect the conditions of increasing muscular fatigue.

Chapter 7 Further research and confirmation presented into the transitional increase of fatigue throughout the duration of the test using both the gold-standard technique and an alternative. Results presented that changes in measured signal instability, through a Fractal Dimension analysis, are reflective in the increasing fatigue of the muscles and can be further used to investigate inter-dependencies between muscles.

Chapter 8 Thesis conclusions and summary, with scope for future work in the continuation of the research performed within the thesis.

2. Literature: Monitoring soft tissue loads

The design of the human body, it's complexity and function, greatly overshadow that of all attempted man-made invention to date. We have spent much of our history exploring the intricate detail and composition of what provides us the scope for existence, makes us who we are, and allows us the gift of movement.

In our ways of classification we label the system responsible for movement as the Musculoskeletal system, the combination of the structural supports (skeleton) and actuation units (soft-tissues) of the human body. This system alone is not solely responsible for movement, working in synergy with other systems of the body (e.g. the nervous, circulatory, and respiratory systems) we achieve efficient and healthy movement. It is however the soft-tissues (muscles, tendons and ligaments) within our Musculoskeletal system which plays a key part in the enclosed research that follows.

As this research introduces and explores a novel measurement technique that evaluates soft-tissue performance, it is necessary to understand and evaluate the current existing analysis systems in use, and subsequent body of literature that support them. This chapter focuses on a brief exploration into the current developments toward the measurement of muscle activity through wearable systems or garments (smart apparel). Exploring where these methods have been used for the measurement of muscular fatigue through traditional or newer, alternative methods. Concluding with a brief overview of the research work encompassing the measurement of the cruciate ligaments using wearable systems.

In lieu of a standard, all-encompassing literature review, much of the relevant work by key researchers pertaining to each topic has been introduced and discussed at the beginning of each relevant chapter to better frame and explore the work.

2.1 Development efforts towards smart apparel

The analysis of exercise performance has long since surpassed the sole interest of sports biomechanists and health practitioners. It has become commonplace for the average consumer to actively capture and analyse their own personal activity data. Motives for such behaviour differ, yet increasing sales of wearable fitness trackers and smartphone fitness solutions are a testament to this paradigm shift [James & Petrone 2016; Moustafa *et al.* 2015].

Identified as one of the ten technologies which will change the world by the European Parliament Scientific and Technology Options Assessment Panel, Market prospects for wearables are very promising with wearables shipments forecasted to increase to $150 billion by 2026 from the estimated level of $30 billion in 2016 (European Commission, 2016). Wearable technologies were the most popular and leading fitness trend in 2016 for the first time, and continued to be so in 2017 [Thompson 2015, 2016] yet they have dropped to the third highest trend leading into 2018 [Thompson 2017], but returning to the lead position in 2019 [Thompson 2018]. A major drawback of smart wearables which may account for this shift is the value that consumers are getting from these devices. In contrast to non-wearable laboratory equipment, wearable devices have a reduced level of accuracy within the technology, posing a challenge to consumers in a market saturated with un-validated products [Düking *et al.* 2016].

To contrast the current magnitude of fitness tracking solutions, one only has to look back a decade when consumers were content to track activity through a single information stream; the heart rate. As both technology and consumer needs evolve, the once prominent lines between Clinical and Consumer measurement systems have become blurred. Constant progression of instrumentation simplification and miniaturisation has led to once cost-prohibitive technology solutions to be widely affordable to the masses. Increasingly it is not only consumer devices but also sporting garments that are adopting this trend and spanning these now blurred lines; Smart devices now scope beyond the wrist with technology-enhanced or *smart* headbands, shirts, jackets, socks and underwear [Düking *et al.* 2016; EU DG Connect 2016].

Of particular focus is that of the progressive developments in compression apparel. Current passive compression garments provide little to no feedback on performance and behaviour to the wearer, functioning mainly as a proprioceptive aid during recovery [Fu *et al.* 2013]. The prominence of these garments within the sporting industry does provide an advantageous avenue for instrumentation of the athlete. Where monitoring select muscle groups and joints directly through a garment affords a transition from lab-based analysis to a wearable platform where evaluated performance is done within the athlete's unique training environment. Novel approaches in material-based sensor technology now allow for integrated *soft sensors* within compression garments, creating smarter apparel that is able to record, store, stream and deliver high-end muscle and joint data for real-time user feedback [Lorussi, Galatolo, Bartalesi, *et al.* 2013; Lorussi, Galatolo & De Rossi 2009].

2.2 Wearable apparel measuring muscle activity

This research deals with smart wearable apparel for muscle performance assessment, the gold standard of which is undeniably electromyography (EMG). Whilst prominent, there are several problems associated with EMG, clearly pointed out by De Luca (1997) which makes it difficult to use EMG in wearables:

- EMG measures the electrical activity of a muscle which the mechanical activity lags behind (electro-mechanical delay).
- The amplitude of the EMG signal is non-linearly correlated to the muscle force, and depends on the number of motor segments recruited on the surface of the muscle, next to the electrodes.
- For optimal measurement electrodes should be located in the midline of the muscle, halfway between innervation zone and the next myotendinous junction.
- Shifting the electrodes along the action line of the muscle decreases the signal amplitude and a sidewards shift decreases the amplitude of higher frequencies (thereby suggesting fatigue if the textile integrated electrode moves sideways).
- Tri-polar electrodes are preferable over bipolar ones, as the former eliminate crosstalk introduced between muscles.

Furthermore, to capture the electrical activity gel/salt-based electrodes are required to reduce the skin resistance and must be incorporated within the design, although special design of embroidered electrodes can overcome this problem [Shafti *et al.* 2017; Taelman *et al.* 2007].

In spite of the issues pointed out above, two companies are selling EMG-based garments for performance analysis: Athos[1] and Myontec[2]. A third company, Leo[3], developed an EMG thigh-sleeve but never sold the product [Early 2016]. B10nix[4] have announced an EMG-based shirt that is not commercially available yet.

Athos, for example, assesses right-left muscle imbalance. Given the fact that precise electrode placement is crucial for accurate results, equal activity levels of muscle groups on the right and left side of the body would generate different signals if the electrode were not placed on the same spot on both right and left muscle groups. A recent research paper [Lynn *et al.* 2018] explored validating the performance of the Athos system against a laboratory system, however does not explore the impact of incorrect placement through improper fit of the Athos garment, in contrast to that of validation performed on Myontec garments by Finni *et al.* (2007).

There are some research papers available that investigate prototypes of EMG-based garments for activity analysis [Finni *et al.* 2007; Manero *et al.* 2016; Shafti *et al.* 2017; Taelman *et al.* 2007]. Finni *et al.* (2007) used traditional EMG electrodes incorporated in a garment, whereas Shafti *et al.* (2017) utilised customised, embroidered electrodes, validated with traditional gel-electrodes. Taelman *et al.* (2007) investigated the effect of electrode misalignment in a smart shirt, in the same

[1] Mad Apparel Inc., Redwood City, CA, USA; https://www.liveathos.com/athletes
[2] Myontec Ltd, Kuopio, Finland; https://www.myontec.com/en
[3] GestureLogic Inc., Ottawa, Canada; https://gesturelogic.squarespace.com
[4] b10NIX Ltd, Milano, Italy; http://wise.b10nix.com

way as Belbasis & Fuss (2015) did. Manero *et al.* (2016), however, did not validate their leggings prototype.

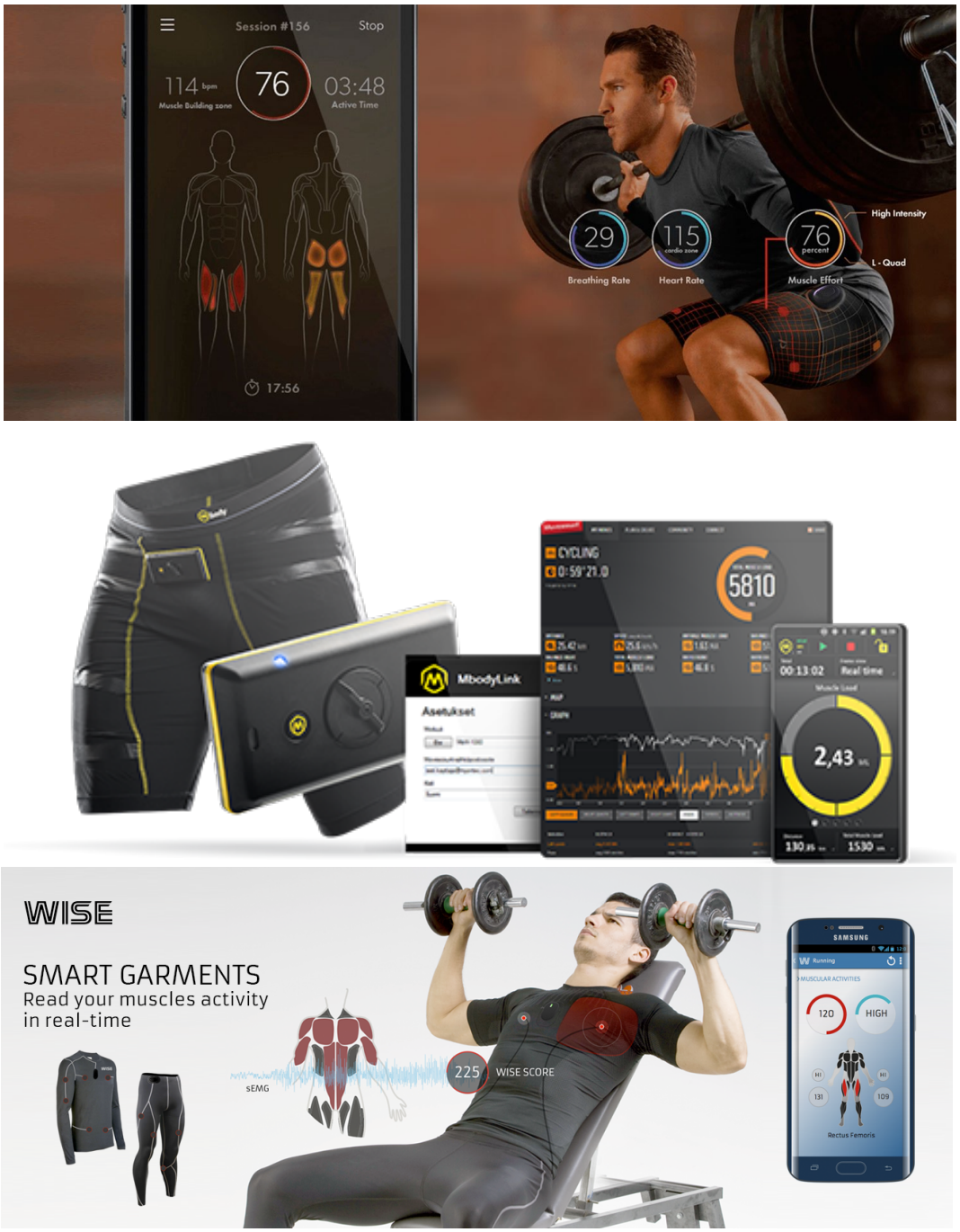

Figure 2.1: Examples of commercially available garments measuring EMG by Athos (top), Myontec (middle) and B10nix (bottom)

2.3 Wearables measuring muscle fatigue

De Luca who was the first to develop the concept of myoelectrical manifestations of localized muscle fatigue [De Luca 1984; Merletti, Afsharipour, *et al.* 2016; Merletti, Knaflitz, *et al.* 1990]. Fatigue is expressed in the EMG signal as an increase in EMG amplitude (increase of motor unit recruitment or synchronization by the central nervous system to maintain the required force level, related to central fatigue) and a shift to the lower frequencies of the EMG frequency spectrum (decrease of the conduction velocity of motor unit action potentials over the muscle, related to peripheral fatigue) [Crozara *et al.* 2015; Mesin *et al.* 2009].

The Myontec garment measures the muscle fatigue threshold (EMGFT2 according to Crozara *et al.,* 2015), i.e. breakpoint in the linear relationship between EMG amplitude and exercise intensity [Lucia *et al.* 1999]. The muscle fatigue threshold, however, is not suitable for measuring the increasing fatigue over time. Manero *et al.* (2016) were the first that attempted to measure fatigue with an EMG garment prototype, by using the instantaneous Average Rectified Value (iARV) signal. However, they did not validate the fatigue data they obtained. For example, although their iARV signal is supposed to increase with fatigue, their initial data at the beginning of the exercise are also very high. Another limitation in this technique is that the introduction of increasing sweat levels drives increases in the iARV signal [Manero *et al.* 2016].

There are several methods available for the assessment of fatigue with EMG, such as FFT-based, time-based, amplitude-based and wavelet-analysis-based methods. Details can be found in comprehensive reviews of Cifrek *et al.* (2009) and González-Izal *et al.* (2012). Both papers mention fractal dimension methods without going into detail. The most common method for assessment of fatigue (gold-standard method) is FFT-based, and the onset of fatigue is characterised by a shift of the median frequency to smaller frequencies [De Luca 1997]. Basmajian & De Luca (1985) conducted an isometric experiment that shows the difference between mechanical fatigue and metabolic fatigue (measured with EMG and FFT method): the muscle force decreased at the failure point, whereas the preceding fatigue point was only detectable with EMG through the decreasing median frequency (Figure 2.2).

Fractal dimension methods for assessing muscle fatigue have increased in importance over the last 10 years, with researchers using different methods, such as the box-counting method [Beretta-Piccoli *et al.* 2015; Boccia *et al.* 2016; Troiano *et al.* 2008] to understand the fractal behaviour. Marri & Swaminathan (2016) used several methods (e.g. Higuchi, Katz, Sevcik, box counting; multifractal analysis). In most cases, Marri and Swaminathan's monofractal algorithms delivered smaller fractal dimensions for fatigued muscles compared to non-fatigue; whilst the opposite was true for multifractal algorithms where the fractal dimension was mostly smaller than a value of 1. In general, a signal's fractal dimension ranges between a value of 1 and 2, i.e. ranging between a straight line or smooth curve, to that of a maximally noisy signal filling up an area [Fuss 2013].

Mesin *et al.* (2009) compared the fractal dimension of EMG signals to other muscle fatigue indexes, indicating that the EMG fractal dimension was least affected by changes in conduction velocity and most related to the level of motor unit synchronisation, and suggesting that the fractal dimension is

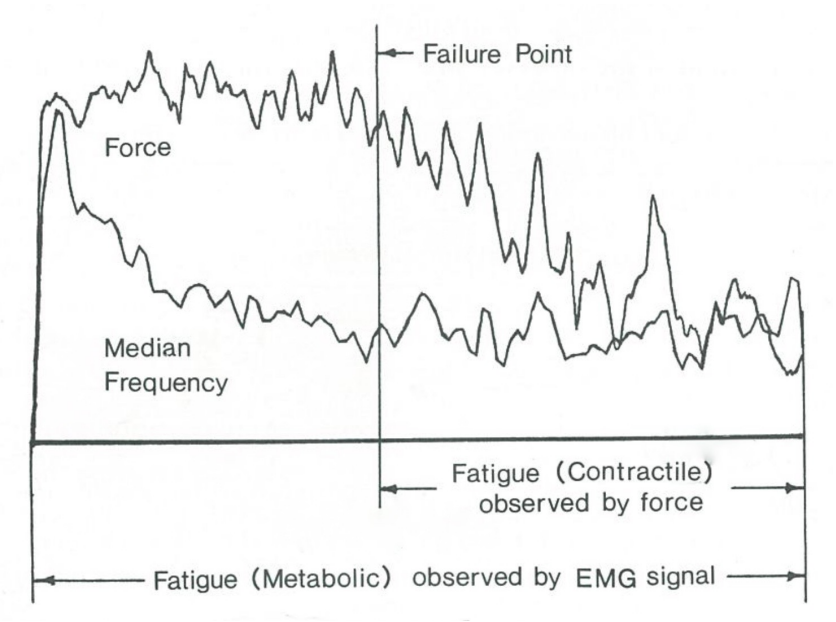

Figure 2.2: Distinction between contractile mechanical fatigue and metabolic fatigue; from Fig. 8.1 of Basmajian & De Luca (1985)

an index of central rather than peripheral fatigue.

Furthermore, Mesin *et al.* (2009) found that in a power trained subject, the Fractal Dimension (FD) does not have a clear trend, indicating that the level of motor unit synchronisation does not change, whereas the rate of change of the median frequency is high. In an endurance trained subject, the rate of change of the median frequency is lower than in the power trained subject, whereas rate of change of FD was high. These results suggest that power trained athletes are affected more by peripheral fatigue, whereas endurance trained athletes suffer more from central fatigue. Consequently, Fractal Dimension of the EMG signal (EMG-FD) appears to be more sensitive in endurance trained muscles, and the Fast Fourier Transform of the same EMG signal (EMG-FFT) more sensitive in power trained muscles when regarding fatigue conditions.

2.4 Alternative muscle measurement: Force Myography

An alternative method to measuring muscle activity through myoelectrical activity (i.e. EMG), is to explore the mechanical changes of the muscles through Mechanomyography (MMG; Islam *et al.*, 2013). In contrast to surface EMG, the quality of the MMG signal is not affected by electrical interference and changes of skin conditions as MMG measures the mechanical action of a muscle. MMG offers two main methodological options:

1. Vibromyography or Acoustic-myogram (phono-myography) using accelerometers and/or microphones. The method assesses the low amplitude sound of lateral oscillations generated by volumetric changes in active muscle fibres at frequencies between 5 to 100Hz with microphones or low mass accelerometers [Fang *et al.* 2015]. However, the signals are affected by limb movements and ambient noise, such that the method is not suitable for sports applications [Islam *et al.* 2013].
2. Force or Pressure sensors used for Force-Myography (FMG). The sensors measure the forces or pressure exerted by the muscles against the skin by volumetric changes of the active muscles [Castellini *et al.* 2014; Connan *et al.* 2016]. Muscle bulging increases the pressure non-linearly with respect to the increase in muscle force [Belbasis, Fuss & Sidhu 2015a].

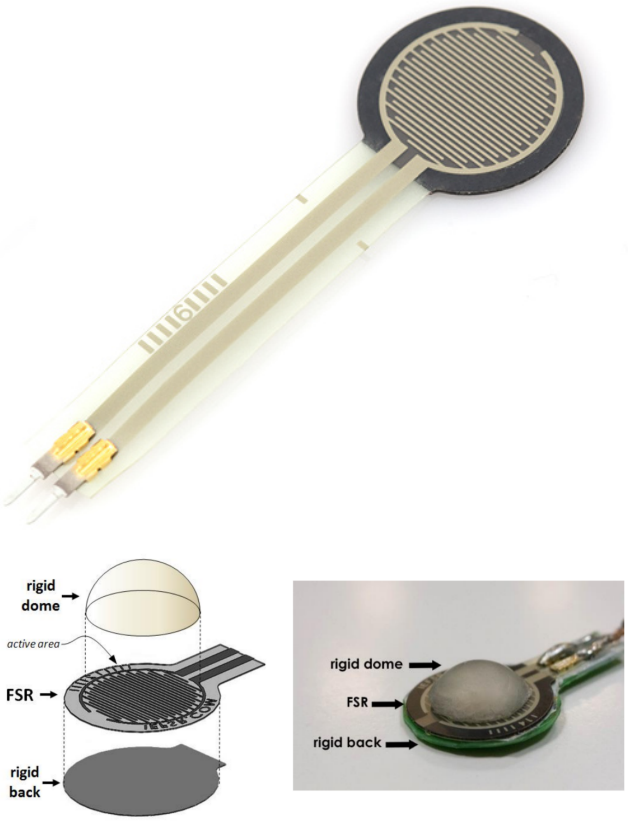

Figure 2.3: Example of a commercially available FSR sensor (top), and the use of a pre-load device to improve sensor performance [Esposito *et al.* 2018] (bottom)

The most common sensors used for FMG purposes are off-the-shelf FSR (Force Sensing Resistive)

sensors (see figure 2.3 above), either as single sensors, several sensors [Connan *et al.* 2016] or sensor matrix arrays [Zhou *et al.* 2017], that are preloaded, either compressed by tight fitting garments or elastic bands to the surface of the relevant muscles [Lukowicz *et al.* 2006; McLaren *et al.* 2010; Zhou *et al.* 2017], Velcro bracelets [Connan *et al.* 2016], integrated in a textile sleeve [Ogris *et al.* 2007], equipped with mechanical preload adjustments [Esposito *et al.* 2018; N. Li *et al.* 2012], or placed inside a forearm orthosis [Wininger 2008]. Belbasis & Fuss (2015) and Belbasis, Fuss & Sidhu (2015ab) used several customised piezoresistive polymer sensors sandwiched between compression garment and skin. Meyer *et al.* (2007) applied a capacitance pressure sensor array embedded in textiles. Alternatively, Jung *et al.* (2015) utilised air-bladders to detect pressure changes underneath a compression band, and Cheng *et al.* (2010) did not use any sensors but instead measured the body capacitance and its changes with movement.

FMG or pressure sensor based garments are a typical example of lateral innovation, i.e. achieving the same goal with other or alternative means, a common precursor of a disruptive technology. Lateral innovation is characterised by e.g. lower costs, higher accuracy, better user-friendliness, smaller hardware, simpler solution, simpler implementation, less affected by error and method, better wearability, providing additional information, or improved manufacturability [Fuss 2017]. However, none of these FMG solutions are commercially available yet.

2.5 Wearables measuring the Cruciate Ligaments

Soft tissue injuries (both acute and chronic overuse syndromes) are among the most prevalent sports injuries. In numerous sporting codes, from the amateur to the elite, every season is plagued by injuries that prevent many participants from full participation. Of key concern is the increasing predominance of non-contact ligament injuries in the lower limbs, specifically the Anterior and Posterior Cruciate Ligaments (ACL, PCL respectively). Several studies have been performed in an effort to quantify the loading of the cruciate ligaments when in use, but ultimately measurement systems rely on data commonly obtained through largely static machines performing either isometric or isokinetic movement.

In the design of the knee joint, it is the cruciate ligaments that function as restraining elements to anterior and posterior movement of the tibial plateau with relation to the distal head of the femur. Both ACL and PCL work under load to compensate for the net horizontal force from the ground reaction force and subsequent supportive muscular activity, where the resultant load on the ligament is highly dependent of the flexion angle of the knee [Fuss 1989; Fuss 1996].

Although significant research has been done into the failure of the cruciate ligaments under various loading conditions [Colby *et al.* 2000; DeMorat *et al.* 2004; Fuss 1989], and the prevalence of injury during due to muscle activity [Withrow *et al.* 2008], gender [Myer *et al.* 2005] or sport [Alentorn-Geli *et al.* 2009a,b], quantifying the real-time loading forces of the cruciate ligaments within the sporting environment has been limited due to the complexity of the joint.

Significant research in ligament structure, composition and failure patterns has led to accurate estimations of soft tissue loading maxima through biomechanical simulations [Zhang *et al.* 2011] and models [Fregly *et al.* 2012; Kinney *et al.* 2013]. However there still exists a need to continue research into the inherent unknowns of the loading condition; the applied load, the subject's health, and ultimately the reflex-driven response. These parameters control how closely we can provide an understanding on when, or how, a ligament will fail. Lin *et al.* (2012) attempted to explore some of these through a stochastic biomechanical model of the risk and risk factors to the ACL, but interestingly found no difference in risk between genders.

The ideal measurement opportunity is through direct access to the soft tissue in question, however practicalities of in-vivo measurement without affecting joint performance pose a challenge to researchers, resulting in novel-approaches being undertaken. Beynnon *et al.* (1992) utilised the arthroscopic installation of in-vivo hall-effect transducers for direct strain measurement of the ACL (see figure 2.4), whereas Taylor *et al.* (2011) opted for the less-intrusive use of biplanar fluoroscopy with motion capture markers and the use of Magnetic Resonance Imagery (MRI) to capture static positional displacement and lengths of the ACL.

Due to clinical requirements and restrictions of in-vivo measurement, much of the investigative research around the joint is done through external capture. Most commonly this is done with motion analysis techniques through either video or more advanced motion capture systems often partnered with force plates to determine the respective ground reaction force.

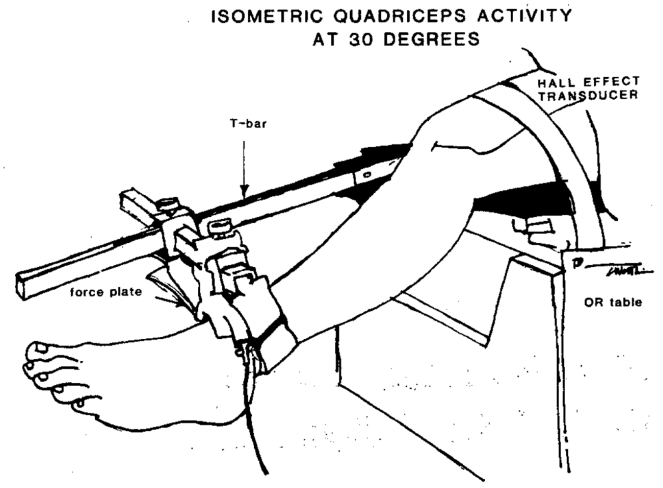

Figure 2.4: Experimental in-vivo setup from Beynnon *et al.* (1992)

Mobility limitations of a combined camera-force plate setup has seen many researchers look to the opportunities to capture data afforded by the ongoing miniaturisation of electrical systems. External attachment of Inertial Measurement Units (IMUs); housing accelerometers, gyroscopes and magnetometers, have allowed researchers to prototype wearables systems that capture gait and knee angle allowing for the determination of preliminary cruciate ligament loading risk [Dowling *et al.* 2011, 2012], with greater mobility outside of a traditional lab environment.

Whilst numerous IMU-based motion capture systems exist, the skill and complexity involved in setup and preparation of a subject for data capture has limited their use outside of the traditionally research and medical applications as validation of the data is often difficult without the use of another (gold-standard) system. For this reason most IMU systems are operated as a capture system, with researchers applying post-capture models on the limb angular data captured.

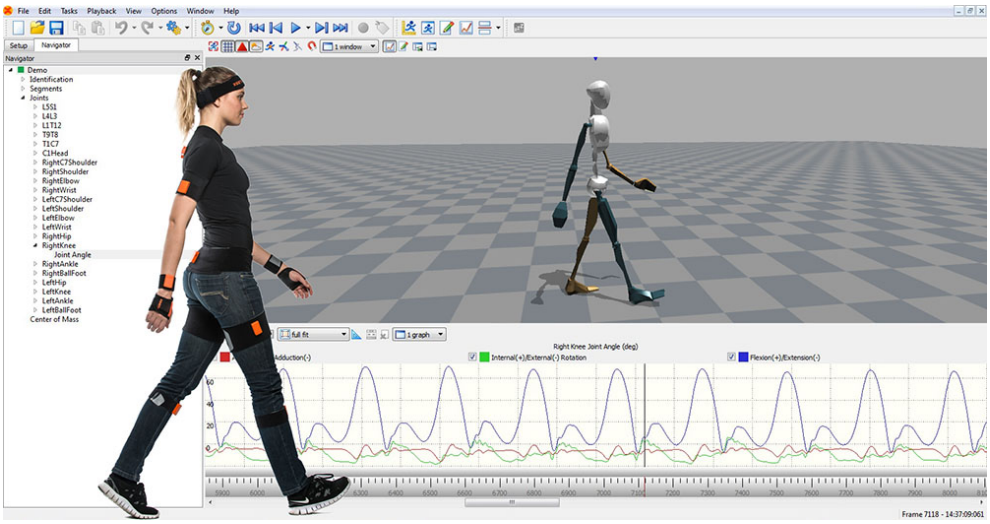

Figure 2.5: Gait analysis using the wearable IMU-based Xsens MVN Awinda system [Xsens Technologies 2019]

2.6 Summary

The literature reviewed shows that there is both a growing research and commercial interest in the synthesis of two bodies of work, namely the monitoring of muscle performance, and the growth and use of wearable devices. The acceptance and capability of wearable technologies are increasing, as are the functional uses of these systems for performance monitoring.

Evaluating the performance of muscle activity has become well established using Electromyography (EMG) techniques, and is accepted as one of the current leading gold-standard methods. Along with its use in both medical and laboratory research environments, EMG has been successfully incorporated into a number of wearable apparel solutions. Limitations in implementing EMG however are driving new thinking into alternate methods for muscle measurement. Force Myography (FMG), a newer yet promising technique, evaluates the muscle activity through the mechanical changes induced by muscle movement. The growing body of research and the respective outcomes for Force Myography largely focuses on measuring muscle activity for control of an external system, and very little has been done on evaluation of the muscle performance.

Evaluation of fatigue behaviour within muscles also relies on EMG as a leading gold standard methodology. However growing research interest is underway into the use of alternative signal processing techniques, such as measurement of the signal's Fractal Dimension, where more information can be extracted from the fatigue behaviour than currently possible through EMG-FFT techniques.

This identifies an opportunity to explore the use both Force Myography and Electromyography to evaluate muscle and limb performance within a wearable system, using both established FFT-based and developing Fractal-based signal processing.

3. Development of a Measurement System

Published Research

The following chapter contains work published within:

- Belbasis, A. & Fuss, F. K. Development of Next-generation Compression Apparel. *Procedia Technology* **20,** 85–90. ISSN: 22120173. `http://linkinghub.elsevier.com/retrieve/pii/S2212017315001929` [2015]

A key need highlighted within the scope of existing literature was the ongoing need to establish performance monitoring smart garments to better understand in-situ biomechanical behaviours. This chapter discusses the selection, design and development of a prototype sensor system to determine the surface pressure under a compression garment and the relative limb orientations of the lower body. A portable monitoring system with the capability of capturing data in a mobile, activity relevant location, outside of the traditional bounds of the research lab.

3.1 A Smart Compression Garment

Complete enjoyment and participation in physical activity is often hindered by a fear of possible injury, a behaviour increasingly common amongst those in recovery from previous injuries. In particular, the muscles and joints in the lower limbs suffer from an increased likelihood of injury due to muscle and ligament overload and straining. A widespread consumer option is the use of elasticated compression apparel to address the concerns of activity-provoked injury by providing additional support to the wearer's body.

In the current state of design, compression apparel is limited only to providing passive muscular and vascular exercise responses; it is in effect a "dumb" garment. In an effort to improve and enhance this, "Smart" apparel introduces the integration of a pressure mapping system into a compression garment. Therein extending the functional support a garment can provide in a range of applications through the real-time collection and processing of information. This solution provides biomechanical information as an indispensable training aid within competitive sports, whilst also

functioning as a rehabilitative tool in the health and medical fields.

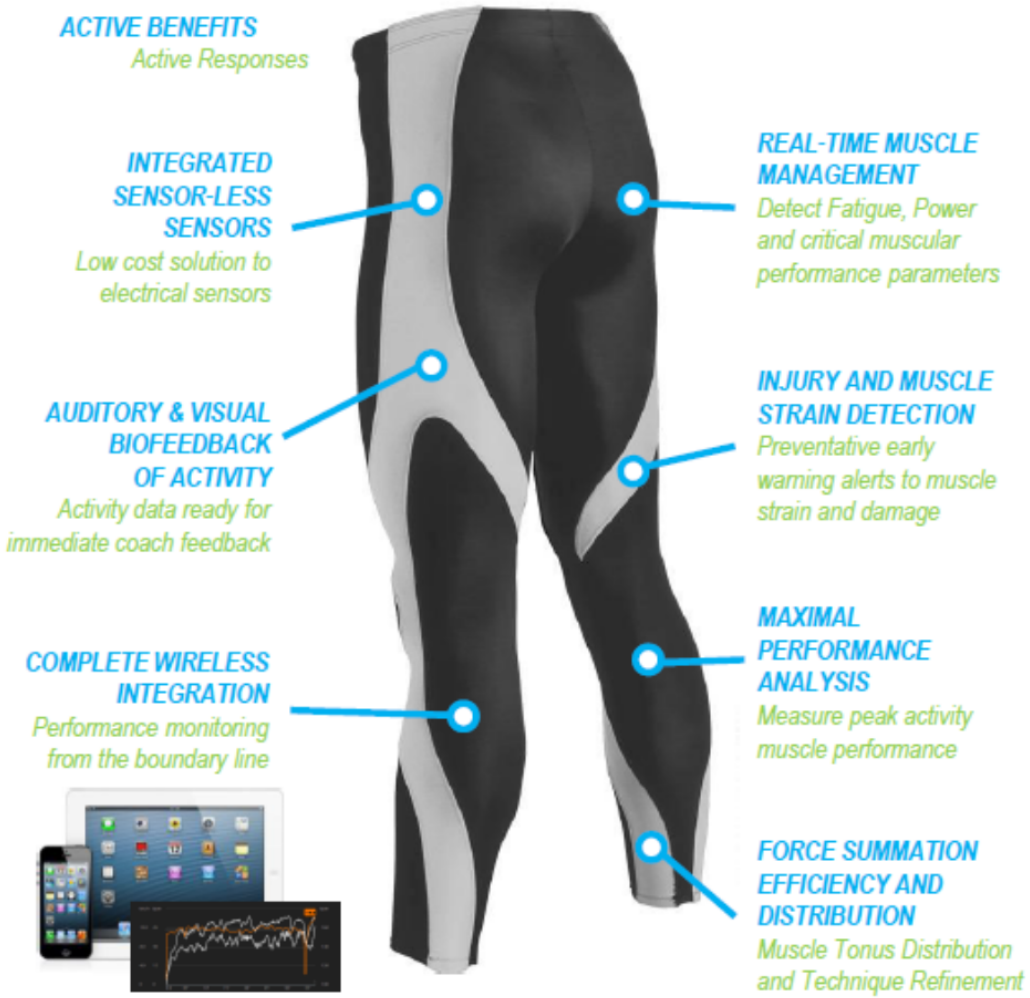

Figure 3.1: Smart Garment concept

3.1.1 Novel Muscle Measurement

The focus of this research was the investigation into the design considerations and developmental steps necessary in producing such a Smart Garment for monitoring biomechanical activity. It investigates a novel approach to quantifying muscular exertion and loading through the measurement of the surface pressures between a target muscular group and a compressive elastic garment during activity. The research goal is that by monitoring and mapping this pressure through garment-integrated sensors, real-time analysis of muscular activity and limb behaviour is possible.

Solely monitoring the pressure exerted by compression garment is not a novel technique; significant approaches have been taken within the fields of garment research to optimise the effectiveness of compression garments [Troynikov *et al.* 2010], and the resultant ranges of pressure they provide during use [Hill *et al.* 2015]. The scope of this document's research builds upon earlier work by

McLaren *et al.* (June 2010) and the Skins Compression Garment company in the development of a separate wearable system measuring pressures for gradient compression garment design. A key difference where this research deviates is the investigation of an integrated garment-sensor system, where the direct pressure variations due to muscle and limb behaviour become the focus of measurement, not the behaviour of the garment. In this way the research also follows developing work by Dordevic *et al.* (2014) with their Tensionmyography technique of determining muscle tension from skin indentations using a discrete load cell attached to the skin. This research however places a specific focus on continuous movement analysis, rather than discrete evaluation of the muscle activity under the singular maximal action that Dordevic *et al.* explores.

3.1.2 Development of a biofeedback system

Presently, no compression garment is capable of entirely assessing active muscle loading, knee ligament strain and co-contraction of paired muscles. Development of an information processing system was undertaken to allow for real-time monitoring of an individual providing a greater understanding of the lower body soft tissue biomechanical loads.

This biofeedback system aims to prevent injury due to excessive inefficient activity by providing sufficient and succinct information to an athlete. At present this system exists in the form of the SmartWear software package, a GUI driven custom MATLAB program written for this research work to provide basic feedback to the user through set threshold values which provide real-time auditory tones and visual indication in graphical display linked to the output from the garment based on level of surface pressure activity.

This biofeedback system presents outputs from the smart compression apparel only relating to changes in surface pressure of the body, allowing for further research into the correlation of the surface pressure to direct muscle loads and limb position [Belbasis, Fuss & Sidhu 2015b], with the resultant cruciate ligament loading [Belbasis, Fuss & Sidhu 2015a] which allows for the system to aid in;

- Monitoring of muscle activity, load, and balance (leg load distribution)
- Assessment of co-contraction of muscle groups
- Alerts to high muscle load and levels of co-contraction
- Monitoring and alerts to ligament loading
- Monitoring and alerts to muscular fatigue

Future developments in the biofeedback system aim to investigate the challenges and solutions used in similar fields of preventative support (diabetes, heart management) where a user-centered design approach has yielded significant improvements into the impact and effectiveness of the critical data relayed to a participant [LeRouge & Wickramasinghe 2013].

3.2 Pressure Sensor Development and Calibration

The unique electro-mechanical relationship between a material's deformation and the resulting change in its electrical resistance is key in the development of a force sensor capable of accurate determination of loads. This relationship, the *piezoresistive response* of a material, is utilised as the core measurement parameter in the design of numerous measurement systems. Specifically, this includes the common thin-foil strain gauges and MEMS-based IMU sensors we see used extensively throughout the field of engineering.

The piezoresistive properties of a material are the aggregate of both mechanical and electrical behaviours exhibited by the material under deformation, each influencing the accuracy and function of the sensor. The mechanical response of the sensor is largely driven by the physical properties of the piezoresistive material utilised. To this effect the material must be selected with consideration of the expected loading profile where measurement is needed. Thin films impregnated with conductive material (i.e. carbon, metals) can have favourable repeatability within elastic loading, and due to their size, are easily integrated into thin sensor constructions.

Electrically, the piezoresistive sensor acts as a force sensitive potentiometer, providing a varied resistance load proportional to the level of force applied. An electrical circuit capable of measuring the changes in the resistance over the sensor is necessary, as such the implementation of a basic voltage divider circuit was utilised. Figure 3.2 depicts a circuit diagram of a voltage divider measuring multiple inputs. A set reference resistor (240Ω) was selected for each channel to measure comparative voltage changes within the circuit allowing for the determination of individual sensor voltages within the target loading profile.

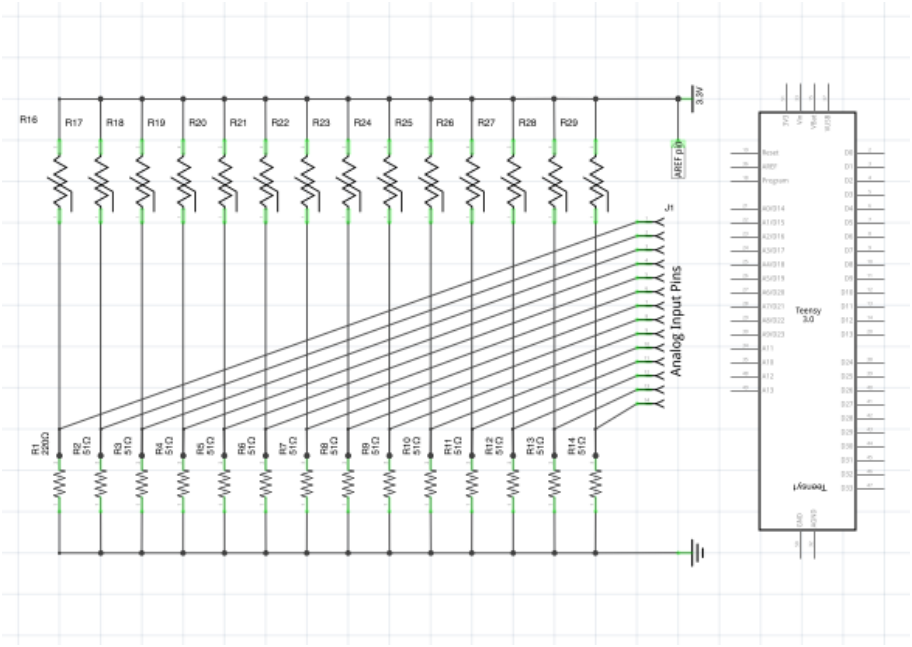

Figure 3.2: Circuit representation diagram of voltage divider measuring multiple (14) sensor inputs through a microcontroller

3.2.1 Design of the sensors

The requirements driven by the research goals outlined a need for a thin, material-based sensor capable of measuring an applied load between the surface of the skin and a compression garment. The thickness of the sensor was critical in minimises the obtrusiveness of the system to the wearer, yet was required to operate within a specified pressure range of 0-3000 Pa [Hill *et al.* 2015]. Successful sensor research and development efforts by the extended RMIT Sports technology team have shown that *Velostat* material, a carbon-impregnated electro-static discharge (ESD) film developed by 3M, produces a significantly high response characteristic to low force applications [Belbasis, Fuss & Sidhu 2015b; Tan, Fuss, Weizman & Azari 2015; Tan, Fuss, Weizman, Woudstra, *et al.* 2015].

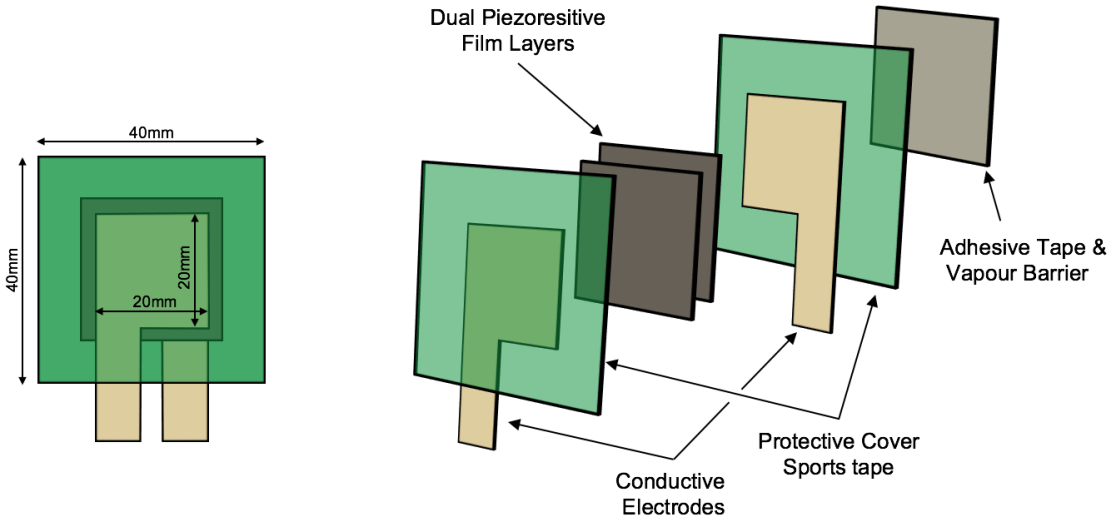

Figure 3.3: Exploded view of piezoresistive pressure sensor

Sensor Construction

Each sensor was constructed from seven material layers bonded together (Figure 3.3). To improve the sensor accuracy and piezoresistive response a dual layer of the Velostat material was utilised as this expands the mechanical and electrical properties of the sensing material. The electrodes of the sensor was constructed from conductive silver-plated ripstop nylon fabric. This was utilised over alternative, rigid layers as it was able to maintain the flexibility necessary for conforming to the skin surface, therefore maximising contact to the piezoresistive layer. Electrode contact area measured 2×2cm (4cm^2), with extended connectivity tabs for the electrode connections.

The individual components of the sensor were enclosed using a material-based elasticised sports strapping tape. Thin double-sided adhesive tape was utilised on one side of the sensor for both attachment to the skin surface, and to act as a vapour barrier to prevent electrical disruption to the readings through permeation of moisture (i.e. sweat) into the sensor.

Useful Nomenclature

n	Analog Sampling Resolution	(bits)
α	Analog sample value	$(0-2^n)$
V_{input}	Input Voltage	(V)
V_{ref}	Reference resistor voltage load	(V)
V_{sensor}	Sensor voltage load	(V)
I	Current in the circuit	(A)
R_{ref}	Resistance of the reference resistor	(Ω)
R_{sensor}	Resistance of sensor	(Ω)
A_s	Area of the sensor	(m^2)
t	Thickness of the sensor material	(m)
ρ	Resistivity of the sensor	(Ωm)
σ	Conductivity of the sensor	($1/\Omega m$)
P_{sensor}	Pressure measured by the sensor	(Pa)

Sensor calibration

Sampling of the sensor's electrical changes was performed through the use of an Analog-to-Digital Converter (ADC), either on a microcontroller or dedicated Data-Acquisition unit (DAQ). The ADC samples the sensor circuit as a scaled value to that of the sampling resolution (n) from the ADC circuit. As such it is necessary to calculate the resultant scaled value of the sensor, this is done within the defined input voltage (typically $V_{input} = 5V$, however this was adjusted where losses in the length of the cable were measured) and the ground (0V), Equation 3.1.

As the circuit measures the voltage load within the reference resistor (V_{ref}), Equation 3.2 is utilised to isolate the voltage load present within the sensor (V_{sensor}).

$$V_{ref} = \frac{V_{input} \times \alpha}{2^n} \tag{3.1}$$

$$V_{sensor} = V_{input} - V_{ref} \tag{3.2}$$

At this stage the V_{sensor} value can be utilised for calibration to a known load, however the loading response of the voltage change in a piezoresistive material is non-linear and as such accurate calibration is difficult to achieve throughout the length of the loading curve (See Figure 3.4).

The conductivity of the sensor exhibits a far better linear behaviour to that of the the (so far) calculated voltage response, calculated based on the unique circuit and sensor properties. This is achieved by calculating the Current (I) and the Resistance of the sensor (R_{sensor}) using Equations 3.3 & 3.4.

$$I = \frac{V_{ref}}{R_{ref}} \tag{3.3}$$

$$R_{sensor} = \frac{V_{sensor}}{I} \tag{3.4}$$

Knowledge of the physical dimensions of the sensor, the electrode area and the thickness of the

piezoresistive material, allows for determination of the Resistivity (ρ) of the sensor, and its inverse the sensor's Conductivity (σ) using Equations 3.5 & 3.6.

$$\rho = \frac{R_{sensor} \times A_s}{t} \tag{3.5}$$

$$\sigma = \frac{1}{\rho} \tag{3.6}$$

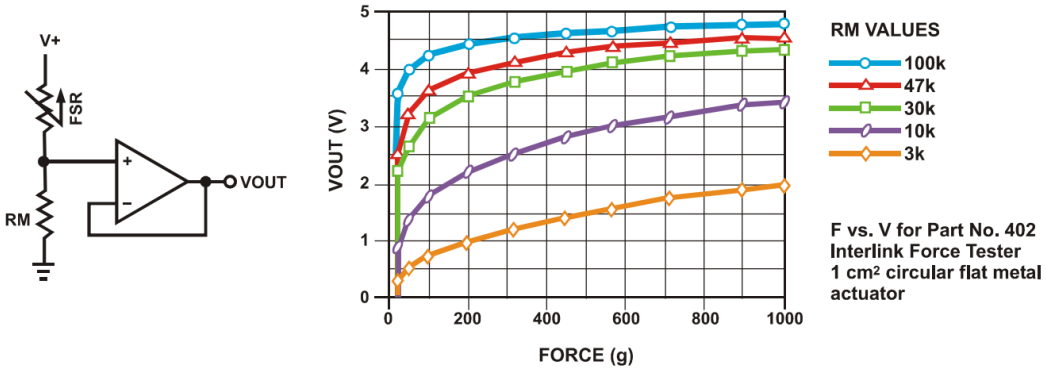

Figure 3.4: Non-linear voltage response behaviour of the sensor under load using simple voltage-divider circuit with various reference resistances, [Interlink Electronics 2016]

Calibration to a commercial sensor

To achieve valid calibration a commercially available force transducer was utilised (Kistler 9317B sensor with Charge Amplifier, Kistler Switzerland). The sensor was positioned in series above the force transducer and both loaded with a variable load over the operational range of the sensor. To ensure and maintain uniform loading over the sensor, 4cm^2 non-conductive rigid plates were used on both sides of the sensor, aligned with the internal electrodes.

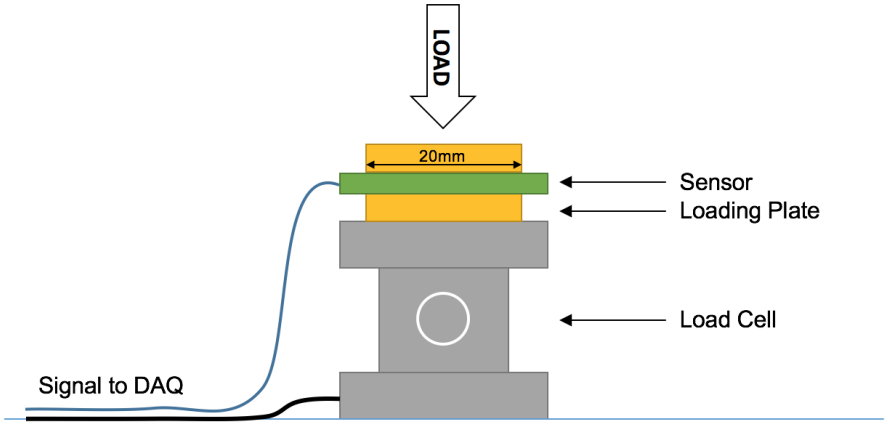

Figure 3.5: Calibration setup with commercial load cell and material sensor

When comparing the peak loading responses from the force transducer to the sensor conductivity a calibration curve can be derived (see Figure 3.6). To do this a curve is fit to the data to calibrate the

material sensor voltages to that of the known transducer values. An example linear function for the single sensor is shown below (Equation 3.7) where the correlation holds accurately throughout the loading envelope ($R^2 = 0.977$). Alternatively an exponential relationship can be utilised (Equation 3.8), where the equation constants (A & B) represent the derived values for the fit respectively for each equation.

$$P_{sensor} = A\sigma + B \tag{3.7}$$

$$P_{sensor} = A\sigma^B \tag{3.8}$$

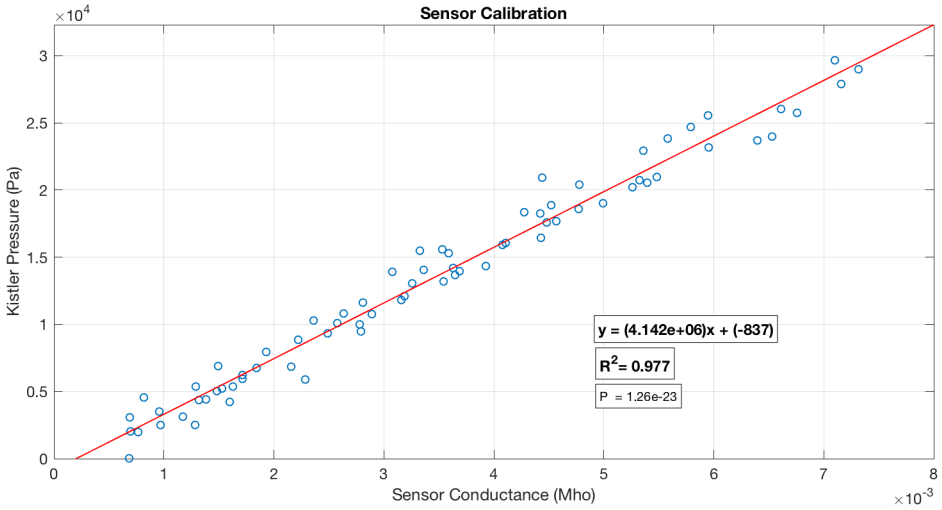

Figure 3.6: Correlation curve of material sensor to force transducer

An important consideration is that the compression force provided by the garment is pressure rather than pinpoint force (although it is resolved to the force over the encompassed area within the calculations). For simplicity it has been assumed that a uniform tangential compressive force in the garment applies a uniform normal pressure over the surface of the sensor, which was made due to the comparative size of the sensor (4cm2) to that of the muscle belly, and the lack of any surface undulations which would present pinpoint localised forces rather than uniform pressure loading. With the sensing based on uniform loading, normal-direction pressure applied to a curved or flat surface will thus be equally measured irrespective of the shape taken due to positioning of the sensors in various locations of the body.

Calibration of the Garment to the User

Muscle capability and performance has long been associated with the visual size and bulge of a muscle; a core premise behind the sport of bodybuilding. Current techniques do not focus on the measurement of this associated change in muscle shape and size under contraction. This is largely due to the accuracy achievable in measuring electrical (EMG) or vibrational motion (Mechanomyography, MMG) of the muscles. This accuracy however comes at the cost of complexity and

portability, reducing the functionality of these systems outside of clinical environments.

Through the measurement of surface pressure the research aims to create a portable monitoring solution that requires minimal setup (installation and calibration) over its alternatives, and provides direct real-time feedback of muscular and limb performance to the individual. As a consequence of the direct feedback, a real-world metric such as pressure in pascals, whilst achievable through comparative calibration, is no-longer paramount to the functionality of the system. Rather, importance is placed upon the biofeedback signal's intuitive relevance to the wearer in understanding their corresponding loading behaviour.

To account for this the Maximum Voluntary Isometric Contraction (MVIC) method is often utilised as a solution in estimation of the forces produced by the muscle, as relevant loading of a muscle can be calibrated and conveyed from a minimally contracted state to the MVIC at 100% effort [De Luca 1997]. This involves the measurement of muscle loads being normalised to the unique characteristics of each individual condition (i.e each participant and the performed action), whereas many of the unknown variables can be discounted through the performance of a calibration routine. Calibration routines consist of a series of activities in which the muscle are activated at various exertion levels from their most relaxed state, to that of a maximal condition (MVIC) state at a given limb angle (see Section 3.2.1). The resultant limitations of the muscle exertion can then be utilised to normalise the exertion level of all further signals. Cautionary observation must be made when calibrating the MVIC using pressure variation. Location of the sensor can result in decreases in pressure with increase in muscle load as the the muscle belly travels away from the sensor location. MVIC calibration therefore must be appropriately normalised considering the absolute pressure change exhibited during the activity.

The resultant scaled metric is significantly more intuitive and perceptible as a biofeedback signal when compared to the standard scientific measurements of the system (N, Pa, mmHg, etc) to a user. Calibration is performed by recording and scaling the range between the base pressure exerted by the compression garment on the relaxed muscle, through to the maximal recorded value through voluntary muscular activity.

Figure 3.7: Measuring MVIC through garment pressure range

It is necessary to note that 100% MVIC is not the maximal limit of a muscles exertion, merely the voluntary limit recorded during the calibration activity. It is possible for muscular exertions to exceed this value during exercise (i.e.>100% MVIC) through involuntary activity. Muscular activity within this involuntary contraction zone is not necessarily damaging, yet if substantial activity forces the user to regularly exceed their MVIC threshold, it is expected that injury likelihood

through overload or straining will increase and acts as a supportive metric to monitor overtraining.

3.3 Goniometry – Limb Angle Measurement

Measurement of key parameters within the testing (i.e. Knee and Hip angles) required the implementation of a system capable of measuring target angles on the body of the subject or on the equipment (i.e crank angle). To accomplish this task a commercially available Motion Capture (MOCAP) system (Qualisys Oqus System, Göteborg, Sweden) was utilised, capturing limb angles and additional motion parameters during the test.

The visual MOCAP system was selected over several other systems which were tested (camera image keyframe and keypoint tracking, IMU-tracking, magnetic-tracking) due to it's higher reliability and accuracy.

3.3.1 Validation System - Qualisys motion capture system

Well established as a gold standard in 3D motion measurement, video-based marker tracking yields significant accuracy due to its globally referenced marker positioning, robustness and ease of use. This is evident in the technology's widespread use throughout the biomechanical and health fields, as well as that of the film and animation industries for reproduction of highly accurate movements.

For the research performed, the volume of interest was observed by 6 infrared motion capture cameras (Qualisys Oqus 500+) with video analysis performed using an additional colour video camera (Qualisys Oqus 210c).

All points were tracked at 100fps and physically represented through spherical 12mm passive retroreflective markers mounted either on the participant or equipment. Calibration of the system was consistently accurate (residuals tracking $<$ 1mm), allowing for confident estimation of limb movement and spatial positioning.

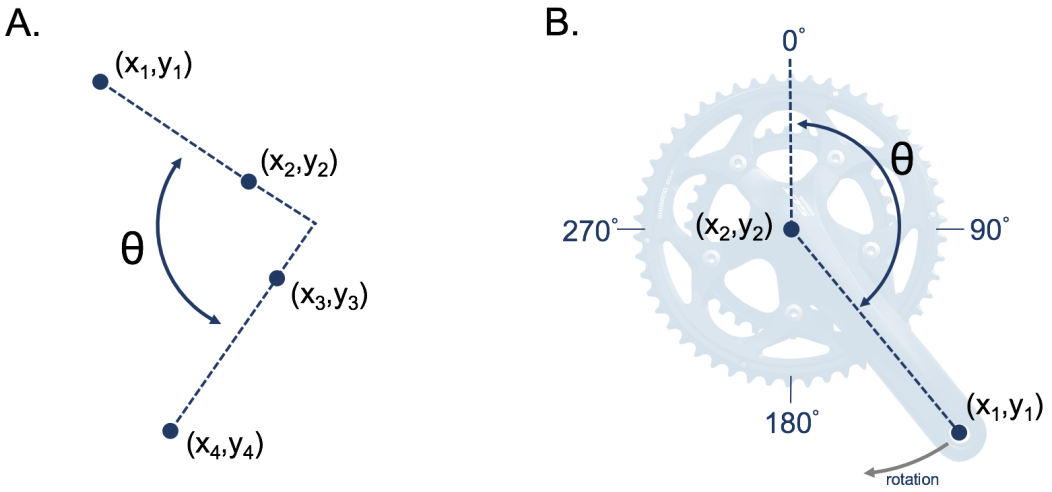

Figure 3.8: Coordinate determination for angle measurement of A) Limbs, and B) Bicycle Crank

Limb Angles

For determination of a subjects limb angles, key observations where made along the sagittal plane of the body (plane separating left and right halves) as it was most critical to the evaluation of knee

flexion. Four retroreflective markers were mounted on the leg of the participant, two on the upper leg and two on the lower leg (see Figure 3.8a). Markers were aligned so the angle between the two groups of markers matched that of the participant's knee flexion angle. In the event of misalignment either; the markers were realigned, or a correction angle (θ_{corr}) was applied by measuring the angular deviation taken when the knee was straightened ($\theta_{KF} = 0°$).

Two vectors were determined through the coordinate points from the markers on each limb segment (Equation 3.9), and the dot product of these vectors utilised to determine the respective angle between them (Equation 3.10).

$$\begin{aligned} v1 &= (x1, y1) - (x2, y2) \\ v2 &= (x3, y3) - (x4, y4) \end{aligned} \tag{3.9}$$

$$\theta = \cos^{-1}\left(\frac{v1 \cdot v2}{|v1||v2|}\right) + \theta_{corr} \tag{3.10}$$

Bicycle Crank Angle

For determination of the crank angle a single marker was utilised. The righthand pedal was fitted with a retroreflective spherical marker mounted on a custom bracket along the axial line of the pedal. This mount eliminated visibility interference (occlusion) from the cyclist's leg on the MOCAP cameras. The sole marker provided reference coordinates (x_1, y_1) for the location of the pedal and crank (see Figure 3.8b).

The crank centre (x_2, y_2) was determined by assessing the centre point of rotation utilising the midpoint theorem[1]. The analytical technique was used as placement of a marker in this location proved difficult due to varied bicycle geometries and the repetitive loss of marker tracking on every pedal stroke; as such this point was derived from the fixed circular path taken by the first marker. With the crank centre restricted from translation by the stationary bicycle trainer, the mid-point of the circular range of the pedal was used to determine the centre point of rotation.

$$(x_2, y_2) = \left(\frac{(x_1)_{max} - (x_1)_{min}}{2}, \frac{(y_1)_{max} - (y_1)_{min}}{2}\right) \tag{3.11}$$

By zeroing the pedal-mounted marker about the coordinates of the crank centre (Equation 3.12), conversion of each pedal stroke from cartesian to polar coordinates using the arctangent (atan2) function[2] yields the respective crank angle (Equation 3.13). To align the resultant polar angle to that of the crank coordinates (i.e angle measured with 0° at top, and clockwise rotation), the coordinates in the standard arctan function were reversed, as well as any negative angles corrected with a 2π rotation (Equation 3.14).

$$(x, y) = (x_1, y_1) - (x_2, y_2) \tag{3.12}$$

[1] Midpoint theorem states that the centre-point between two coordinates can be determined by taking the mean distance between the two respective coordinates. In the use case presented this is the maxima and minima of the circular path taken in both axes.

[2] atan2 is utilised as it extends the standard arctangent range from $\pm\pi/2$ to $\pm\pi$ to resolve the full range (2π) of the pedal stroke.

$$\theta = \text{atan2}(x, y) \tag{3.13}$$

$$\theta = \begin{cases} \theta + 2\pi, & \text{if } \theta < 0 \\ \theta, & \text{otherwise} \end{cases} \tag{3.14}$$

3.4 Physiological Monitoring - EMG and Pressure

3.4.1 Placement of EMG sensors

Due to the nature of detection, EMG is particularly prone to misalignment errors where incorrect placement increases noise and crosstalk within the signal. To overcome this and improve the accuracy of the EMG results, the electrode placement can be optimised through a 5-point signal analysis test to determine best placement. Through comparison of the ratio of peak magnitude and median frequency of all five of the measurement sites, an indication of the optimal location to place the electrode is evident [De Luca 1997], where signal to noise ratio was maximised, and crosstalk from nearby muscles minimised (Figure 3.9)[Belbasis, Fuss & Sidhu 2015b].

It is the use of this localisation testing, or an established guide, which is necessary to determine the correct placement location. For the performed tests the subject was fitted with wireless EMG measurement units (Zwave Zero-wire Cometa Systems, Italy) for each target muscle. Due to the impracticality of performing a 5-point test for every muscle on every participant, the general placement of the electrodes followed the recommendations of Hermens *et al.* (2000) and SENIAM (1999) alongside the Cometa Software providing a visual placement guide for the determination of optimal placement sites with automated warning of poor signal quality. Figure 3.9 demonstrates an example of the 5-point test, whereas the correct placement of the electrodes yields the optimal signal from the central position.

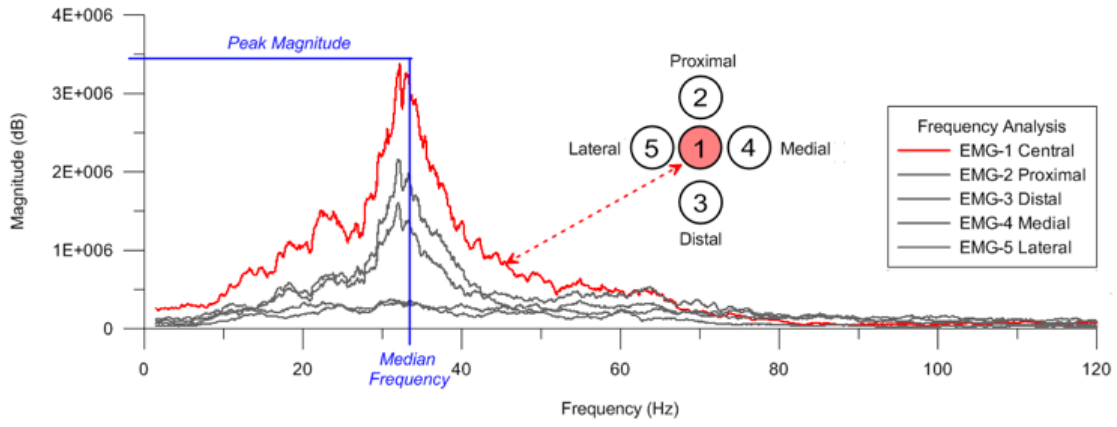

Figure 3.9: Example of the 5-point EMG localisation test, where the central electrode (red line) indicates optimal placement [Belbasis, Fuss & Sidhu 2015b]

3.4.2 Placement of Pressure sensors

The measured pressure response exists as a result of the mechanical deformation of the muscle, as such it is not prone to the electrical crosstalk of neighbouring muscle groups that must be overcome in EMG placement. For the purpose of the research case, achieving a maximal pressure differential drove placement optimisation. Therefore, placement (where possible) was selected to be above the target muscle belly centre of pressure when under maximal contraction. This aided in maximising the pressure reading and further improving the signal to noise ratio of the measurements. For most

muscles the optimal position was aligned with the EMG placement, whereas pressure sensors were positioned between the two EMG electrodes.

To reduce the impact of the EMG electrodes on the pressure sensors, only the EMG gel electrodes were placed underneath the garment, with wiring exposed through small holes in the garment connecting the EMG sensor units which were mounted on the the 'outside' of the garment above (but off-axis) to the muscles. This allowed for minimal disruption to the garment providing compression to the pressure sensors, and allowing the necessary electrical EMG measurements to be taken simultaneously.

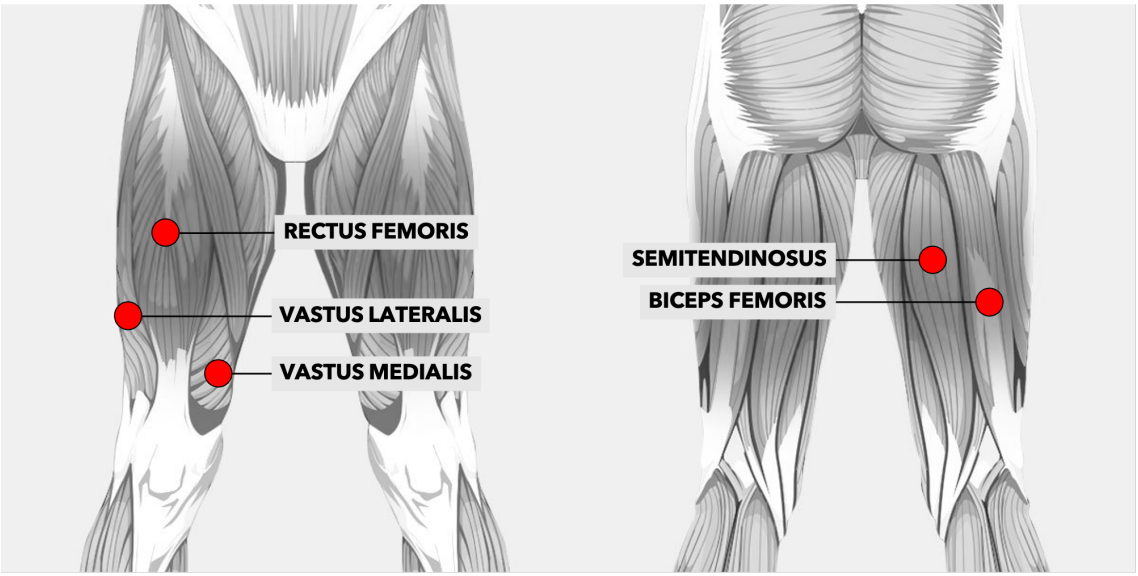

Figure 3.10: Generalised placement location of the ten sensors (5 EMG, 5 FMG) on the right leg quadriceps and hamstrings

Whilst not affected by an electrical crosstalk as with EMG, pressure measurements are adversely affected by the mechanical connection shared with the encompassing compression garment. This mechanical crosstalk condition exists as a result of localised pressure increases transferred over the circumferential stretch of the garment. An example would be when quadricep-only extension of the knee creates increased compression through increased thigh volume, the uniform compression provided by the garment applies increased pressure to the sensors of the hamstring muscles resulting in phantom hamstring muscle activity.

To overcome this the muscles require individual compression conditions, thus the selected commercial garments utilised for testing specifically isolated muscle groups through the use of siliconised regions on the internal face (show in figure 3.12) which increased friction on the skin around key muscle groups. This allowed for prevention of localised muscle pressure changes transferring to other regions of the garment.

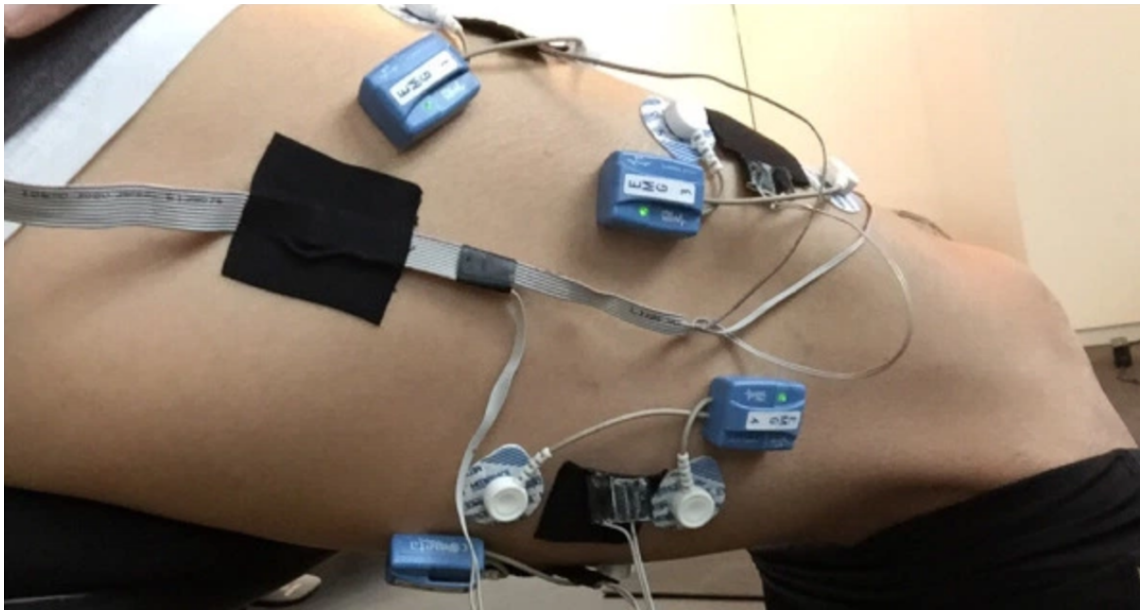

Figure 3.11: Layout of EMG electrodes and Pressure sensors on the upper leg

3.4.3 Calibrating the Dynamic Zero Baseline pressure

With EMG measurements, non-muscular activity exhibits a baseline measurement near constant zero, where a constant offset in the baseline value is easily zeroed. Pressure measurement over the garment however is non-consistent, changing with different participants, garments and limb angles. Therefore an additional consideration when performing muscle pressure measurements was the identification of the dynamic zero baseline pressure of the relaxed muscle at varied limb angles. Whilst during static contraction this pressure remains constant, when the limb angle is altered, the position of the muscle belly mass in relation to the sensor is affected, thus altering the baseline pressure value.

To counter this, at the beginning of every test session a dynamic zero baseline is recorded for each sensor by the external manipulation of the participant's relaxed limb throughout the full angular range of the knee joint. The baseline pressure measurement are then subtracted from the recorded test data for each relevant test according to the respective knee angle, isolating the pressure provided by the active muscular contraction from that of the relaxed muscle.

3.4.4 Conditioning the EMG signal

A key step in the use of Electromyography, is the conditioning methodology utilised in the analysis of the captured signals. The method utilised within this research follows the guidelines proposed by Carlo DeLuca a foremost leading expert and pioneer in the research of EMG [De Luca 1997; Luca 2003]. To counter both low and high frequency noise artefacts a 6th order butterworth bandpass filter was utilised to isolate frequencies between 10-350Hz where muscular activity is present and a full wave rectification performed to the signal.

Figure 3.12: Internal siliconised friction regions ensuring localised garment compression of the quadricep muscles; 2XU MCS compression tights (left), Puma ACTV compression tights (right)

Debate continues within the field of EMG over the most appropriate determination of the EMG signal strength for analysis, significant evidence has led to an industry recommendation that the signal's RMS value shows greatest robustness in reflecting the signal power of the muscle [De Luca 1997]. As such an RMS function was applied to the signal with a sliding window of 0.1 seconds.

3.5 Summary

Initial research into the development of Smart Apparel has yielded positive results into its viability as a muscle diagnostics and injury prevention garment through its novel approach to quantifying muscular exertion and loading. Preliminary testing of the surface pressures between a target muscular group and a compressive elastic garment shows repeatable pressure change that can be measured and normalised to a user's muscular exertion levels, allowing for the real-time feedback of key muscle, ligament and joint loading conditions.

To allow for the capture of the under-garment pressures, material-based pressure sensors have been developed and calibrated to a known industry standard, as well as a methodology introduced for on-body calibration. Advantages and disadvantages of the use of gold-standard techniques in the form of EMG and Motion Capture have been highlighted, with the experimental setup detailed for use in later chapters.

Lastly a biofeedback tool has been developed to assist an individual in mitigating potential injury conditions and further enhance the quantifiable nature of their activity. The research will continue further work into the correlation of the associated movement to that of the known muscle force through inverse dynamics calculations, and also to another forward dynamics system, namely EMG, where direct forces are attributed to the loading of the muscle based upon surface pressure.

II Research Implementation

4. Estimation of Muscle Activity

Published Research

The following chapter contains work published within:

- Belbasis, A., Fuss, F. K. & Sidhu, J. Muscle activity analysis with a smart compression garment. *Procedia Engineering* **112,** 163–168. ISSN: 18777058 [2015]

Compression garments have seen a significant increase in their use within the sporting and fitness domains, both as fashionable sporting attire and as post-activity recovery wear through passive soft-tissue compression. This proliferation has allowed for new opportunities in capturing detailed insights through integration of wearable technology upon the human body via a convenient scaffolding form factor that users are well accustomed to. The establishment of a measurement system in the previous chapter allows the research focus of this chapter to be placed on developing the ability to determine the muscular activity captured through such an instrumented compression garment.

The following work explores the scope of measuring muscle surface pressure in an effort to identify the activity and load conditions present. Specifically, this research section looks at how monitoring the deformation changes on the physical surface of a limb (muscle surface pressure caused by the garment compressing the muscle) can be utilised for quantifying the muscular activity levels, doing so with respect to Surface Electromyography (EMG) the established gold standard within the field. It demonstrates that with increasing loading of the muscles, a corresponding increase in both electrical and mechanical activity is present. Furthermore both measured systems show alignment to the analytical loading model derived from the biomechanics of the lower limb.

4.1 Determining Muscle Activity Patterns

It is clear that as a consequence of the physical deformation of the muscle, pressure between the skin and the compression garment is altered. Inherently, variation of this pressure will be affected by the level of muscular exertion and the position of the sensor in relation to the changing shape of the muscle. Unfortunately both of these factors are instrumental as to whether the occurring pressure change will be positive or negative in direction with respect to the increased muscle activity.

A challenge lies in the correlative association of the this pressure change to the activity of the muscle, and if possible the level of force involved. De Luca (1997; 2003) and Liu *et al.* (2002) each demonstrated using EMG that the measured activation level of the muscle fibres exhibit a non-linear relationship to that of the corresponding forces exerted. This is due in part to the numerous variables conditional on muscle fibre activation, distribution and conditioning, where reliance on an accurate model is difficult to achieve due to the influences of genetic and preconditioning variances within the population. Wininger (2008) however demonstrated that the use of Force Myography (surface muscle pressures) on the proximal forearm can produce sufficiently accurate representation of grip forces when compared to a grip dynamometer from rest to 100% MVIC, with near realtime representation of muscular activity. Noting however that this did not measure the direct force of each muscle, but the resultant output at the grip. Moreover, Yungher *et al.* (2011) measured the surface pressures over the three superficial heads of the quadriceps (RF, VM, VL), with correlation to the EMG behaviour to assess walking gait, highlighting clinical relevancy in surface pressures furthering our understanding of muscle function patterns, however stopped short of determining specific muscle forces.

4.1.1 Experimental Method

To estimate the muscles force patterns in the upper leg an activity was selected where motion, and subsequently the forces produced, could be readily modelled. The selected activity was required to isolate a target muscle (or group) such that resolved forces were associated where possible with the respective muscle of action and no others. To achieve this the basic actions of leg extension and flexion were selected for force derivation, as both of these activities enforced a condition where only the quadriceps or hamstring muscles were activated at any one time. Simple extension or flexion of the knee was performed from a seated (extension, quadriceps loaded) or standing (flexion, hamstrings loaded) position with either an unweighted or weighted shank at the ankle (Figure 4.1).

As the selected activity was one where the desired behaviour of the motion was known it operates as an inverse-dynamic biomechanical approach to determine the muscle forces in the quadriceps and hamstrings. This affords an opportunity to better understand the relationship between the muscle force to that of the corresponding pressure variation experienced above the skin at the muscle's surface. Given that Force Myography (FMG) pressure mapping of the muscles relies upon pressure measurements to infer resultant motion, it functions as a forward-dynamic system, so to assist in validation of results Electromyography (EMG), another forward-dynamic system, was incorporated into the testing.

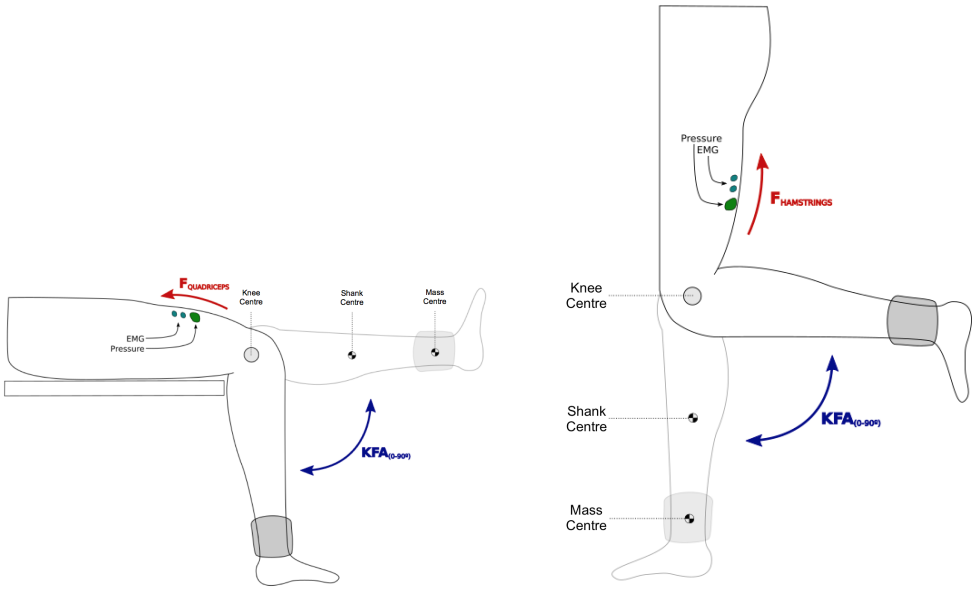

Figure 4.1: Quadriceps driven leg extensions (left) and Hamstring driven leg flexion (right) with weighted shank

Quadricep Extension Test

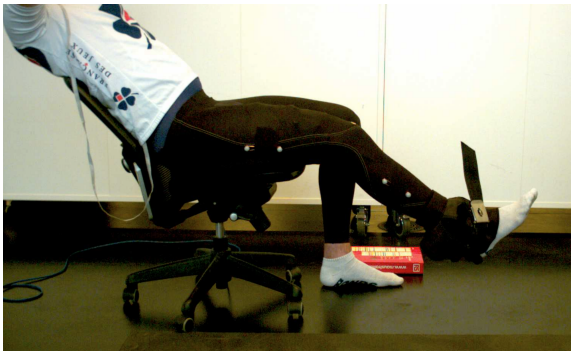

Figure 4.2: Video frame from Quadricep extension testing

Quadricep-driven leg extension was performed from a seated position. A slightly reclined position was used to open the hip joint and enforce full utilisation of the Rectus Femoris muscle. Optional padding was utilised underneath the posterior-distal section of the femur for alignment to the horizontal ($0°$), and the lower leg allowed to freely swing into a resting position ($\sim \theta_{KFA} = 90°$).

Participants were tasked with slowly ($\sim$3-5 seconds each direction) extending the knee joint to full extension ($\sim \theta_{KFA} = 0°$) and then back to a resting position. To prevent overstimulation of the quadricep muscles at maximal extension, participants were instructed not to 'lock-out' their knee, a condition nearing hyperextension which would over-contract the muscles with no additional support to the extension activity.

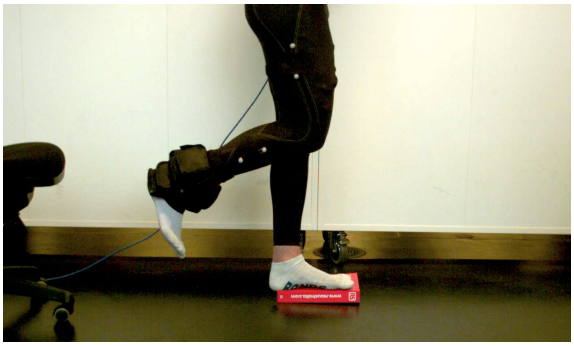

Figure 4.3: Video frame from Hamstring flexion testing

Hamstring Flexion Test

Hamstring-driven leg flexion was performed from a standing position. Participants utilised two points of contact for stability; the wall as a minimal contact support, and a raised platform on the floor for the majority of their bodyweight supported through the left-leg. The raised platform, namely a book, was utilised to allow unrestricted movement of the right-leg from contact with the ground. Additional monitoring was provided by the research team to ensure any hip tilt (in the coronal plane) caused by the raised platform was corrected for by the participant. In this position the leg was allowed to freely swing into a resting position at full extension ($\sim \theta_{KFA} = 0^{\circ}$).

Similarly to the quadricep activity, participants were tasked with slowly (~3-5 seconds each direction) flexing the knee joint to near full flexion ($\sim \theta_{KFA} = 110^{\circ}$) and then back to a resting position. To prevent overstimulation of the hamstring muscles providing additional engagement, participants were instructed not to 'bounce' the weight at the peak of the leg flexion, rather to decelerate and pause and then proceed to extend the knee.

4.1.2 Participants

Six male participants were involved in the testing. This study was granted Ethics approval by the RMIT University Human Ethics Committee (approval no. ASEHAPP 45-15) and adhered to the Declaration of Helsinki. Participants were briefed to the requirements of the test and an informed consent form was filled in by all the participants before the start of the experiment.

4.1.3 Data Collection

A motion capture system (9 Camera - Qualisys Oqus System, Göteborg, Sweden) was utilised to capture the limb segment angles of the participants. The data sampling frequency for motion tracking was set at 100 Hz. The smart compression prototype garment [Belbasis & Fuss 2015; Belbasis, Fuss & Sidhu 2015a,b] was utilised for the testing of each participant. The garment provided capability for measuring and mapping changes in the surface pressure above a muscle where the active movement of the muscle under the compression fabric was detected by a distributed network of pressure sensors. The low-pressure sensors were manufactured from two layers of a conductive piezoresistive polymer, with an almost linear calibration curve of the average equation of $p = 97282000\sigma^{1.184335}$ for 2 layers, where p is the pressure in Pascal, and σ is the conductivity

in Siemens [Fuss 2016]. A sensor was positioned over each of the five thigh muscles (Rectus Femoris, RF; Vasti Medialis and Lateralis, VM & VL; Biceps Femoris, BF; and Semitendinosus, ST) of the participant's right leg.

In addition to the utilisation of pressure sensors, a 16-channel wireless EMG system (Wave Plus Wireless EMG, Cometa Systems, Bareggio, Italy) was used for recording the electrical signal of the same muscles. The general placement of the electrodes followed the recommendations of [SENIAM 1999] and the optimum placement of the electrodes was achieved by using the method of Belbasis, Fuss & Sidhu (2015a).

The raw data of both pressure and EMG signals were recorded in volts and millivolts respectively, at a frequency of 2000 Hz, simultaneously and synchronised with the motion capture data utilising a centralised trigger device. Retroreflective marker on the right upper and lower leg were utilised to determine respective knee flexion angles.

4.1.4 Data Analysis and Statistics

For the muscle activity analysis, the signal amplitude (of FMG pressure and EMG signals) for ± 1.5 standard deviation (removal of outliers) was assigned to the knee flexion angle. The summed output from each muscle group (quadriceps - RF, VM, VL; hamstrings - BF, ST) were summed and normalised. The average amplitude was calculated with a running median filter of a window width of 35 datapoints. Subsequently, the average knee extension/flexion data were normalised across all measurements. In order to calculate the average signal of each muscle across all participants, the data of all participants were averaged, squared (thereby assigning a greater weight to higher data), and normalised once again.

Derivation of Muscle Force

As it is necessary to account for the complexity of forces in the knee joint, a key objective of the analysis was the determination of the resultant moment (rotational force) produced about the knee (M_{Knee})[1]. Earlier derivations by Fuss (1989) on knee joint mechanics were used to estimate the resultant force required of the activated muscles to compensate the moment. Critical to these calculations was the determination of the knee flexion angle (θ_{KF}), measured through the motion capture setup.

Measurements were taken for the length from the knee's rotation centre to the centre of mass of both the shank (x_{leg}), and added weight positioned on the ankle joint (x_{weight}). These parameters allowed for the further calculation of the moment acting about the knee (M_{knee}); a function of the effective moment arm that is dependent on θ_{KF}, and the estimated total combined mass of the leg (m_{leg}) taken based on the participant's measured or calculated body proportions [Contini *et al.*

[1] As with most ongoing research, complimentary streams of research occur in parallel with one another. Derivation of knee-based forces is discussed in further detail within the next chapter, however a subset of the calculations associated with knee forces are utilised here. For greater explanation and expansion on these calculations please see Chapter 5.

1963], and that of the added weight (m_{weight}).

$$M_{leg} = (x_{leg} \times m_{leg}) \cos(\theta_{KF}) \tag{4.1}$$

$$M_{weight} = (x_{weight} \times m_{weight}) \cos(\theta_{KF}) \tag{4.2}$$

$$M_{Knee} = M_{leg} + M_{weight} \tag{4.3}$$

As the patella acts as a force multiplier between the quadriceps tendon and patellar ligament [Fuss 1989], the mechanical advantage of the patella ($MA_{patella}$) at a given θ_{KF}, along with the moment arm of the patellar ligament (x_{PL}), was determined to resolve the knee moment to that of the force produced by the quadriceps (Equation 4.4).

$$F_{Quadriceps} = \frac{M_{Knee}}{MA_{patella} \times x_{PL}} \tag{4.4}$$

Alternatively Equations 4.1-4.4 can be combined to produce Equation 4.5.

$$F_{Quadriceps} = \frac{(x_{leg} m_{leg}) \cos(\theta_{KF}) + (x_{weight} m_{weight}) \cos(\theta_{KF})}{MA_{patella} \times x_{PL}} \tag{4.5}$$

The resultant force produced by the hamstrings through the moment arm of the hamstring tendon (x_{HT}) is also determined (Equation 4.6). The lack of a force multiplier on the posterior side of the joint results in a simplified force equation dividing the applied moment over the force offset distance of the hamstring tendon from the rotation centre of the joint (x_{HT}).

$$F_{Hamstrings} = \frac{M_{Knee}}{x_{HT}} \tag{4.6}$$

The resultant polynomial relationships allow for the calculation of the required force in the quadriceps or the hamstrings with respect to the θ_{KF} (between 0-90°), holding true where no co-contraction of the quadriceps and hamstrings occurs. For example, the force in the quadriceps is solely responsible for the moment about the knee joint when performing quadriceps-only extensions. Conversely the hamstrings responsible for the moment about the knee during flexion. Figure 4.4 utilises both Equations 4.4 (extension) and 4.6 (flexion) to represent the calculated resultant loading curve for an adult male (90kg/180cm) performing the test activities with gradated weighting conditions (0-10kg) of the shank.

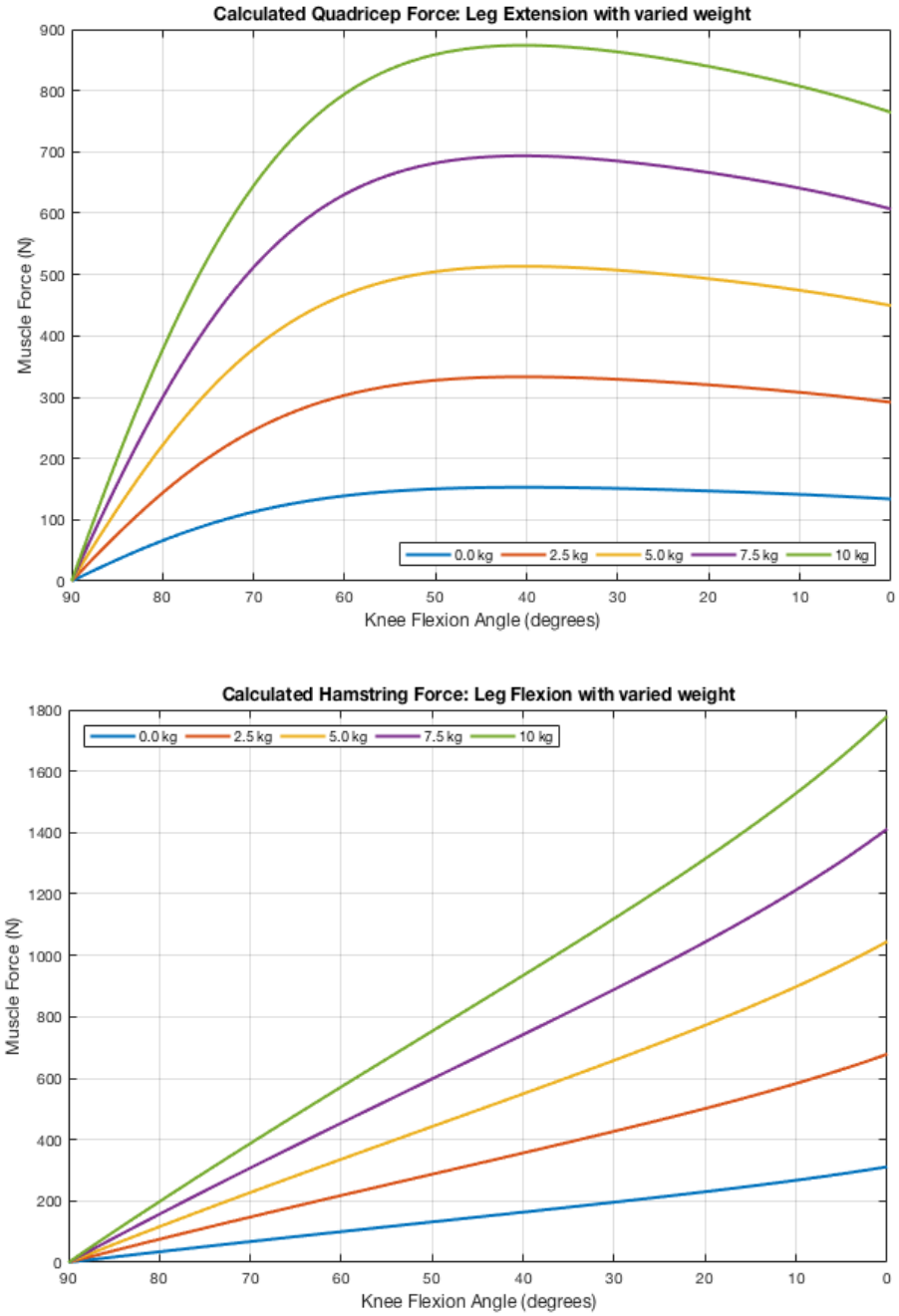

Figure 4.4: Calculated loading curves for quadricep and hamstring extension-flexion exercises

4.2 Discussion of knee extension-flexion results

For the purposes of the study concentric and eccentric movements for the activity were isolated and only concentric movements identified for further analysis. An averaged dataset for each muscle group (Quadriceps and Hamstrings) was taken across all participants, values were normalised between the maximum and minimum range of measured results and plotted against the measured θ_{KFA} for both tests. This allowed for direct comparison of both pressure and EMG signals to that of the calculated force loading of the muscle from the performed activity, the resultant aggregated performance curves are shown below within Figure 4.5.

4.2.1 Quadriceps Extension

Quadricep results demonstrated clear separation of the muscle activity with increasing loading across the extension test for both EMG and FMG pressure measurements, following the calculated biomechanical model. Increases in muscular activity with increasing loads (0, 5, 10kg) applied to the shank was clearly defined in EMG activity throughout the whole range ($\theta_{KF} = 90^\circ \rightarrow 0^\circ$), with near even separation of the three curves as the additional weight was applied. Muscle activity measured through FMG pressure sensing was less consistent over the entire extension range, however clear separation of the three grouped results was demonstrated over a majority of the test extension range ($\theta_{KF} = 85^\circ \rightarrow 22^\circ$), expected reasons for this behaviour at low and high angles will be discussed further below.

Prominent within both EMG and FMG pressure results was the presence of muscle activation prior to the start of the loading ($\theta_{KFA} \geq 90^\circ$), an apparent indication of pre-engagement of the quadricep muscles. Early engagement of the quadriceps at the start of the test was present for several participants and is reflective within the grouped results for both EMG and FMG pressure with apparent muscle engagement (non-zero values) prior to beginning the activity, noticeably higher within the FMG pressure measurements. Possible causes for this behaviour could stem from the following;

- Muscle pre-engagement: Participants activating their quadricep muscles in anticipation of the force required in completing the extension task. The existence of pre-engagement on both EMG and FMG pressure indicates that a portion of this behaviour was not measurement system dependent and indeed is a reflection of muscle engagement (both electrically and mechanically). However without a consistent load to necessitate the engagement of the primary quadriceps, this contractile behaviour could indicate potential crosstalk from the activation of secondary stability-support muscles in the upper leg.
- Incorrect angle measurement: Incorrect alignment of the upper and lower leg motion capture markers would result in the measured angle not representing the true knee flexion angle. This would be consistent across both testing measurements as they were taken simultaneously and the markers were not moved. The low zero value of the 0kg EMG test provides evidence that there is a low possibility this is the cause of the early muscle activation.
- Incorrect zeroed baseline: The noticeable existence of muscle activation of the FMG pressure results could stem from a failure to address correctly the dynamic zero baseline throughout the

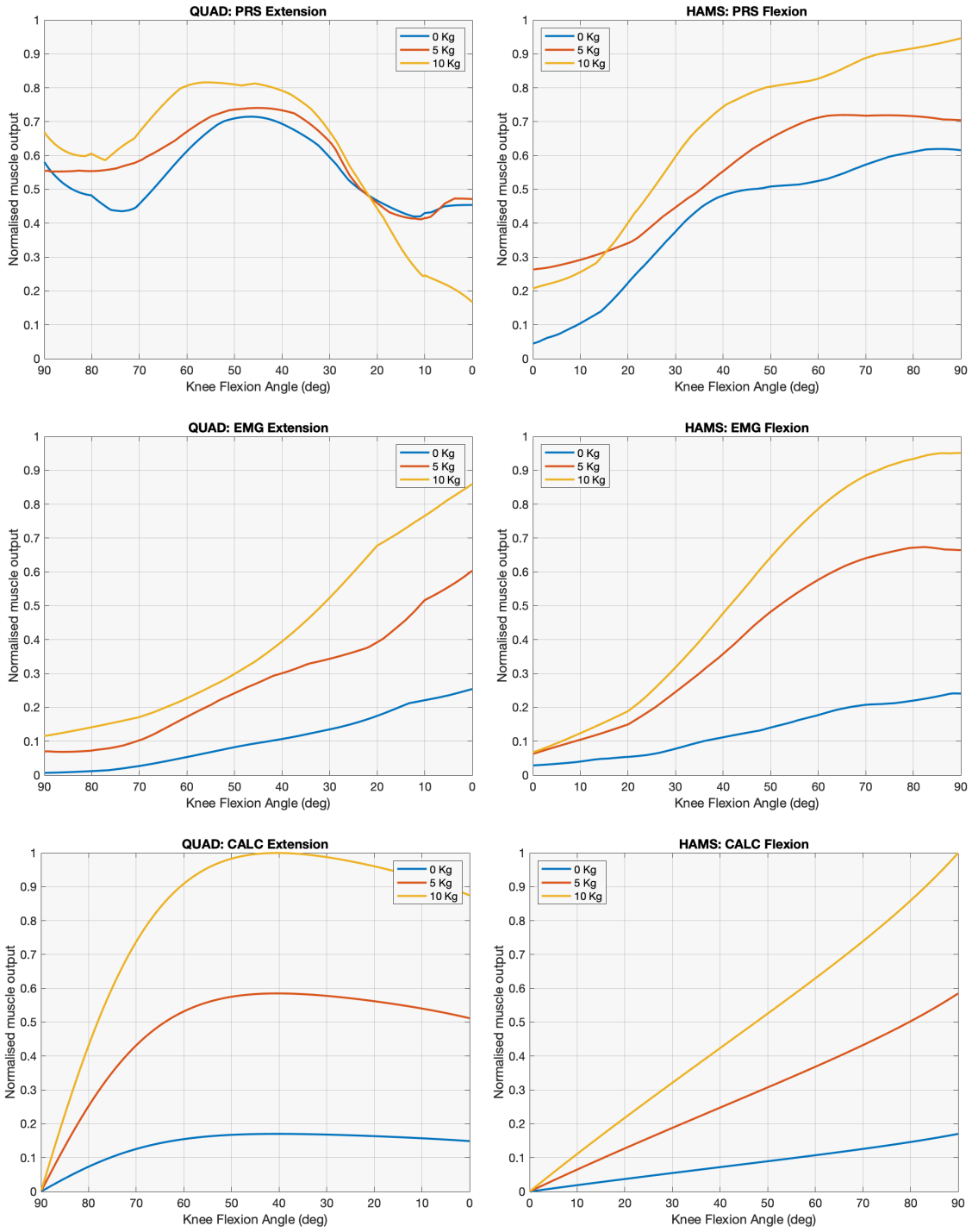

Figure 4.5: Averaged grouped results for extension (left) and flexion (right) tests. Showing measurement differences for FMG pressure (top), EMG (centre) and Calculated (bottom) normalised muscle activity.

range of motion (see Section 3.4.3). Although the research team manually manipulated the leg for the participant whilst monitoring a zero muscle activity state, this external manipulation may not truly demonstrate the pattern exhibited by the muscle under a participant's own action, therefore producing a differing baseline profile. Heightened initial activation of the pressure values over EMG support this, however the existence of these EMG values provides indication that muscle activation was in fact still present and not completely a result of incorrect baseline controls.

- Knee joint complexity: Additional to the early engagement of the muscle, FMG pressure measurements for the 0kg and 10kg tests demonstrated a decline in measured load during the initial 15 degrees ($90-75^\circ$) of the test. It is unclear whether this is due to a free-swinging of the shank during relative low-loading, afforded by the complex structure of the knee joint, or an activation-relaxation behaviour to accelerate the dead-weight of the shank at the beginning of the activity. This engagement of muscle at low angles retracts muscle bulk from directly under the sensor as the muscle stiffens to perform the activity, and as a consequence lowers the apparent muscle measurement.

Future testing will require a more rigorous control of setup and testing to ensure that potential inconsistencies in the experimental process are eliminated and the route cause of this behaviour isolated to determine the biomechanical relevance to the activity.

With higher extension angles the force multiplier afforded by the patella bone reduces the necessary muscle force required, and as such peak loading was expected to occur at approximately midway through the extension activity ($\theta_{KF} \approx 40^\circ$). EMG results did not follow this pattern and demonstrated an increasing trend through to maximal extension before reaching peak loading. This is reflective of the increased muscle fibre activation, not the subsequent mechanical force produced. As FMG measures the mechanical output of the muscle, peak muscle loading for FMG measurements were demonstrative of the patella's force multiplier effect ($\theta_{KF} = 40^\circ - 55^\circ$) before significantly reducing in loading, differing to the theoretical model as an interception of all three pressure values occurs at approximately $\theta_{KFA} = 22^\circ$. From here the 0kg and 5kg tests show uniform behaviour, decreasing to a minima at $\theta_{KF} \approx 12^\circ$. The 10kg test however continues a negative pressure change through to the full extension of the leg ($\theta_{KFA} = 0^\circ$).

This behaviour shows an indication that across all participant the muscle belly has traversed across the pressure sensors (prior to the intercept point at 22°), and sensor measurements of the muscular engagement for the remaining extension have become less sensitive to tracking muscle behaviour. The continued drop of the 10kg results show indication that contraction along the length of the muscle, shortening due to the concentric behaviour, is reducing the measured pressure even though the muscle is still being engaged further as evident in both the EMG result and the calculated biomechanical model.

4.2.2 Hamstring Flexion

Hamstring response across both tests demonstrated clear evidence that muscle loading produced a corresponding increase in the electrical (EMG) and mechanical (FMG) activity of the muscle,

aligning strongly with the biomechanical model. As was with the quadricep extension testing, pre-activation of the muscles was again present, however significantly less so. Interestingly the pre-activation of the hamstring muscles was higher amongst the FMG pressure values for the 5kg test over the 10kg. This could be an artefact as a result of grouping all participants, however from $\theta_{KF} > 15^\circ$ signals follow that of the EMG and Calculated model, and clear separation of the three results demonstrates the clear stepped muscle activity as a result of increasing loads.

The calculated behaviour for the hamstring biomechanical model, whilst near linear, indicates a growing muscle activation as the loaded shank is flexed through to 90 degrees where the moment arm is longest, and thus maximal torque expected about the rotational centre of the knee. Contrary to this, both the EMG and FMG pressure signals demonstrate a plateauing, diminishing behaviour as the higher angles of flexion, seen between $60-70^\circ$, where the muscle activation slows with increasingly higher angles.

Without the complexity of the patella, the flexion activity operates as a simple hinged joint. Knowing that the moment arm hasn't shortened (expected only at angles where $\theta_{KFA} > 90^\circ$), mathematically the source of the diminishing performance must occur as a component of the force produced (see Equation 4.6). Given the fixed loading, and thus constant force, this behaviour must originate as a consequence of the sensor measurement on the hamstring muscles. Thus similar to the observed behaviour of the Quadriceps, due to the gross movement of the muscle belly for both the Biceps Femoris and Semitendinosus over the flexion range, it can be presumed that as a result of the muscle belly moving away from the sensors the corresponding electrical (EMG) and mechanical (FMG) measurements are decreasing and not capturing the true muscle performance (shown in Figure 4.6).

4.2.3 Signal comparison

To explore the similarity in muscle activity responses between each measurement system (EMG, FMG, Calculated) correlation was determined using the Pearson correlation coefficient (R^2) through linear, quadratic and cubic fits. An averaged mean of each R^2 value was taken across each of the respective load (0, 5, 10kg) as to determine a single grouped behaviour, affording better insight into the similarities between the calculated and measured systems. For Quadriceps and Hamstrings these are shown in Tables 4.1 and 4.2 respectively.

Table 4.1: Correlation coefficient (R^2, as percentages) of Quadricep grouped performance of the three results across the activity range of motion

Correlation signals	θ_{KFA} range	Linear	Quadratic	Cubic
Calculated Model to FMG Measurement	$90^\circ \rightarrow 0^\circ$	5.45	16.75	24.56
Calculated Model to EMG Measurement	$90^\circ \rightarrow 0^\circ$	35.42	37.75	39.93
FMG Measurement to EMG Measurement	$90^\circ \rightarrow 0^\circ$	27.82	70.15	86.54

Due to the effects of the patella on the quadricep muscles, it was anticipated that a linear correlation to the calculated model for both systems would be low. This is reflected in the results with both systems showing low linear correlation values (EMG, $R^2 = 0.354$; FMG, $R^2 = 0.055$). Even

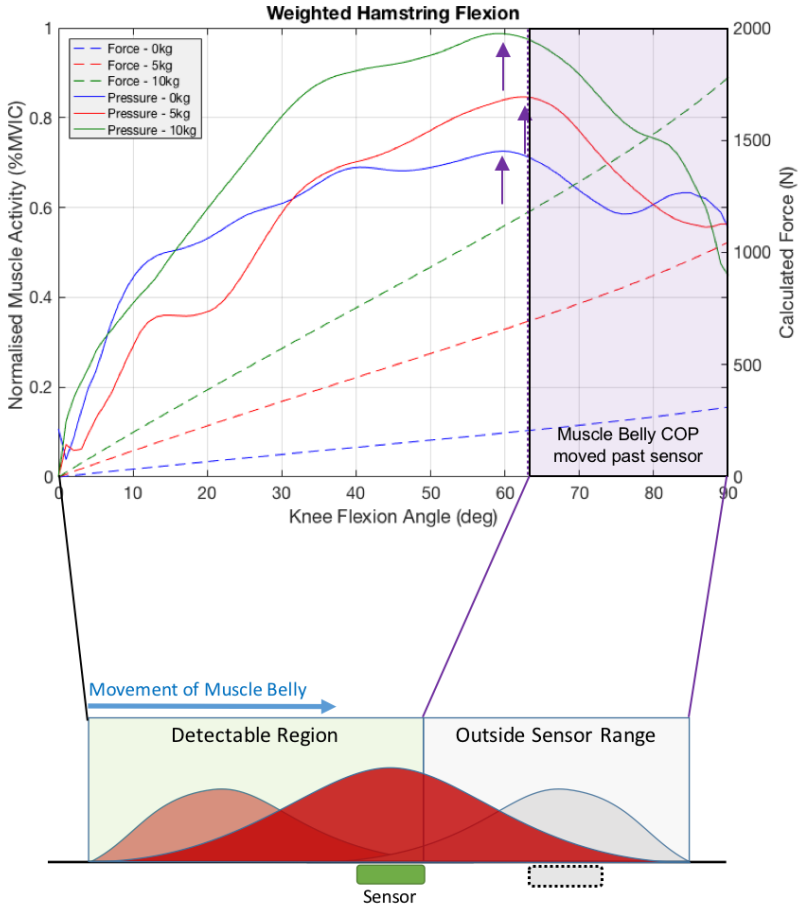

Figure 4.6: Peak muscle loading results demonstrating the implication of longitudinal movement of the muscle belly centre of pressure beyond the range of the pressure sensor.

when considering higher order polynomial quadratic and cubic fits, the correlation does not improve significantly further highlighting the discussion points raised in Section 4.2.1. It was also expected that the two measured systems (both forward-dynamic in nature) would demonstrate higher correlation to one another, however the results demonstrate that unique characteristics centred around the electrical and mechanical loading of the quadriceps differs, and a strong linear relationship between the two does not exist ($R^2 = 0.278$).

Table 4.2: Correlation coefficient (R^2, as percentages) of Hamstring grouped performance of the three results across the activity range of motion

Correlation signals	θ_{KFA} range	Linear	Quadratic	Cubic
Calculated Model to FMG Measurement	$0° \rightarrow 90°$	88.83	97.32	98.32
Calculated Model to EMG Measurement	$0° \rightarrow 90°$	96.95	97.54	99.81
FMG Measurement to EMG Measurement	$0° \rightarrow 90°$	91.28	98.08	99.55

As can be clearly seen within Figure 4.5, Hamstring behaviour across all three systems exhibits similar responses in both magnitude and direction. This is reflective in the strong linear correlation

values found in Table 4.2. The simpler mechanical operation of the joint in flexion results in higher linear correlation of the measured values to the calculated forces (EMG, $R^2 = 0.969$; FMG, $R^2 = 0.888$), and amongst each other (EMG to FMG, $R^2 = 0.913$). Use of higher order fits improves the correlation further with the additional flexibility in accomodating the diminishing performance of the sensors at higher flexion angles.

4.3 Summary

This study explored the measurement of participants conducting defined target muscle activity (leg extension and flexion) whilst recording FMG pressures, EMG and motion capture data. The system was calibrated through voluntary contractions of target muscles, where the surface pressure range and EMG data allowed for the quantification of activity and exertion levels whilst the participant performed leg extension and flexion activities. Each sensor tasked with monitoring mechanical and electrical activity (FMG and EMG respectively), successfully measured a viable range of exertion for each muscle group investigated. The summed data collected from the pressure and EMG signals allowed for confident estimation of normalised muscle exertion levels of participants during the dynamic flexion and extension exercises.

A key investigation of the study was to determine whether measured changes in muscle surface pressure correlate with respect to increases in muscular loading during an activity. Preliminary relationships were drawn between the two forward-dynamic systems (EMG and FMG pressure mapping), with comparison of the measured results to that of the inverse-dynamic analytical approach taken to determine the muscle loads. The analytical model, derived from the biomechanics of the knee joint and upper leg muscles, provided indication that with increases in loading to the shank we can expect higher forces present within the muscles on the upper leg.

Established literature across the field shows that increases in muscle load are reflective in greater electrical activity within a measured EMG signal. This relationship is nonlinear and multiple factors attribute to its shape. This understood behaviour was confirmed within our testing with clear delineation between all measured EMG signals with increases to loading of the shank during flexion and extension activity. Confirmation of muscle activity increase through this forward-dynamic system allowed for the identification of loading behaviour through another forward-dynamic system, measurement of muscle surface pressures.

The key finding from the results was that surface pressure testing demonstrate that it is clearly reflective of increases within the surface pressure of the muscle, demonstrating that increase in additional shank mass is reflected in the normalised muscle activity for both mechanical and electrical activity. Clear stepped separation in the monitored activity was evident across all three 0kg, 5kg and 10kg loading profiles for the grouped results.

There existed separate loading curve profiles for quadricep extension, with understanding that the complexity of the quadricep muscle support functions and force multiplier effect introduced by the patella require further improvement to the testing methodology to better identify grouped muscle behaviour. More consistency across all testing was present within the hamstring muscle group. The results showed increases in electrical and mechanical activity corresponding to loading increases, with the profile of the curve largely showing consistency in shape, and primary growth in amplification as a result of increased weighting applied to the shank.

Additional key findings of the test results was the observable traits in the signals and how these differed between subjects, actions and measurement systems, highlighting limitations in the pro-

posed test setup and methodology. A summary of these observations were presented, with their findings establishing improvements in the design and analysis of further testing methodologies. Critical to the pressure measurement is the need to address the calibration of the garment to that of the range of knee flexion angles. Longitudinal positioning of sensors along the limb is critical for both EMG and FMG sensor measurement due to the movement of the muscle belly during dynamic, large angle movements 'beyond' the sensor placement. This results in lower muscle activity values and does not truly represent the loading condition. Notably in literature this is often overlooked within EMG studies, or commonly mentioned as for future consideration. Capturing the behaviour of the muscle belly as it travels across (and past) the sensor will require further implementation techniques with either additional sensors applied along the longitudinal direction of the muscle, and/or calibration and post-processing corrections.

Further research of the smart garment will look into the relationship of these two measurement systems in greater detail, with a focus upon improved fit accuracy along with the inclusion of a matched biofeedback signal capable of alerting the wearer to the condition of the muscles, such as the loading strain and co-contraction activity. This research continues to show that further development into the smart garment concept promotes an innovative and smart solution for wearable sports technology, aiding in the training, performance assessment and physical welfare of participants in physical activities.

5. Estimating Cruciate Ligament Loads

Published Research

The following chapter contains work published within:

- Belbasis, A., Fuss, F. K. & Sidhu, J. Estimation of cruciate ligament forces via smart compression garments. *Procedia Engineering* **112,** 169–174. ISSN: 18777058 [2015]
- Fuss, F. K. & Belbasis, A. Soft tissue management method and system. *WIPO PCT Patent (filed)* **WO2016065404A1** [May 2016]

Our ability to load the lower limbs during dynamic activity is largely possible by the complex internal support structure of the knee, a network of soft-tissues which allow for multi-directional loading at the full range of the joint. In particular, the dominant anterior and posterior loading forces at the tibial-femoral plane are supported by the Anterior (ACL) and Posterior (PCL) Cruciate Ligaments. With growing participation in both physical activity and the pursuit of personal performance, there is an increasing need to better understand and raise awareness of the loading conditions of the cruciate ligaments, and importantly provide an intuitive understanding to their safe working range whilst in use during an activity.

Within the field of biomechanics loading of the ACL and PCL ligaments are heavily investigated in an effort to further understand the causes of their catastrophic failure. Yet they continue to pose a challenge [Kinney *et al.* 2013] to the research community, where *"The most significant barrier to model-based treatment design is validation of model-based estimates of in vivo contact and muscle forces"* [Fregly *et al.* 2012]. This can be predominately attributed to the encapsulated position they hold within the knee, where the scope of invasive, in-situ measurement is largely unattainable due to the interference with the performed activity of interest [Belbasis, Fuss & Sidhu 2015a].

To counter the limitations of experimental measurement, much research has shifted to the development of controlled modelling simulations to aid in the predictive ability to determine real-time loading conditions [McLean *et al.* 2015]. Fregly *et al.* (2012) highlights the paradox of model-based evaluation of the knee joint, where to accurately determine the validity of the model's output an invasive technique is needed, which in turn is detrimental to true loading measurements of the joint.

5.1 A novel model for fast calculation of cruciate ligament loads

Whilst there exists within literature a high number of prominent developed works and predictive models into calculating internal ligament forces of the knee, the step towards real-time, unrestricted (free-mobility) calculation of loading conditions has been limited [Fregly *et al.* 2012; Kinney *et al.* 2013]. This is especially true where the use of muscle activity analysis through systems such as EMG should be treated with caution [De Luca 1997; Hug 2011] when used outside of the controlled conditions of the experimental setup. This largely is attributed to the overwhelming *unknown forces* present during *unknown activities* a user may perform, and the complexities that arise under these conditions.

A large focus has been placed on honing each specific model for accuracy, where this astute attention to detail results in the model's growth in both complexity and limitation. As a result, the ability for direct application of an early-stage broad implementation within an unconstrained environment is limited. Put simply, within a laboratory testing environment the models hold with high accuracy, but when exposed to unconstrained training environments where an athlete is free to determine the loading nature of the joint, we see a significant drop in predictive performance of these same models.

It is within this scope that the development of a new model is proposed, one that does not intend at its beginning to produce a clinical-level accuracy on the summed internal forces of the knee joint. Rather, to act as a provisional early indication of loading conditions through minimal complexity and non-invasive techniques that are both readily available and easily implemented. In this way the model follows a lateral-thinking approach of developing an improved understanding of the CL forces through early awareness and actionability to their overload or overuse.

5.1.1 Measurement of parameters

Following this lateral mindset, an alternative approach to the mainstay of literature was introduced. The model begins with the consideration of the internal components of the knee joint as a *black box*, a closed system. This allows for the complexity of the joint's soft tissue, range of use and resultant internal forces to be isolated for analysis. A macro view of the loading scenario can therefore be considered. We turn our attention to the loading of the knee from the external forces providing inputs (or outputs) to the joint as a closed system, and the assumption that this blackbox operates as a loss-less[1] system with all forces effectively transferred.

During a common loading scenario, inputs to the joint come in the form of the Ground Reaction Force (F_{GR}) and the subsequent moment produced around the joint's instantaneous centre of rotation (M_K). Outputs are therefore the compensatory muscle reactions to provide a balanced steady state within the joint. These are provided through the two large muscle groups in the upper leg; the Quadriceps and Hamstrings. Therefore much like a balanced equation, the collection of three key parameters critical to the resolution of the cruciate ligament forces are;

[1] Whilst no biomechanical system is truly loss-less, the comparative magnitude of the losses present to that of the loads applied within the knee joint allows for this assumption to hold true.

Quadriceps Force (F_Q) The summed force generated by the four Quadricep muscles; Rectus Femoris, Vastus Medialis, Vastus Lateralis and Vastus Intermedialis. These muscles are largely responsible for the extension of the knee, whilst also providing significant stabilisation support during movement.

Hamstrings Force (F_H) The summed force generated by the Hamstring muscles; Biceps Femoris, Semitendinosus, Semimembranosus. The antagonistic muscle group to the quadriceps, these muscles control flexion of the knee and stabilisation support.

Knee Flexion Angle (θ_{KF}) The flexion angle of the knee; where at full extension of the shank (a straightened leg) $\theta_{KF} = 0°$, and at active maximum flexion (fully bent knee) $\theta_{KF} \approx 140°$. The measured angle is taken along the femoral-tibial line within the sagittal plane.

The proposed model allows for the determination of the above parameters through multiple measurement systems (i.e. EMG, Video, Motion Capture, Force plates), however within the context of this research the FMG and EMG measurement techniques were utilised. This involved the application of the following:

- Pressure sensors at anterior skin surface of the thigh to measure F_Q.
- Pressure sensors at posterior skin surface of the thigh to measure F_H.
- Motion capture system with at least two reflective markers on the lateral skeletal line of the thigh, and at least two reflective markers on the lateral skeletal line of the shank to determine knee flexion angle (θ_{KF}).

5.1.2 Further parameters calculated from Knee Flexion Angle

Earlier research by Fuss (1996) showed that the knee flexion angle governed the relevant parameters of key soft tissues within the knee, not excluding that of the cruciate ligaments. The study involved the dissection and measurement of knee joints from adult male cadavers and showed that key angles and lengths of these soft tissues could be accurately determined with respect to the overall knee angle in the form of derived polynomial functions. Of critical importance to the further calculation of the model, the following parameters are outlined below with respective components listed in Table 5.1.

ACL Angle The angle of the Anterior Cruciate Ligament (θ_{ACL}) with respect to the tibial plateau within the knee joint.

$$\theta_{ACL} = ACL_a + ACL_b(\theta_{KF}) + ACL_c(\theta_{KF})^2 + ACL_d(\theta_{KF})^3 \tag{5.1}$$

PCL Angle The angle of the Posterior Cruciate Ligament (θ_{PCL}) with respect to the tibial plateau within the knee joint.

$$\theta_{PCL} = PCL_a + PCL_b(\theta_{KF}) + PCL_c(\theta_{KF})^2 + PCL_d(\theta_{KF})^3 \tag{5.2}$$

Patellar Ligament Angle The angle of the patellar ligament (θ_{PL}) with a perpendicular to the tibial plateau within the knee joint. At extension of the leg the value is positive, negative

when in flexion.

$$\theta_{PL} = PL_a + PL_b(\theta_{KF}) + PL_c(\theta_{KF})^2 + PL_d(\theta_{KF})^3 \tag{5.3}$$

Hamstring Tendon Angle The averaged angle of the hamstring tendons with a perpendicular to the tibial plateau (θ_{HT}). The coordinate system is taken along the sagittal plane and the posterior direction of the hamstrings, yielding a negative value.

$$\theta_{HT} = HT_a + HT_b(\theta_{KF}) + HT_c(\theta_{KF})^2 + HTL_d(\theta_{KF})^3 \tag{5.4}$$

Mechanical Advantage of Patella The Mechanical Advantage due to the lever arm of the Patella bone (MA_P) and its resultant effects on the force transfer from the quadriceps tendon the the patellar ligament.

$$\begin{aligned} MA_P = \{&MAP_a + MAP_b(\theta_{KF}) + MAP_c(\theta_{KF})^2 + MAP_d(\theta_{KF})^3 \\ &+ MAP_d(\theta_{KF})^4 + MAP_d(\theta_{KF})^5\} \end{aligned} \tag{5.5}$$

Patellar Ligament Moment Arm The moment arm of the Patellar Ligament (L_{PL}), yielding a positive result to the equation.

$$L_{PL} = LPL_a + LPL_b(\theta_{KF}) + LPL_c(\theta_{KF})^2 + LPL_d(\theta_{KF})^3 \tag{5.6}$$

Hamstring Tendon Moment Arm The averaged moment arm of the Hamstring Tendons (L_{HT}), yielding a negative result to the equation.

$$L_{HT} = HT_a + LHT_b(\theta_{KF}) + LHT_c(\theta_{KF})^2 + LHT_d(\theta_{KF})^3 \tag{5.7}$$

Table 5.1: Coefficients for determination of parameters of the knee [Fuss 1996]

Parameter	Coefficient	A	B	C	D	E	F
θ_{ACL}	ACL_n	60.0849	-0.1105	-0.0022	1.1896E-05	-	-
θ_{PCL}	PCL_n	52.0700	-0.1323	0.0042	-1.6752E-05	-	-
θ_{PL}	PL_n	24.1122	-0.09492	-0.0041	2.1612E-05	-	-
θ_{HT}	HT_n	-7.6190	-0.4261	-0.0067	2.4484E-05	-	-
MAP	MAP_n	1.3999	-0.0057	1.0478E-05	-3.8194E-06	5.3082E-08	-1.7975E-10
L_{PL}	LPL_n	5.0003	-0.0122	-8.7046E-05	7.4877E-07	-	-
L_{HT}	LHT_n	-3.0081	-0.0471	0.0003	1.8671E-07	-	-

* Where physical user parameters of: body height = 1.8m, shank height = 0.285m, foot height = 0.039m

5.1.3 Calculation of external force

To continue resolution of the internal forces within the knee, the external loading conditions around the knee joint require calculation. The analytical model continues with the assumption that the applied load balanced between the upper and lower leg at the knee is as of a result of the supporting

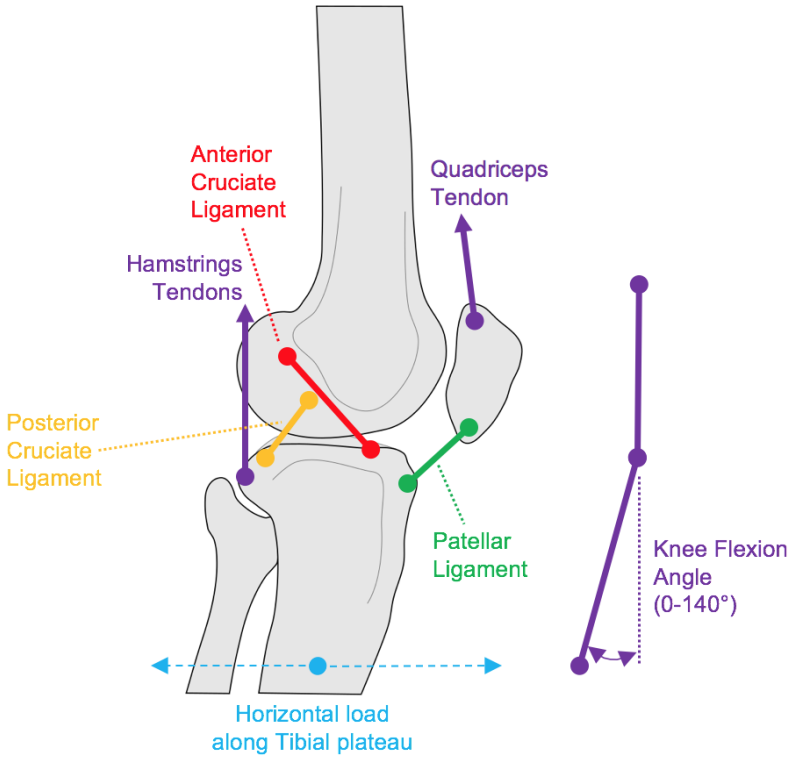

Figure 5.1: Key parameters of the Knee Joint - Angles of ligaments and tendons

forces provided by the quadricep and hamstring muscle groups. The varied loading condition between the two muscle groups is of a result of the given angle of the knee joint.

A loading scenario of the knee is considered during running. Upon the foot strike of a runner's stride, a resultant ground reaction force creates a moment load around the knee joint, requiring the activation of both quadricep and hamstring muscles to stabilise the joint. Whilst other muscles in the lower limb also activated for stability, the antagonistic quadricep-hamstring pair are solely responsible for maintaining and supporting the angle of the knee. Fundamentally to maintain the knee angle, the resultant moment they provide around the instant centre of the knee should be that of equal magnitude to the external moment produced by the ground reaction force.

Moments about the Knee Joint

Combining the force produced by the quadriceps and the mechanical advantage of the patella bone (MA_P), allows for determination of the resultant force (F_{PL}) transferred to the patellar ligament (Equation 5.8). The force multiplier effect of the Patella at varied θ_{KF} is evident at this stage; where at $\theta_{KF} = 90^\circ$ the $MA_P \approx 0.6$, resulting in the F_{PL} loaded 1.67 times higher than the quadriceps force (F_Q).

$$F_{PL} = \frac{F_Q}{MA_P} \tag{5.8}$$

This now permits calculation of the moment about the knee instant centre produced by the quadriceps (M_{PL}) via the patellar ligament. Determination of M_{PL} (Equation 5.9) will always yield a

positive value.

$$M_{PL} = F_{PL} \times L_{PL} \tag{5.9}$$

The force produced by the hamstring muscles (F_H) is also responsible for producing a resultant moment (M_H) about the knee instant center (Equation 5.10). As the L_H is negative due to the coordinate system taken, M_H is also negative.

$$M_H = F_H \times L_H \tag{5.10}$$

The coupling of M_H and M_{PL} determines the overall moment about the knee (M_K). This in turn is balanced by the external moment, the directional sign of which will dictate whether extension (positive) or flexion (negative) of the knee is occurring.

$$M_K = M_{PL} + M_H \tag{5.11}$$

As the M_K is a product of the muscles balancing the ground reaction force (F_{GR}), the horizontal component of the external force (F_{GRx}) is calculated based upon the relative moment arm from the instant center of the knee to the point of ground contact. For this the body height (BH) of the subject is considered where the relative shank length (L_{shank}) and foot height (h_{foot}) are calculated (28.8% and 3.9% of BH respectively) [Contini *et al.* 1963; Drillis *et al.* 1964] or for greater accuracy measured directly.

$$F_{ext} = \frac{M_K}{BH(0.285+0.039)} \quad \text{or} \quad \frac{M_K}{L_{shank}+h_{foot}} \tag{5.12}$$

Ground reaction force error

Alignment of the localised coordinate system is selected so the vertical (y) component of the coordinate system is in-line with the longitudinal length of the tibial bone, and the horizontal (x) component with the tibial plateau. This allows for the simplification of the analysis as ground reactions forces travelling along the y-component are negated as they do not stress the cruciate ligaments. The simplistic model is limited to determining ground contact always at the intersection of the longitudinal axis and the bottom surface of the foot. In this respect it does not currently take into account the additional effects produced by plantar and dorsiflexion of the foot.

The existence of an error due to the unknown point of ground contact, and consequently the changes in moment produced about the knee, limits the accuracy of the proposed model. Further research developments are needed within both the analytical model and the smart garment progress to account for the plantar/dorsi-flexion of the foot as well as the location of impact to determine the additional impact of the F_{GR}.

The model however considers an important biomechanical understanding - internal joint forces (thus ligaments) are largely loaded as a consequence of the muscular forces, not external loads (i.e. ground reaction force). This is due to the comparative length of the moment arms for the muscles to that of the ground reaction force. Knee loading is produced by the external moment about the

knee, a product of the ground reaction force and the length of the shank height. The muscles tasked with balancing these moments rely on significantly smaller moment arms, and as a consequence are required to produce higher compensatory forces.

Horizontal Loads at the Tibial Plateau

The cruciate ligaments support and transfer horizontal loads along the tibial plateau to the distal femoral head, therefore it is necessary to isolate and sum the horizontal (x) components of F_H, F_{PL} and F_{ext} for the net horizontal shank force (Fx_{net}) acting upon the ligaments. For the calculation of the horizontal component of F_{PL} and F_H it is necessary to utilise the angles determined above by Equations 5.3 (positive) and 5.4 (negative). A forward (positive) result for Fx_{net} (Equation 5.15) is compensated by the ACL, whilst a backward (negative) result by the PCL.

$$F_{PLx} = F_{PL}\sin(\theta_{PL}) \tag{5.13}$$

$$F_{Hx} = F_H \sin(\theta_{HT}) \tag{5.14}$$

$$Fx_{net} = F_{PLx} + F_{Hx} + F_{ext} \tag{5.15}$$

5.1.4 Calculation of cruciate ligament forces

Finally the forces within the anterior (F_{ACL}) and posterior (F_{PCL}) cruciate ligaments can be determined through the angles of the individual cruciate ligaments based on the current measured θ_{KF} (equations 5.1 and 5.2).

$$F_{ACL} = \frac{Fx_{net}}{\cos(\theta_{ACL})} \tag{5.16}$$

$$F_{PCL} = \frac{-Fx_{net}}{\cos(\theta_{PCL})} \tag{5.17}$$

As ligament tissue does not provide support under compression and the cruciate (crossed) configuration of the ACL and PCL means they both cannot be under tension at the same time, equations for decision making are required to determine which ligament is under tension. A negative result (denoting compression) in Equations 5.16 and 5.17 is zeroed and only the positive results deemed relevant to the loading conditions.

$$\begin{aligned} &\text{If } Fx_{net} > 0 \text{ (positive) then } F_{ACL} > 0 \text{ and } F_{PCL} = 0 \\ &\text{If } Fx_{net} < 0 \text{ (negative) then } F_{PCL} > 0 \text{ and } F_{ACL} = 0 \end{aligned}$$

Thus mathematically determined:

$$F_{ACL} = H(Fx_{net}) \times \frac{Fx_{net}}{\cos(\theta_{ACL})} \tag{5.18}$$

$$F_{PCL} = [H(Fx_{net}) - 1] \times \frac{Fx_{net}}{\cos(\theta_{PCL})} \tag{5.19}$$

Where H denotes the Heaviside function (unit step function); and $sgn()$ denotes the sign function.

$$H(x) = \frac{sgn(x)+1}{2} \tag{5.20}$$

Published Research

The preceding methodology has been successfully filed as an international patent:

- Fuss, F. K. & Belbasis, A. Soft tissue management method and system. *WIPO PCT Patent (filed)* **WO2016065404A1** [May 2016]

International filing within the following domains:

- Australia
- United States
- China
- Europe
- New Zealand
- Canada
- Japan

5.2 Cruciate Loading: Static Testing

To evaluate the function of the proposed model, static loading tests of the cruciate ligaments were conducted utilising the Smart garment to measure both muscle surface pressure changes (FMG) and muscle electrical activity (EMG). The tests were designed to alternatively strain either the ACL or PCL ligaments under specific muscle activation and knee flexion angles. In total, four tests were conducted where the θ_{KF} was held constant and the muscles of the Quadriceps and/or Hamstrings activated maximally to extend or flex the knee against a stationary anchor at maximal voluntary isometric contraction (MVIC).

5.2.1 Testing Procedure

The MVIC was used as a means of normalising the force in the muscle with respect to both systems of measurement. The tests were designed to selectively load either one of the cruciate ligaments maximally; test 1 loaded only the ACL at maximal extension, tests 2 & 3b the PCL at full flexion and 90 degrees (respectively), and test 3a loading of neither cruciate ligaments (provided no hamstring co-contraction occurred) at a 90 degree flexion angle. A summary of the testing conditions is shown within Table 5.2.

Table 5.2: Ligament load testing conditions

Test	Knee Flexion	Active Muscle	Action	Ligament Load
1	5°	Quadriceps	Full Extension	Maximal ACL
2	138°	Quadriceps	Full Extension	Maximal PCL
3a	90°	Quadriceps	Full Extension	None
3b	90°	Hamstrings	Full Flexion	Maximal PCL

5.2.2 Calculating Knee Ligament Loading

The calculation of cruciate ligament forces was achieved by extending Fuss' inverse-dynamic method [Fuss 1989] to a forward-dynamic one as described within the model above. Through the measurement of the knee flexion angle (θ_{KF}) several key parameters could be derived to determine critical soft tissue conditions within the knee joint (see Table 5.3). Measured θ_{KF} values allowed for the average angles (relative to the normal of the tibial plateau) of the ACL (θ_{ACL}), PCL (θ_{PCL}), patellar ligament (θ_{PL}) and average hamstring tendons (θ_{HT}) to be calculated. Furthermore, the θ_{KF} was utilised to determine the mechanical advantage created by the patella (MA_P), and the respective moment arms of both the patellar ligament (L_{PL}) and hamstring tendons (L_{HT}).

5.2.3 Results and Discussion

The data for the static cruciate loading was compared across all tests, with specific focus placed upon matching calculated loading conditions (shown within Table 5.2) with that of outputs from the SCG. The outcomes for all four tests, for both Pressure and EMG measurements, were processed through the presented mathematical model and the relationship of each system inferred from the muscle activity to the resultant ligament loads.

Results for all the tests (1, 2, 3a, & 3b) showed strong correlations (R^2) values of 0.7812, 0.8129,

Table 5.3: Soft tissue parameters based on knee flexion angle [Belbasis, Fuss & Sidhu 2015a]

Parameter		5°	90°	138°
ACL angle	θ_{ACL}	59.5°	40.9°	34.1°
PCL angle	θ_{PCL}	51.5°	61.9°	69.7°
Patellar ligament angle	θ_{PL}	23.5°	−1.8°	−10.0°
Hamstring tendon angle	θ_{HT}	−9.9°	−82.7°	−130.4°
Mechanical advantage of patella	MA_P	1.37	0.61	1.03
Patellar ligament moment arm	L_{PL}	49mm	37mm	36mm
Hamstring tendon moment arm	L_{HT}	32mm	46mm	31mm

0.8422, 0.8722 respectively between both pressure and EMG signals for each test, further confirming evidence that muscle electrical activity correlates to that of surface pressure changes of the active muscle group.

Test 1: Leg extension at $\theta_{KF} = 5°$

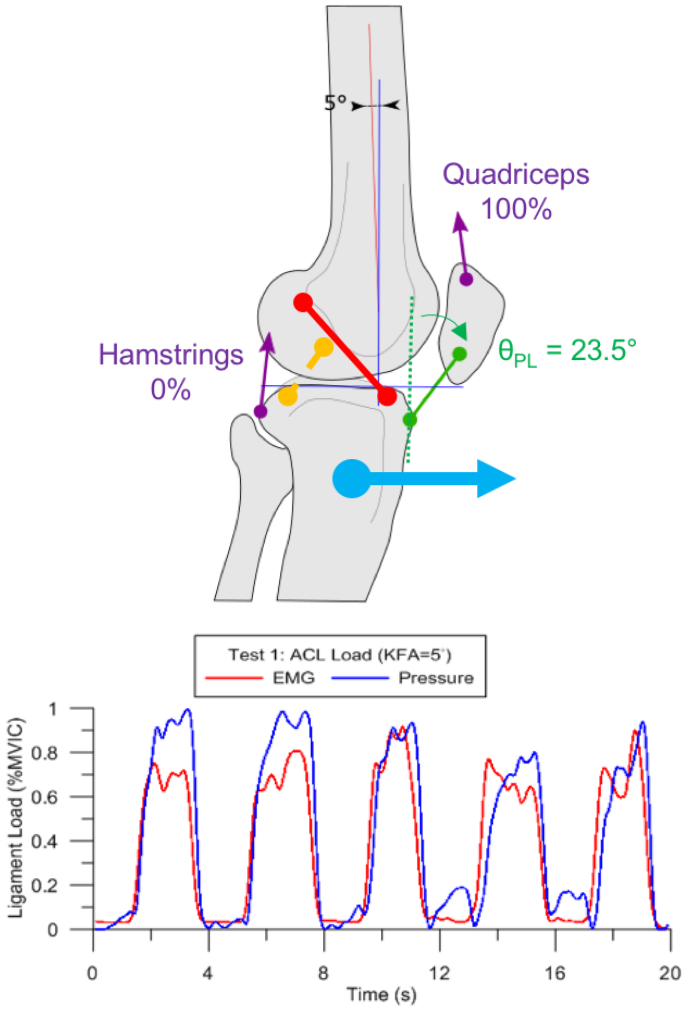

Figure 5.2: Test 1: ACL loading at $\theta_{KF} = 5°$

Whilst at full extension, the patellar ligament is drawn forward by the patella ($\theta_{PL} = 23.5°$), and subsequent loading forces from the quadriceps produce a mixture of Fx_{net} and Fy_{net} loads (see Figure 5.2). Test 1 specifically assesses this condition, where at close to full extension ($\theta_{KF} = 5°$) the contraction of the quadriceps to extend the leg fully produces a positive Fx_{net} load, compensated solely by the ACL.

Extension of the leg does not utilise the hamstring muscle group, however should inadvertent activation of the hamstring muscles occur, the angle of the hamstring tendons ($\theta_{HT} = -9.9°$) produces additional positive Fx_{net} loads, as well as significant Fy_{net} loads. This action is detrimental to the intended task with the antagonistic action reducing the quadricep extension force, whilst also producing an unnecessary increase in the summed ACL load.

Test 2: Leg extension at $\theta_{KF} = 138°$

When the leg is at near full flexion ($\approx 138°$) the patella draws the Patellar Ligament rearward ($\theta_{PL} = -10.0°$). This ensures any resultant activation of the quadricep muscles performing a

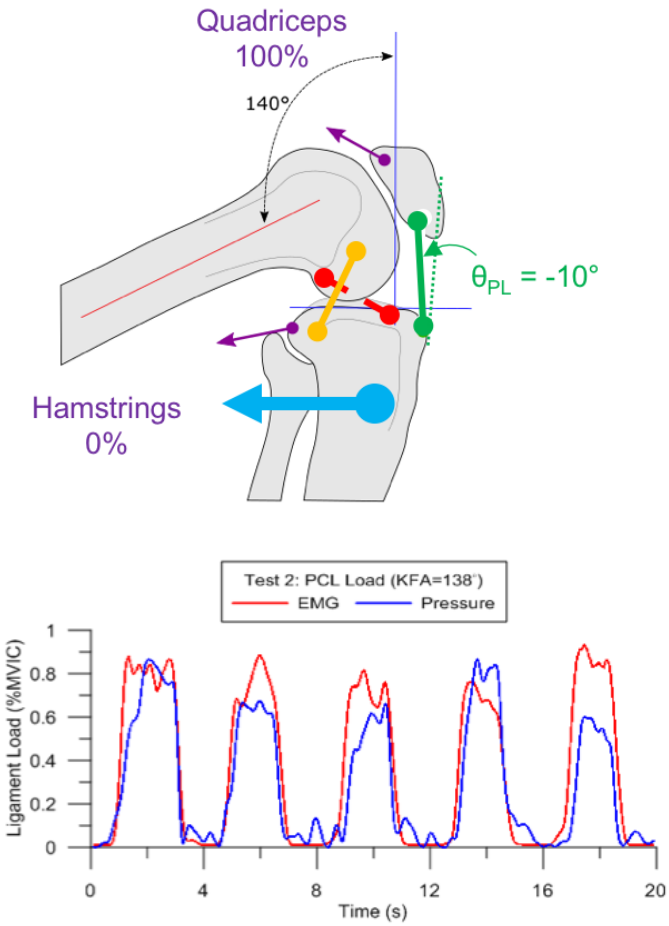

Figure 5.3: Test 2: PCL loading at $\theta_{KF} = 138°$

leg extension creates a negative Fx_{net} force, thus loading the PCL. Similarly as with test 1, any activation of the hamstring muscle group is unnecessary and detrimental to the intended leg extension as $\theta_{HT} = -130.4°$, where co-contraction of the antagonistic muscle group produces significant additional Fx_{net} loading to the tibial plateau, thus transferring additional loading to the PCL.

Test 3: Leg extension (3a) and flexion (3b) at $\theta_{KF} = 90°$

Test 3 evaluates the effect of quadricep and hamstring activity when the knee is positioned at 90 degrees. At this angle the patellar ligament is closely aligned with the normal to the tibial plateau ($\theta_{PL} = -1.8°$), and there exists only a small resultant Fx_{net} produced by quadriceps activity. As such, horizontal net force is provided through the activation of the hamstrings muscles, as the hamstring tendon is almost parallel to the tibial plateau ($\theta_{HT} = -82.7°$).

Furthermore when at $\theta_{KF} = 90°$, the mechanical advantage of the patella is at its lowest ($MA_P = 0.61$) and plays a significant role in the internal joint forces. Loads transferred from the quadricep tendon to the patellar ligament are increased by 1.67 times through the lever-effect of the patella bone. This results in any quadricep activity (even at the reduced θ_{PL} value) amplified in its effects on the cruciate ligaments.

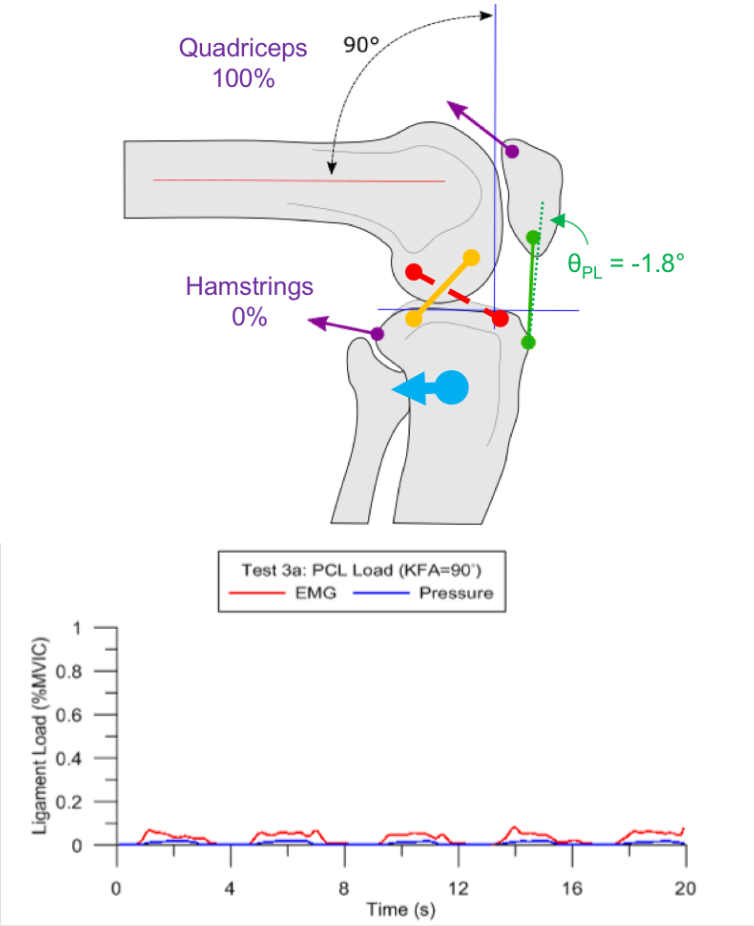

Figure 5.4: Test 3a: PCL loading at $\theta_{KF} = 90°$

Test 3a evaluates the resultant CL loading through quadricep-driven leg extension at $\theta_{KF} = 90°$. As both θ_{PL} and θ_{HT} are negative angles, any loading from either the quadriceps or hamstrings results in a posterior force transfer to the tibial plateau; stressing the PCL. This is evident in the results of Test 3a where the PCL is minimally stressed through inadvertent hamstring co-contraction activity (confirmed through EMG activity) whilst the quadriceps is used maximally to extend the knee.

Test 3b evaluates the resultant CL loading through hamstring-driven leg flexion at $\theta_{KF} = 90°$. When the hamstring muscles are activated to further flex the knee, the PCL becomes maximally stressed, this relationship is clearly shown in Figure 5.5. As with test 3a, co-contraction of the quadriceps only increases the PCL loading, however the effect of which is minimal due to the alignment of the patellar ligament.

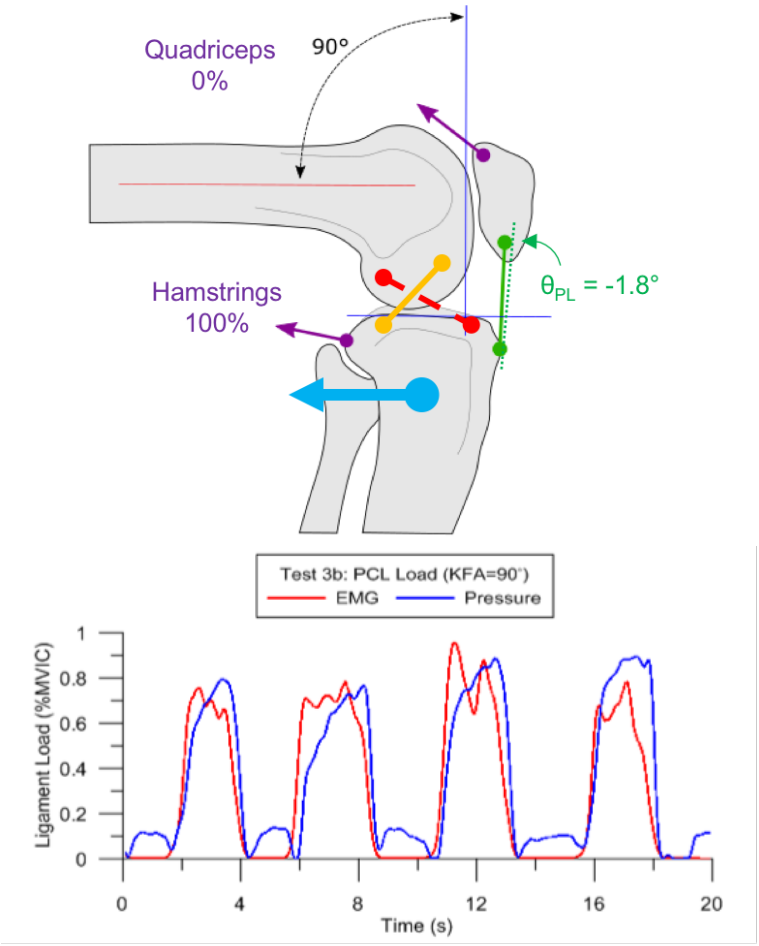

Figure 5.5: Test 3b: PCL loading at $\theta_{KF} = 90°$

5.3 Summary

The utilisation of a smart compression garment and the proposed model functions as a new approach at creating a wearable system capable of assessing active muscle loading, knee ligament strain and co-contraction of paired muscles in a real-time capacity during physical activity. The mathematical approach presented allows for the calculation of cruciate ligaments loads through the knowledge of the forces in the lower leg, and the respective angle of the knee.

Preliminary research shows that the selective loading of the cruciate ligaments by both varied muscle activation and knee flexion angle can be calculated by measuring both the electrical activity within the muscle, and the subsequent surface pressure variations under a compression garment as the muscle contracts to apply a force. As with all models developed for internal knee loading, further testing is required to improve accuracy and reliability of the proposed model, however as presented the model provides an informative view of the loading conditions within the knee within a realtime capacity, specifically driving a focus to allowing use within an open free-activity environment. A limitation of this work is the difficulty in determining the accuracy of the model using both EMG and FMG. Further work is required to benchmark the performance of this novel model against other models within literature to aid in avoiding the danger of highly correlated, yet incorrect model predictions.

Continued development of not only the smart garment but also the associated information processing and calculation methods allows for the real-time monitoring of an individual's CL loading forces, providing metrics for improved exercise performance and safety. The development of this novel method is critically necessary to overcome the limitations of lab-focused monitoring, which although providing high accuracy of the knee mechanics, do not allow for a broad range of loading conditions and activity monitoring of the joint significantly affecting their usefulness and applicability.

6. Testing for Muscle Activity and Fatigue

Published Research

The following chapter contains work published within:

- Belbasis, A. & Fuss, F. K. Muscle performance investigated with a novel smart compression garment based on pressure sensor force myography and its validation against emg. *Frontiers in Physiology* **9** [2018]
- Fuss, F. K., Belbasis, A., Sidhu, J., *et al. Fractal dimension analysis of muscle fatigue with muscle surface pressure measured via compression garments* in *Proceedings of ICSST 2016, 2nd International Conference in Sports Science and Technology* [Nanyang Technological University, Singapore, 2016]

In recent years, cycling has grown into one of the world's most popular exercise activities, with active participation for a number of purposes; from general exercise, a means for transportation, to racing both on- and off-road. Along with the growth in participant number, there exists a corresponding growth in the number of injuries sustained within the sport.

While cycling is traditionally considered a low impact sport and has been suggested as a therapeutic activity with use in rehabilitation [Fleming *et al.* 1999], the considerable time spent on the bike, both in training and racing (upwards of 3 hours and often more than 5) and the repetitive nature of pedalling leads to unique patterns of overuse injury within the sport. Up to 85% of cyclists reported one or more non-contact, overuse injuries and 30% requiring medical intervention [Kim *et al.* 2006; Wilber *et al.* 1995]. Where one of the most common sites for overuse injury (41.7%) was that of the knee joint [Holmes *et al.* 1994].

There are two major causes for knee injury in cyclists, the first is that muscle fatigue produces changes in pedalling technique and leads to stress and imbalances in the kinetic chain [Asplund & St Pierre 2004]. The second major cause is an overdevelopment of the knee flexors. The pedal cycle has been extensively studied, and there are several models that describe the lower limb biomechanics [Raasch *et al.* 1997; Thelen *et al.* 2003; Zajac 2002]. The prime drivers for generating energy in the pedal cycle are the knee extensor muscle group (Rectus Femoris, Vastus Medialis

& Vastus Lateralis) [Zajac 2002], and so many cyclists focus their training on these muscles, this however may increase their risk of knee injury [Raasch *et al.* 1997] through muscle fatigue caused by overtraining and overuse.

This chapter explores the evaluation of muscle fatigue during a controlled exhaustive cycling activity through the measurement of an athlete's muscular and biomechanical performance. The test structure implemented enforces a fatigue condition on the participant, providing a means to collect muscle performance data under the known conditions of non-fatigued and fatigued states. Established fatigue measurement techniques include both analysis of the changes in the muscular firing patterns (EMG) and the changes in the athletes muscular surface pressure during the activity as they fatigue.

6.1 Changes in activation timing of the muscle

The use of FMG pressure readings for detection and measurement of muscle activation patterns during activity is a key technique discussed within Chapter 3 and further explored in Chapter 4. With the additional motion capture of the pedal stroke movement, muscle activity can be resolved to the corresponding angle of the crank where each individual muscle was utilised.

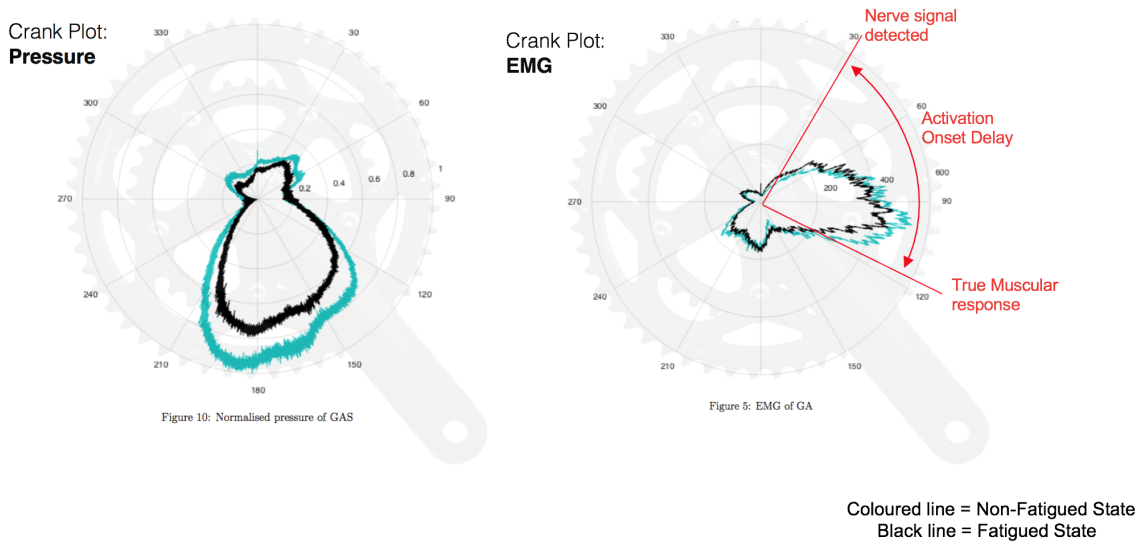

Figure 6.1: Gastrocnemius activation onset differences highlighted in the timing between Pressure (left) and EMG (right) measurements at a cadence of 92 rpm [Fuss, Belbasis, Sidhu, *et al.* 2016]

Utilisation of a polar representation of the EMG and FMG pressure signals aids the intuitive understanding of the muscle activation throughout the 360 degree pedal stroke. Figure 6.1 shows both the non-fatigued (coloured) and subsequently fatigued (black) states of the muscle after performing the exhaustive second test. This visual furthers an understanding of how the muscle is activated throughout the pedal stroke, along with displaying some insight into the affect fatigue has on the muscle behaviour and performance across two differing measurement techniques.

6.1.1 Electromechanical delay of the muscle

It can be seen above that the maxima of the polar plots for EMG and FMG pressure do not coincide (Figure 6.1), the phase shift of which reflects the fact that the activation onset of the EMG signal precedes the increasing muscle force [De Luca 1997]. Essentially, EMG measurements are reflective of the electrical (nerve) activity within the muscle, not the (later) force generating physical response which tends to be the desired measurement objective, as demonstrated by Cavanagh & Komi (1979) in Figure 6.2.

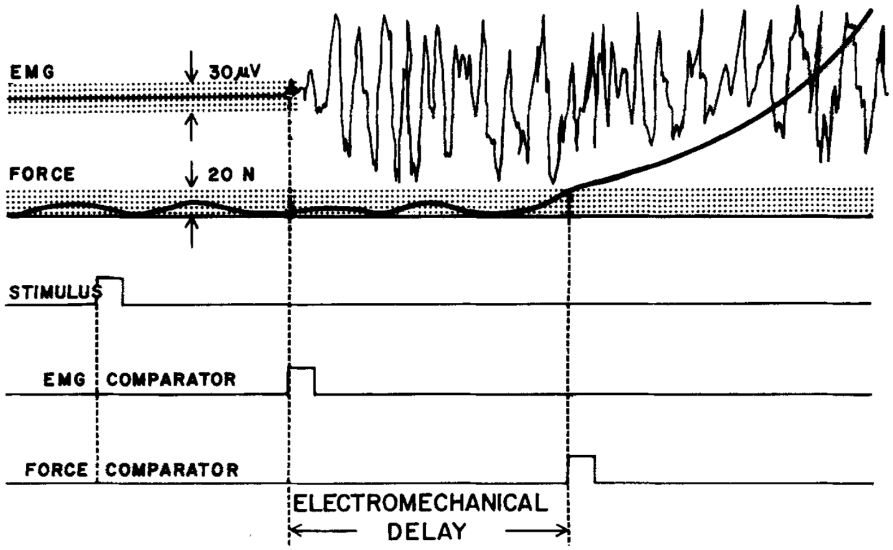

Figure 6.2: Electromechanical delay between the EMG signal and the produced muscle force [Cavanagh & Komi 1979]

This electromechanical delay phenomenon poses a significant issue when observing EMG behaviour during high speed activity such as cycling. Due to the increased frequency of muscle activation, higher cadence speeds result in greater angular deviation of the measured EMG signal (see Figure 6.3). Although activation onset durations differ by both subject and muscle, research has shown most fall within a range of 30-100ms [Cavanagh & Komi 1979].

Therefore, taking this onset delay range and the mean cadence of Session 2 results from further in this chapter (73 RPM), the observable muscle activation response will precede the physical response by between 19-64 degrees. If this deviation is not accounted for, significant misrepresentation of the data is possible. However due to physiological differences between individual muscles, the onset latency of the muscle is often difficult to ascertain [Cavanagh & Komi 1979], particularly during cycling [L. Li & Baum 2004], and thus difficult to accurately correct for at these higher activation rates and across different participants.

Alternatively, the measurement of muscle pressure through FMG is a direct analysis of the muscle's physical state change due to mechanical activity. With this technique an onset delay largely only exists in two forms; through the electro-mechanical response of the sensor (a negligible delay), and the mechanical response of the muscle in relation to the sensor position.

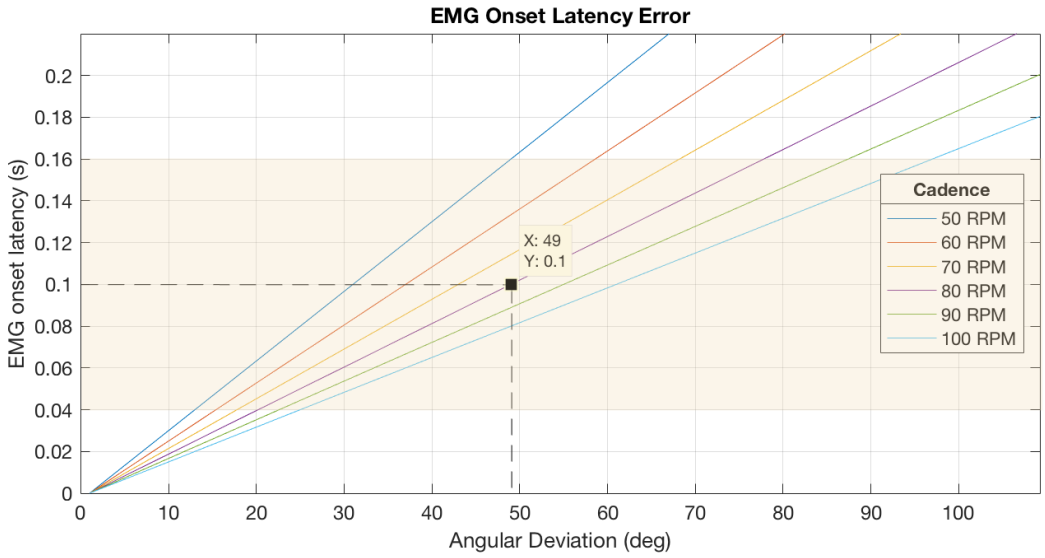

Figure 6.3: Angular deviation impact of EMG muscle activation onset delay at increasing cycling cadence speeds

Provided the pressure sensor is positioned above the muscle belly at the time of initial activation, the sensor response and thus recorded muscle activation timing is a true representation of the muscle mechanical behaviour during the activity. This gives further support to the analysis of the muscle force with FMG surface pressure as a possible alternative technique when knowledge of real-time activation behaviour is key to the analysis.

6.2 Methodology

6.2.1 Experimental method

A fatigue-inducing regiment based upon work by Dorel *et al.* (2009) was utilised to quantify the effects of fatigue during cycling. The test protocol deliberately introduced fatigue to the active muscles, allowing for the analysis of muscle activity and performance under two known definitive conditions, namely a non-fatigued and fatigued state. To allow for sufficient muscle recovery, participants were asked to follow the following testing procedures over two testing sessions which were separated by at least four recovery days.

The tests were performed on the participant's own bicycle mounted on the stationary ergometer (Wahoo Kickr, Wahoo Fitness USA). To ensure that muscles were activated during the upstroke of the pedal phase (180°-360° of the crank cycle) clip-in shoe/pedal combinations or caged pedals were utilised to prevent separation of the foot and pedal.

Session One: FTP Ramp Test

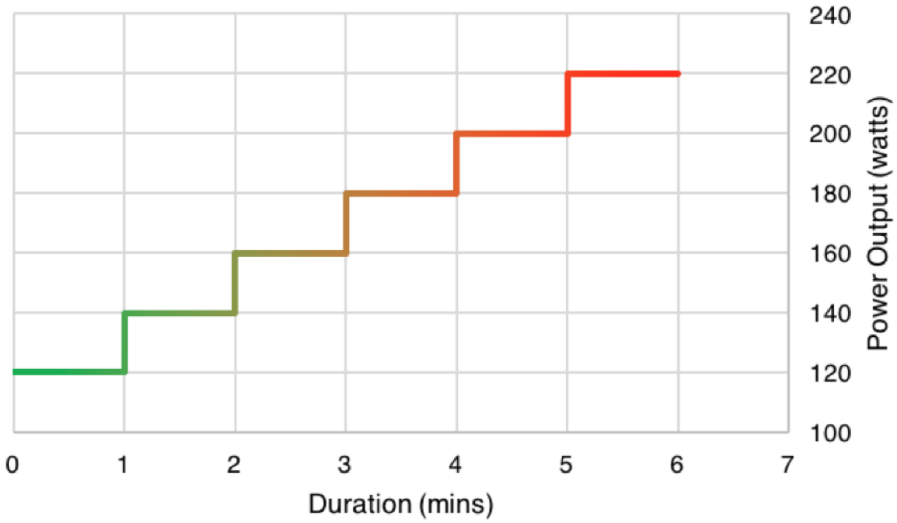

Figure 6.4: Example of proposed testing power profile for Session 1: Incremental power test reaching FTP = 220W after 6 minutes

Each participant was tasked with completing an incremental cycling exercise (Ramp test). This involved the incremental ramp-up of generated power to determine the exercise limitations of the participant. Other than a heart-rate strap for ensuring safety of participants, no instrumentation of the participant's body was necessary for this session. All testing begun at a target power output of 120 Watts with increasing workload increments of 20 W/min until the target power could no longer be satisfactorily sustained.

To ensure consistent power output during the test the ERG-mode setting of the Wahoo Kickr ergometer was utilised. This setting constantly monitors the generated power and cadence (angular velocity), and enforces a consistent target power output through automatic adjustments to the cycling resistance level (torque) through a magnetic actuator.

To prevent artificially enforcing an earlier end to the test, reasonable changes in both cadence and gearing were permitted for the participant to find their comfort zone to complete the task. The Functional Threshold Power (FTP), defined as the last stage that was completed in its entirety, was used to calculate the appropriate workload imposed by the cycle ergometer during the second test session.

Session Two: 80% FTP Fatigue Test

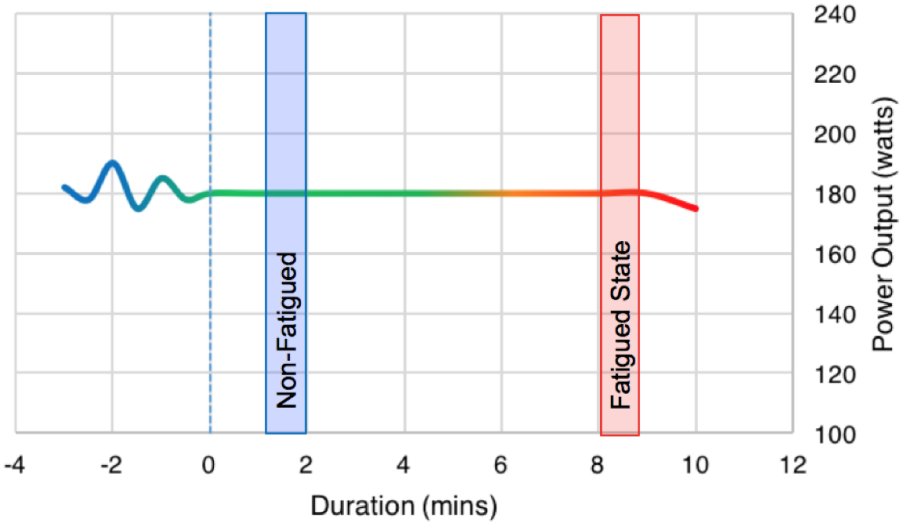

Figure 6.5: Example of proposed testing power profile for Session 2: Induced fatigue test set at 80% FTP = 176W.

The second session, notably the primary data collection session, involved the complete instrumentation of the participant's right upper leg with EMG, Motion capture and FMG pressure sensor equipment. Participants performed a self-directed warm-up routine consisting of at least 3 minutes of cycling at a lower power output to the test condition, ensuring sufficient preparation of the participant for the test. Following the warm-up, subjects performed a cycling exercise at a constant power output equating to 80% of their measured FTP for as long as physically maintainable. The ergometer was set at a fixed resistance setting and the participant instructed to maintain the two target parameters displayed to them; the target power output (80% FTP), and a constant cadence freely adopted from the end of the warm-up session. FMG surface muscle pressures, EMG activity and angular parameters were recorded continuously throughout the session.

To enforce repetitive muscle activation, participants were asked to maintain a single cycling position, where shifting along the saddle or handlebars was not allowed. The test continued until the cyclists voluntarily chose to stop the exercise (fatigue-induced exhaustion) or until they were no longer able to maintain their initial test cadence ($\pm$5 rpm), which was considered as a failure to maintain the required task (the target power output at a constant cadence).

6.2.2 Data Analysis and Statistics

The raw data of both FMG pressure and EMG signals were recorded in volts and millivolts respectively, at a frequency of 2000 Hz, simultaneously and synchronised with the motion capture

data utilising a centralised trigger device. Utilising the retroreflective marker on the right pedal, the top dead centre of the crank (highest marker position) was set as zero position (0°) with positive increases in crank angle in the clockwise direction as viewed from right-hand side of the bicycle.

For the muscle activity analysis, the signal amplitude (of FMG and EMG signals) for ± 1.5 standard deviation (removal of outliers) was assigned to the crank angle. The average amplitude was calculated with a running median filter of a window width of 7.5 degrees. Subsequently, the average crank cycle data were normalised across all measurements. In order to calculate the average signal of each muscle across all 7 participants, the data of all participants were averaged, squared (thereby assigning a greater weight to higher data), and normalised once again.

It was anticipated that both the performance limiting affect of fatigue and the mechanical/electrical nature of both FMG and EMG measurement systems respectively would have an observable impact on the radial activation behaviour of the muscles. Unlike the electromechanical onset delay within EMG measurement, fatigue can influence activation behaviour in both earlier and later timing to that of the non-fatigued state. For these reasons the calculation of the average crank angle was determined for each muscle as the angle that divides the areas under the signal into two equal parts (integration window = 180°). The average crank angle represents the position of the activated muscle on the crank diagram as a single number for comparative purposes.

Finally, the angular phase shift of the Fatigued and Non-Fatigued conditions are compared to determine the respective movement as a factor of the introduced fatigue; the radial phase shift angle ($\Delta\theta$). A positive value reflective of a delayed activation by the muscle, or conversely a negative value representative of earlier activation during the pedal stroke.

6.2.3 Participants

Seven male participants (age: 28 ± 3.6 yrs; body height: 1.751 ± 0.059 m; body mass: 78.7 ± 7.9 kg) were involved in the testing. This study was granted Ethics approval by the RMIT University Human Ethics Committee (approval no. ASEHAPP 45-15) and adhered to the Declaration of Helsinki. Participants were briefed to the requirements of the test and an informed consent form was filled in by all the participants before the start of the experiment.

All participants were deemed healthy volunteers, passing the health and fitness requirements for ethics committee approval for to sustain the level of exertion required during the testing procedures. All participants were of above-average levels of fitness, regularly participating in various sports such as running (participant 1 and 5), soccer (2 and 4) and cycling (3,6 and 7) at least 3 times a week, where their typical training sessions would meet or exceed the physical requirements of the testing. The overall cycling skill ranged from an Amateur cyclist (participant 2), through to Semi-elite cyclists (participants 3 and 7).

6.2.4 Data Collection

A 9-camera motion capture system (Qualisys Oqus System, Göteborg, Sweden) was utilised to capture the limb segment angles of the participants, as well as providing tracking for the rotational

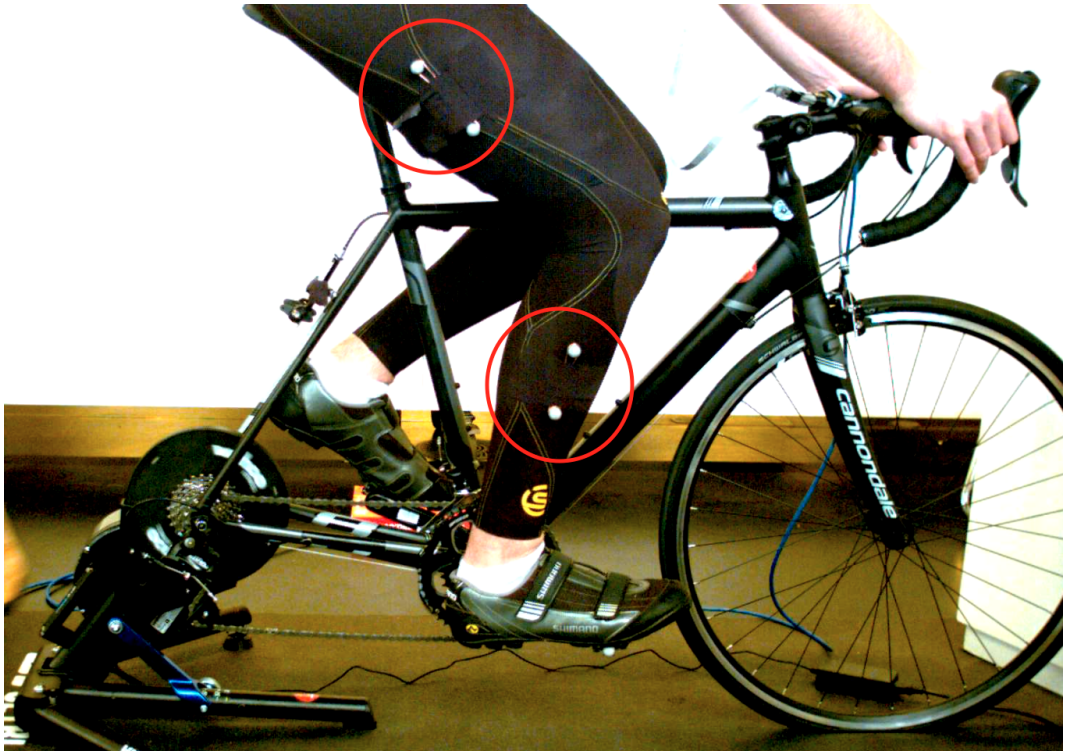

Figure 6.6: Motion capture markers (highlighted red circles) mounted on the participants upper and lower leg whilst wearing the smart garment.

crank angle of the bicycle (Figure 6.7.A,B). The data sampling frequency for motion tracking was set at 100 Hz, with the marker positions mounted as per the installation requirements detailed in Section 3.3 on the right leg of the participating cyclist, are shown highlighted in Figure 6.6.

The smart compression prototype garment [Belbasis & Fuss 2015; Belbasis, Fuss & Sidhu 2015a,b] was utilised for the testing of each athlete. The garment provided capability for measuring and mapping changes in the surface pressure above a muscle (Figure 6.7.D) where the active movement of the muscle under the compression fabric was detected by a distributed network of pressure sensors. The low-pressure sensors were manufactured from two layers of a conductive piezoresistive polymer, with an almost linear calibration curve of the average equation of $p = 97282000\sigma^{1.184335}$ for 2 layers, where p is the pressure in Pascal, and σ is the conductivity in Siemens [Fuss 2016].

The sensors were positioned over five of the thigh muscles (rectus femoris, vasti medialis and lateralis, biceps femoris, and semitendinosus) of the participant's right leg. In addition to the utilisation of pressure sensors, a 16-channel wireless EMG system (Wave Plus Wireless EMG, Cometa Systems, Bareggio, Italy) was used for recording the electrical signal (Figure 6.7c) of the same muscles.

The general placement of the electrodes followed the recommendations of [SENIAM 1999] and the optimum placement of the electrodes was achieved by using the method of Belbasis, Fuss & Sidhu (2015). To ensure accurate capture of the muscle behaviour throughout the tests a data sampling frequency of 2000 Hz was utilised for both the FMG and EMG sensors. Table 6.1 contains a

Table 6.1: Test measurement equipment and monitored data

Measurement Equipment	**Data Parameter**
Wahoo Kickr Cycle Trainer	• Cycling Power • Cycling Cadence
Wahoo TickrX heart rate monitor	• Heart Rate
Qualisys MOCAP Cameras	• Knee Angle • Crank Angle
Qualisys DAQ (wired pressure sensors)	• Muscle Pressures: - Rectus Femoris (RF) - Vastus Lateralis (VM) - Vastus Medialis (VL) - Biceps Femoris (BF) - Semitendinosus (ST)
Cometa EMG System (wireless connection)	• Muscle sEMG: • Muscles as above

summary of the variables captured and recorded for the purpose of testing and data analysis.

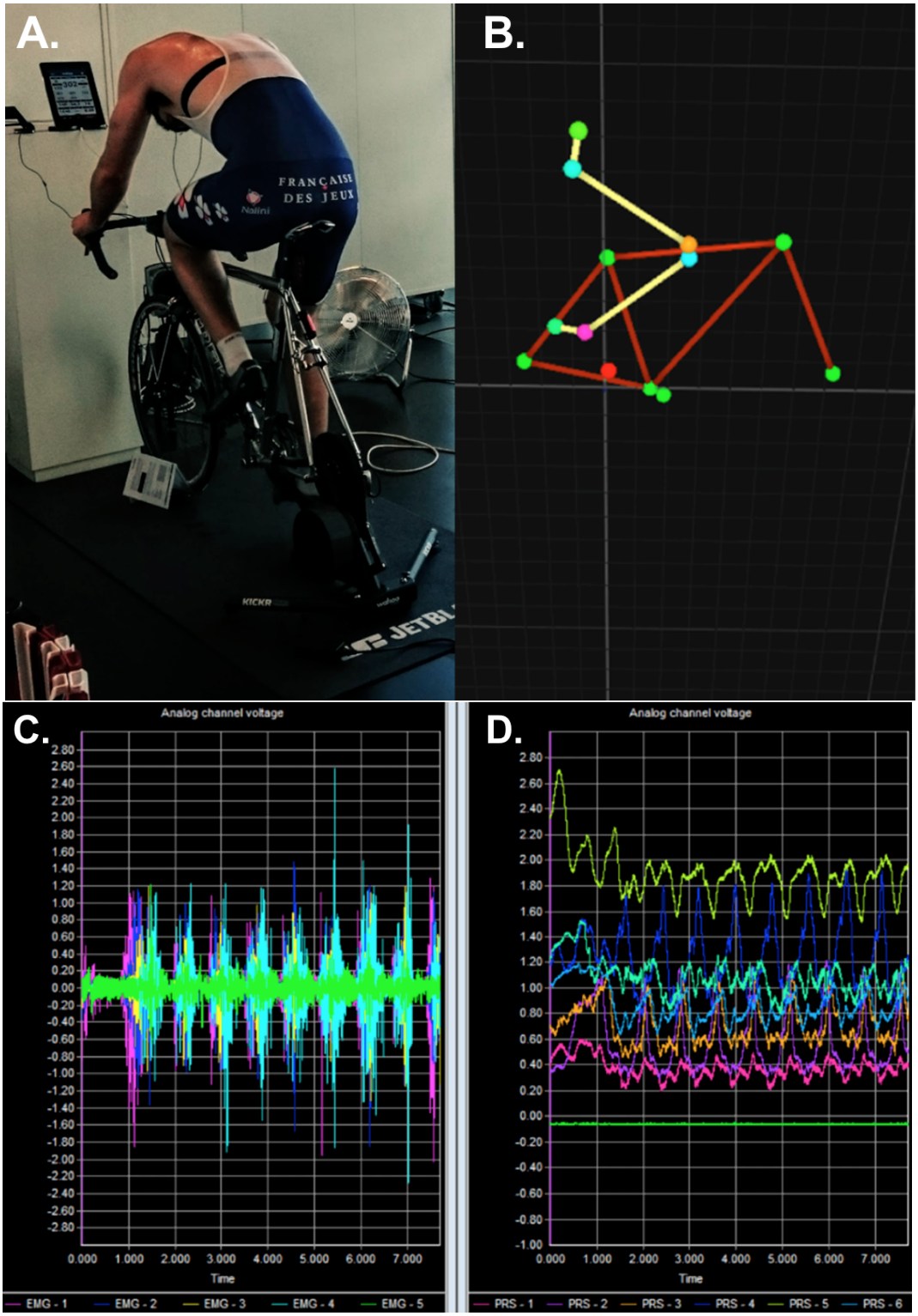

Figure 6.7: Qualisys software outputs of muscular behaviour (8 second window) exhibited during the Fatigue test; A) Raw video, B) Motion Capture, C) EMG data, D) FMG data

6.3 Results

6.3.1 Power Data: Session 1

The primary objective of the first testing session was to determine each participant's achievable FTP wattage level, allowing for the normalised testing FTP target during the second test. Outputs from the cycling trainer pertaining to the participant's performance data was collected and is shown below within Table 6.2.

Table 6.2: Session One activity summary

Participant	Time (m:s)	Time (s)	FTP Level (W)	Total Work (kJ)	Mean Cadence (rpm)	Mean Cadence (rad/s)	Mean Power (W)	Mean Torque (Nm)
1	10:35	635	320	141	88	9.2	222	24.1
2	6:09	369	220	62	58	6.1	168	27.7
3	17:11	1031	420	272	82	8.6	264	30.7
4	12:12	732	320	151	74	7.7	206	26.6
5	9:11	551	260	100	70	7.3	181	24.8
6	12:14	734	340	167	90	9.4	228	24.1
7	13:07	787	360	189	68	7.1	240	33.7
mean	11:31	691	320	154.6	75.71	7.9	216	27.4
st.dev	3:26	206	65.32	66.92	11.57	1.2	33	3.7

Application of the ramp test specifically assessed an individual's ability to increasingly deliver higher power output over time, as such we expect a distribution in the resultant efforts throughout the sample group due to differences in physical ability and familiarisation with the task. Due to the similarity in skill set and fitness between the participants, five participants fell within the bounds of one standard deviation from the mean of the duration and achieved FTP level. The other two participants; namely the least experienced cyclist (participant 2, below), and the most experienced (participant 3, above) were within two standard deviations.

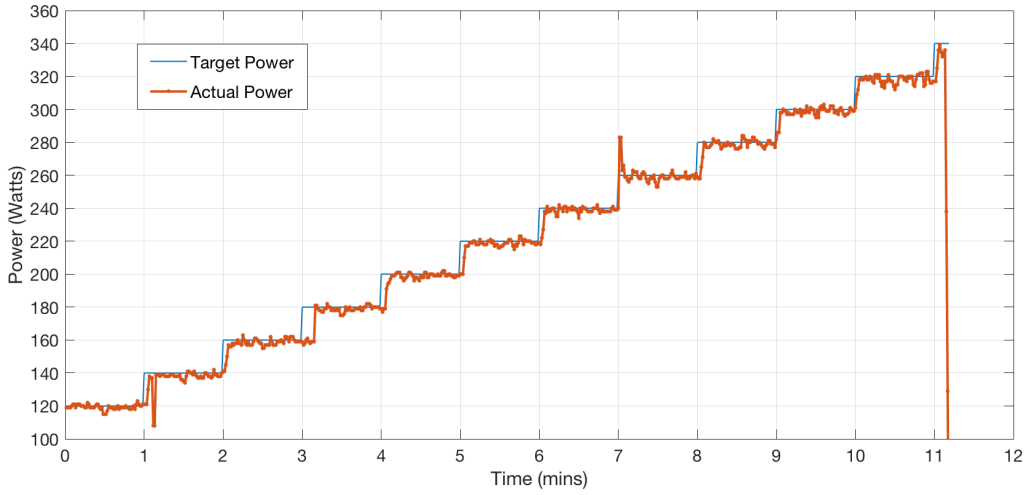

Figure 6.8: Power profile of a Ramp test taken by a participant

The test result profile shown in Figure 6.8 is an example of a participant successfully completing an

FTP level of 320W after 11 minutes. The next step level (340W) was attempted by the participant, however fatigue induced failure led to voluntary completion of the test.

6.3.2 Power Data: Session 2

Following the determination of the participant's FTP level, individual 80%FTP calculations were made for each participant and utilised for the second session to produce the fatigue profile. This inclusion of the additional biomechanical measurement systems (FMG, EMG and MOCAP) within the second test session allowed for greater insight into the onset and continued fatigue of the muscles in the lower limbs where the muscle behaviour for all key muscles were recorded and displayed throughout the second session. Figure 6.9 shows an example of the captured Power, Heart-rate and Cadence measurements of the fatigue test.

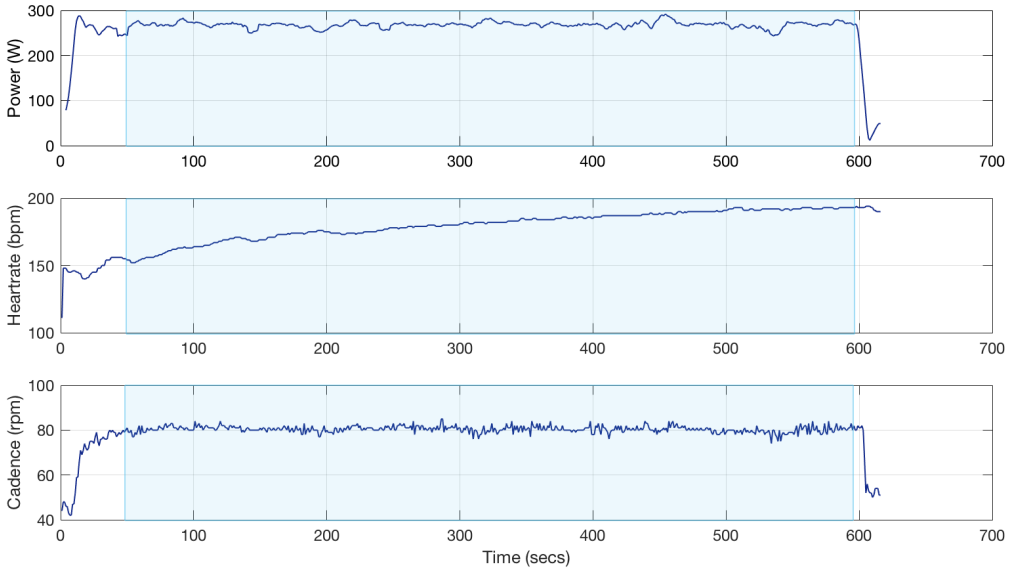

Figure 6.9: Fatigue test data of a participant, showing Power output, Heart-rate and Cadence. Blue shading represents the test period

All but one measurement for the seven participants was captured correctly throughout the full duration of the tests. Due to a lack of adhesion of the electrode, the Semitendinosus EMG measurement of participant 1 was corrupted mid-test and therefore is omitted from the following analyses. It is worth noting, that whilst the maturity of the FMG pressure monitoring technique is still in development, the majority of experimental issues (restarts, corrupted data, time-consumed) was attributed to the installation and affixment of both the EMG electrodes and equipment, and the motion capture markers. The simplicity and robustness of the pressure measurement system limited the prevalence of experimental failures.

A summary of key test data relating to each test is displayed within Table 6.3. Accuracy of achieving the target $\sim$ 80% FTP loading required was met within a satisfactory range (5%) for each participant with the mean accuracy within 1% of the grouped aim.

A noticeable deviation in the results was the duration of the test for participant 2 (least experienced).

Table 6.3: Session Two activity summary

Participant	Time (m:s)	Time (s)	Mean Power (W)	Total Work (kJ)	Mean Cadence (rpm)	Mean Cadence (rad/s)	Mean Torque (Nm)	Target Power (W)	Target Accuracy (%)
1	9:28	568	259	147	84	8.8	29.4	256	98.84
2	3:28	208	175	36	68	7.1	24.6	176	100.57
3	11:18	678	330	224	81	8.5	38.9	336	101.82
4	9:15	555	257	143	71	7.4	34.6	256	99.61
5	12:41	761	208	158	64	6.7	31.0	208	100
6	9:52	592	268	159	80	8.4	32.0	272	101.49
7	12:00	720	275	198	66	6.9	39.8	288	104.73
mean	9:33	583	253	152	73	7.7	32.9	256	101.01
st.dev	3.40	183	49.6	59.1	8.1	0.8	5.4	52.3	1.94

Whilst all other participants concluded the test within one standard deviation of the test mean (9:33 minutes of exercise), the low fatigue tolerance for participant 2 forced an end to the test after only 3:28 minutes. This result aligns with the experience level of the participant in comparison to that of the other participants, where duration of the test is largely driven on the physiological and psychological conditioned nature of the muscle and participant to operate under increasing fatigue limiting conditions. The experience level also correlated with the mean power and torque (Table 6.3) such that the least (participant 2) and most experienced (participants 3 and 7) participants exhibited the lowest and highest values, respectively.

6.3.3 Overall muscle activation

Through the motion capture of the pedal stroke movement, the muscle activity was resolved to the corresponding angle of the crank where each individual muscle was utilised, shown on polar diagrams. The polar diagrams of three representative participants (3, 6 & 7) are shown in Figure 6.10 for both the EMG and FMG measurements.

The EMG graphs of the extensors (Quadricep muscles: Rectus Femoris RF, Vastus Medialis VM, Vastus Lateralis VL) exhibited overlapping activity in the same sector of the diagram, with individual differences: in Figure 6.10A and 6.10C overlap of the muscles occurred at 330°-360°, whereas in Figure 6.10B this was observed at 30°. The FMG pressure-based activity deviated from the EMG-based activity in general by a clock-wise phase shift, indicative of the expected electromechanical delay of the muscles. For example, it can be seen in Figure 6.10C, the extensors still sizeably overlap, although not as perfectly as in the EMG plot, where the peak activities are shifted by 30° to 60° clockwise.

In Figure 6.10B, RF behaviour for both FMG and EMG activity aligns in the same sector. Whereas for VM, the pressure signal is shifted counter clockwise by approximately 30° with respect to the EMG signal, and VL is shifted clockwise by more than 60°.

In Figure 6.10A, RF and VM are shifted clockwise by 30° and 70°, respectively, and VL by almost 180°. Comparing the three FMG pressure plots, the activity of RF ranges from 20° to 30°, of VM

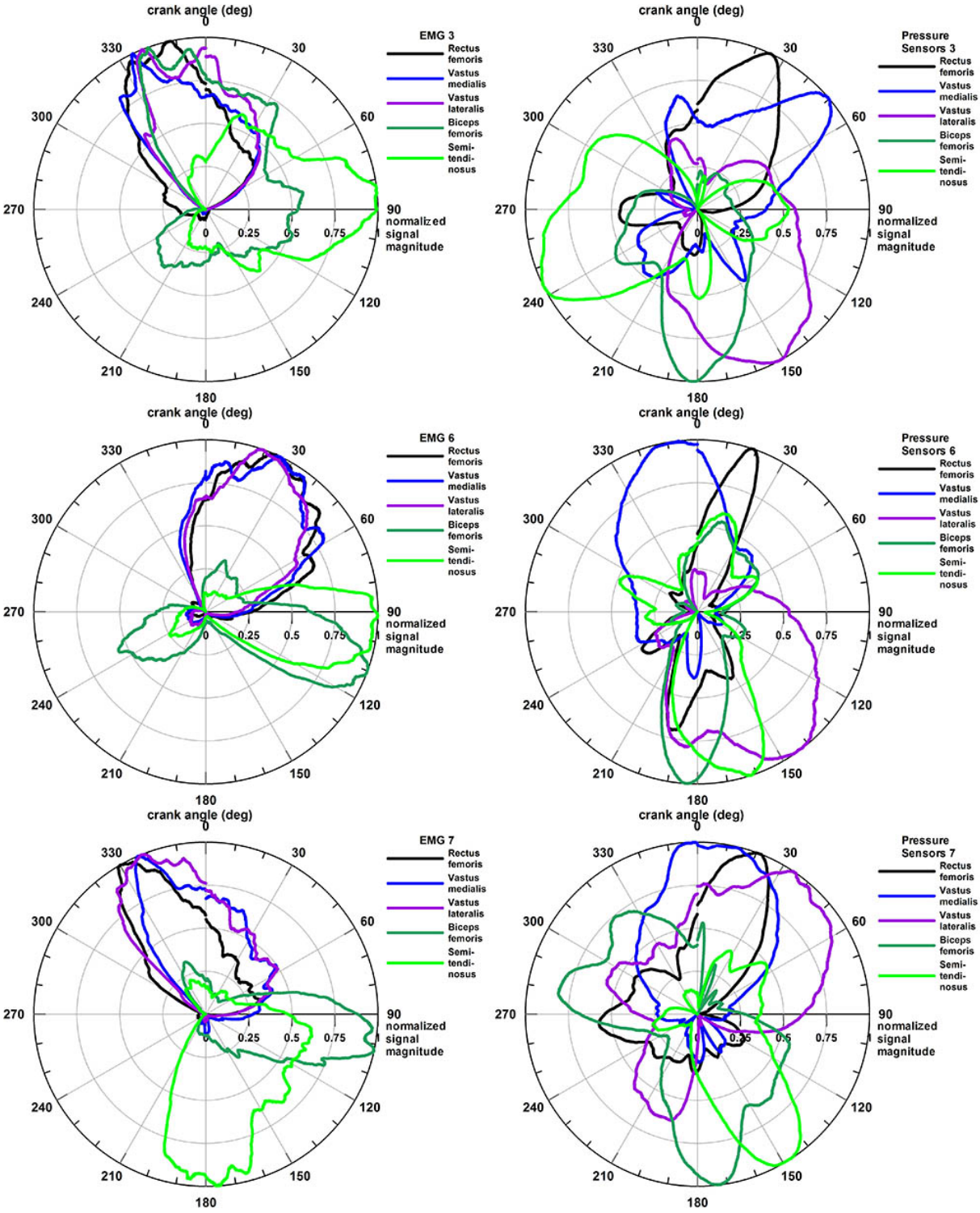

Figure 6.10: Polar plots of the activity of five muscles and three participants; Left column: EMG data, Right column: FMG (pressure data).

from -10° to 50°, and VL from 40° to 150°.

The flexor muscles (Hamstrings: Biceps Femoris BF and Semitendinosus ST) showed less consistent EMG activation patterns than the extensors: ST at 90°, 90°, and 180°; and BF at 100°, 110°, and 340°. The FMG pressure activation patterns are, in general, shifted clockwise as already seen in the extensor muscles, namely the BF by 70°, 70° and 200°; and the ST by -30°, 70°, 150°. Comparing the three FMG pressure plots, the peak activity of BF occurs around 170° to 180°, whereas the one of ST ranges from 150° to 240°.

Figure 6.10A shows a co-contraction of the three extensors and the BF on the EMG plot, whereas the FMG plot confines the co-contraction to VL and BF. The same is true for both hamstrings and the VL on the FMG plot (Figure 6.10B), whereas the EMG plot appears to be free of co-contractions. The latter is true for both FMG and EMG plots in Figure 6.10C.

Figure 6.11 shows the average muscle activation patterns of all 7 participants combined, thereby highlighting the sectors used by most participants. In general, while the muscle activities, measured with EMG or FMG, are relatively consistent across athletes, they do not coincide when the two different methods are compared directly (Figures 6.10 and 6.11).

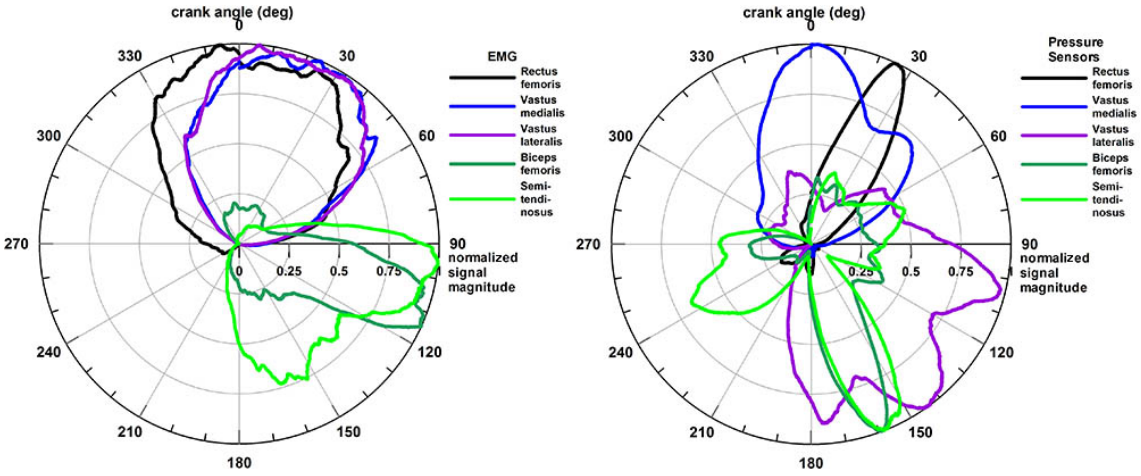

Figure 6.11: Combined polar plots of the activity of five muscles of all seven participants; Left plot: EMG data, Right plot: FMG (pressure data).

Table 6.4: Average angles and resultant phase shift

Muscle	Average Angle (FMG)	Average Angle (EMG)	Phase Shift
RF	-8°	-24°	+16°
VM	-24°	-8°	-16°
VL	-23°	-124°	+101°
BF	-110°	-143°	+33°
ST	-122°	-156°	+34°
mean	-57.4°	-91°	+33.6°
st.dev	54°	69.6°	42.8°

The average angles of the EMG signal are highlighted within Table 6.4. The FMG pressure plots

of all but one muscle are characterised by a clockwise phase shift with respect to the EMG plots of 16° to 101°. Only VM is shifted counter-clockwise by 16°. This phase shift phenomenon is attributed to the electromechanical delay of the muscle signal, which will be explained in detail in the Discussion section.

6.3.4 Fatigue induced radial phase shift

Radial phase shift angle ($\Delta\theta$) for all tests is displayed within Tables 6.5 & 6.6 for EMG and FMG measurements respectively and within Figure 6.12. The results are further averaged using the median values to determine central tendency by muscle and participant. This allows for observing the signal distribution pattern of each test with reference to the direction and magnitude of the radial shift angle, affording better insight into how fatigue-induced activation has influenced the muscles over the duration of the test.

Table 6.5: Muscle EMG activation angle (degrees) shift due to fatigue.

Subject	RF	VM	VL	BF	ST	median
1	-17.36	-5.24	-6.06	2.94	-	-5.65
2	-1.23	0.99	-0.96	-2.31	-3.79	-1.23
3	-6.43	-3.49	23.3	-16.29	18.47	-3.49
4	8.14	3.14	1.05	5.7	18.75	5.7
5	-8.85	-3.78	-0.2	0.29	8.02	-0.2
6	17.42	1.32	-6.55	12.38	6.28	6.28
7	-14.94	-20.12	-15.55	-4.41	3.13	-14.94
median	-6.43	-3.49	-0.96	0.29	7.15	-0.58

Table 6.6: Muscle FMG activation angle (degrees) shift due to fatigue.

Subject	RF	VM	VL	BF	ST	median
1	-6.43	-20.94	8.72	-17.08	90.66	-6.43
2	-2.89	1.43	-8.78	-4.41	-8.21	-4.41
3	-55.58	-0	-22.22	-20.74	-6.23	-20.74
4	55.54	-5.83	-4.73	2.9	-2.23	-2.23
5	-134.64	-68.35	32.31	-17.31	-2.09	-17.31
6	-148.91	-19.43	-12.65	-59.57	-11.98	-19.43
7	-24.22	-27.01	-42.91	-23.39	-3.76	-24.22
median	-24.22	-19.43	-8.78	-17.31	-3.76	-8.78

With respect to the EMG measurements, radial shift was balanced between earlier and later peak activity between muscles and participants with an aggregated average shift toward an earlier activation ($\Delta\theta_{avg} = -0.58$). Earlier peak muscle activation was highest amongst the three power generating extensor muscles (RF $= -6.43°$, VM $= -3.49°$ & VL $= -0.96°$). The stabilising flexors (BF $= 0.29°$ & ST $= 7.15°$) both demonstrated a tendency toward later activation. The maximal range of angular shift was between $-20.12°$ and $23.3°$.

Radial phase shift in peak activity was distinctly more prominent within the FMG pressure results, ranging at maximums between $-148.91°$ and $90.66°$. Unlike in EMG results, these results showed

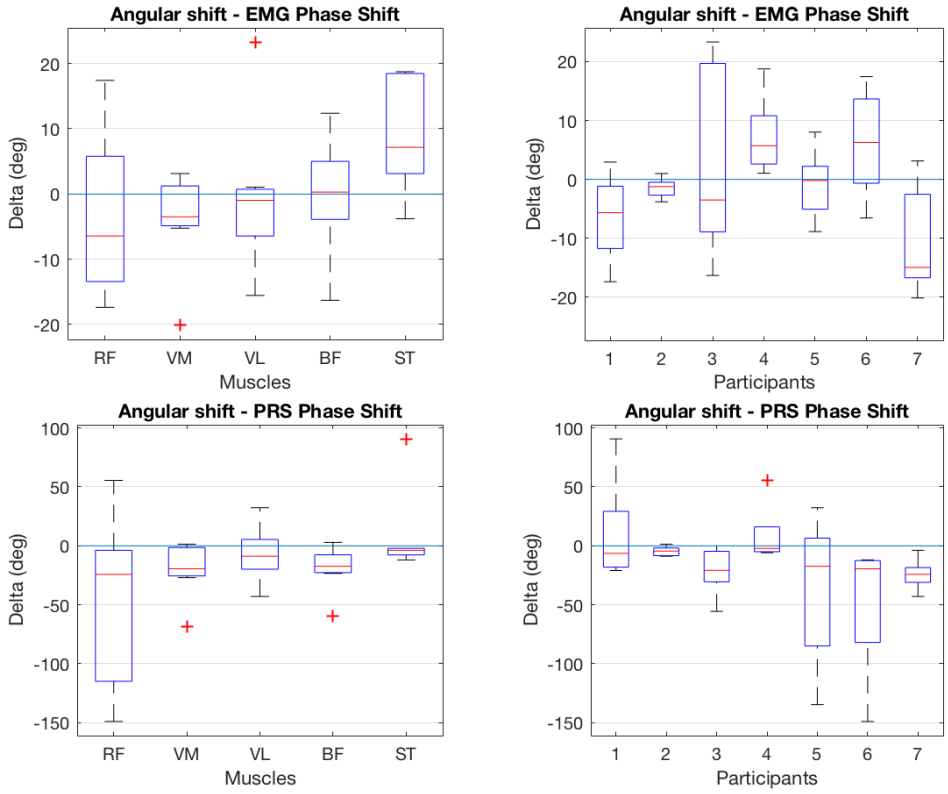

Figure 6.12: Radial shift in activation angles for (top) EMG and (bottom) FMG (denoted as PRS) measurements separated by muscles (left) and participants (right).

a higher skew toward earlier peak muscle activation for both muscles and participants, and a higher aggregated average radial phase shift ($\Delta\theta_{avg} = -8.78$). Less distinction was present between the power generating extensor muscles and the stability flexor muscles, with the RF ($-24.22°$), VM ($-19.43°$) and BF ($-17.31°$) demonstrating high earlier shifts, and the VL ($-8.78°$) and ST ($-3.76°$) lower due to spread across the participants. A connection to activity conditioning may be present here, as the highest shifts were present amongst the participants who primarily identify as cyclists (3 , 6 & 7), with the soccer identifying participants (2 & 4) presenting the lowest changes to peak activation timing.

6.4 Discussion

The purpose of this study was to explore the applicability of a smart compression garment based on force myography with pressure sensors [Belbasis & Fuss 2015; Belbasis, Fuss & Sidhu 2015a,b], measuring muscle contraction, for assessment of muscle activity and fatigue, as an alternative to EMG during a cycling exercise. The goal of which was addressing whether muscle activity can be assessed and measured with the smart compression garment. The signals obtained, related to the contraction pattern when cycling, were highly comparable and consistent on the polar diagrams, with some individual differences between participants.

The constant-load cycling task was chosen as it employs a mixed combination of muscle groups within the leg that provide either power generation, or stability throughout the activity. These muscle groups work together to produce a consistent power output to the crank, however as fatigue sets in the muscular performance of each group is affected differently. A common behaviour observed within the signal magnitude response of the test results is the decrease in performance of the stability-support (hamstring) muscles with the increasing presence of fatigue. Whilst in comparison, the power-generating Vasti muscles of the quadriceps (Vastus Medialis & Lateralis), experience increases in the amplitude of the signal over the test duration, demonstrating an increase in overall muscle activity (Figure 6.13).

Sanderson & Black (2003) showed that during a fixed-load fatiguing activity, reduced performance within stabilising muscles is compensated through the muscles tasked with power generation. Thus as a result of the fixed-power output requirements of the test, to maintain the test objective compensatory muscle force is necessary from the dominant knee extensor muscles to overcome decreasing performance of the stability-support muscles. It is important to note that the Quadricep muscles, particularly the Vasti pair (VM & VL), play a significant role in the activity of cycling. As such the regular engaged nature of the test participants within the sport leads to higher physical conditioning of these muscles, this leads to an increased ability to compensate an induced fatiguing condition in these dominant muscles. The Rectus Femoris (RF), unlike the two other measured quadricep muscles (VM, VL), does not always mimic the same behaviour in performance. This can be attributed to the activity relying upon the RF for two components of the stroke cycle; once during the knee extension phase (0-90 degrees) when down-force is applied to the pedal (alongside both Vasti), and again during the hip flexion phase (270-0 degrees) when up-force is necessary to lift the pedal. As the Rectus Femoris fatigues primarily through the weaker hip-flexion activity, the lift force it can apply to the pedal is effectively reduced. During this upstroke however, the pedal is 180 degrees out of phase with the opposite leg, where this performance decrease is directly compensated in some part by the opposing Vasti muscles. The increased fatigue associated by this behaviour in the RF muscle may be the cause for the increased comparative variability in phase shift observed in the RF to the other four muscles (as shown in Figure 6.12).

Further, the variation in the VL to the other knee extensors as measured using FMG was not as yet determined clearly as to the source of this behaviour, which differed between participants as shown in Figure 6.10. Due to the elongated nature of the VL muscle it experienced the

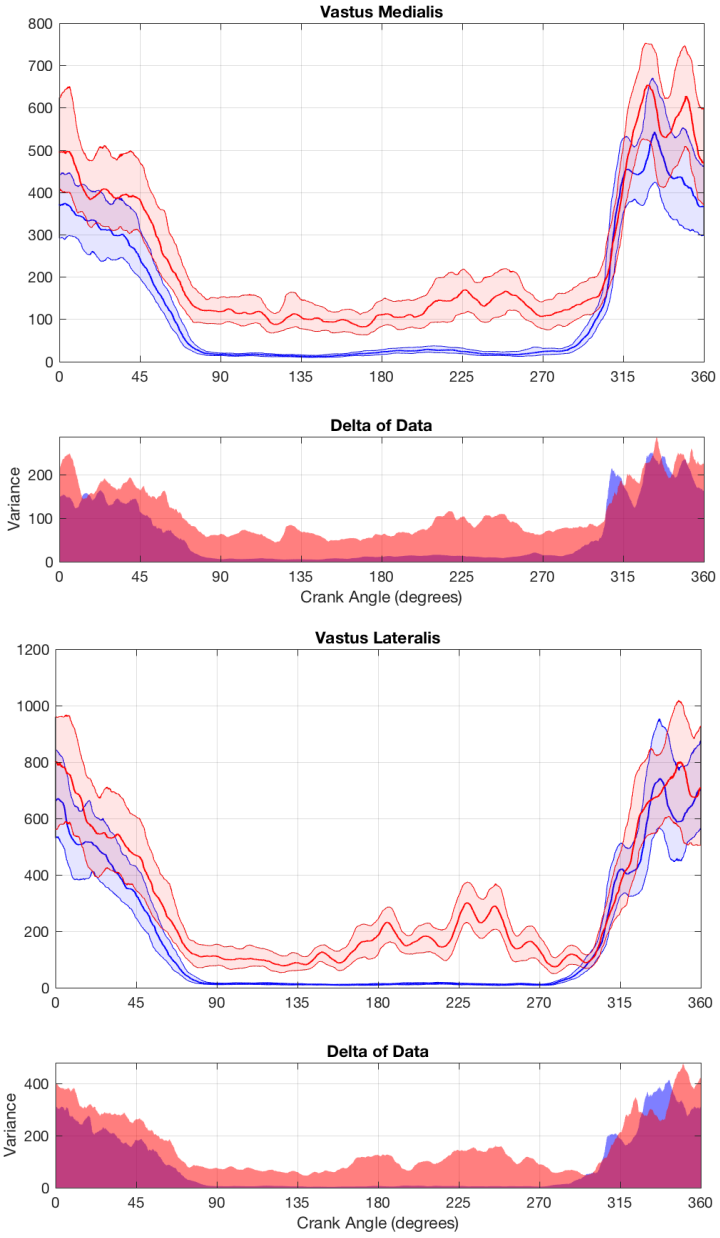

Figure 6.13: Increased EMG activity in the Vasti muscles to accommodate loss of power from supporting muscles during the 90-270 degree component of the pedal stroke. (Blue indicates non-fatigued muscle, Red that of fatigued muscle)

smallest values of pressure variation (i.e 'bulging') before normalisation and proved to be the most difficult to determine the optimal placement for measurement of pressure behaviour. Subsequently measurement of this muscle was more prone to a 'signal to noise' measurement errors and will require further exploration.

A secondary objective of this study was to validate the muscle activity pattern obtained from the smart compression garment with a gold standard, i.e. a lab-based EMG system. However, the muscle activation patterns obtained from EMG and the smart compression garment were, to some

extent, not comparable (Figures 6.10 and 6.11). The reason for this is not the inferiority of the smart compression garment, which could be easily deduced from the data, but rather the choice of the gold standard. Undoubtedly, EMG is the (even if the only) gold standard for assessment of muscle activity and fatigue. Yet, EMG measures the electrical activity of the muscle, whereas the smart compression garment detects the mechanical activity, i.e. muscle bulging that compresses the FMG pressure sensors between skin and garment.

The difference between EMG and FMG polar plots simply reflects the difference between electrical and mechanical activity. The electro-mechanical delay [De Luca 1997] of the contraction force with respect to the electrical stimulation of a muscle is explained from the time difference between onset of electrical activity and the increasing muscle force. This delay is also dependent on muscle fibre distribution, measured by the percentage of fast and slow twitch fibres. For example, to reach a contraction level of 50% of the maximal muscle force, it takes a fast and slow twitch fibre approximately 0.15 and 0.25 seconds, respectively [De Luca 1997]. When cycling at a cadence of 73 rpm (average cadence from Table 6.3), these two delay times would cause, in theory, a phase shift of between 66° and 110° on the polar diagram. The differences seen in the EMG and FMG sensor polar diagrams are therefore expected.

According to EMG data of Jorge & Hull (1986) and Hug *et al.* (2010), the quadriceps extensors are active from 300° to 130° and from 235° to 162°, respectively, and the hamstrings from 15° to 255° and from 324° to 288°, respectively (maximal ranges). The data seen in Figure 6.11 perfectly fit into these ranges, which the exception of the VL, which exceeds 130°. Jorge & Hull (1986) also reference other papers, the results of which show considerable differences and fluctuations, suggesting that there is considerable variety of EMG results.

The fatigue induced phase shift present within both electrical and mechanical measurements could suggest an influencing cause behind the variety of results across the literature. The test results demonstrated that for both measured systems (EMG and FMG) there was significant individual movements both forward and backward in the position of the average crank angle for each muscle between a non-fatigue and fatigued state. The influence of which presented more readily within the FMG pressure results, with nearly all muscles shifting to earlier peak effort (median $= -8.78°$) suggesting either a reduction in the electromechanical delay, or a pre-emptive action by the muscles to compensate for reduced performance. The activation phase shift of the EMG results were less influenced by the presence of fatigue (median $= -0.58°$).

The balanced spread across the subjects in the EMG results with no clear skew to earlier or later activation suggests a dependency not on the muscle group performing the same task across all participants, but rather its conditioning and muscle fibre (i.e. fast and slow twitch) distribution which is unique to each participant. Evidence for this is further supported by the grouping of participants in the FMG pressure results by their defined primary sport, where the cyclist (participants 3, 6 & 7) all experienced far earlier average activation phase shifts than the soccer players (2 & 4), activities which call on different muscle conditioning and as such would reflect within the participant results.

Nevertheless, EMG is still a gold standard for validating the smart garment, as there is no other

system available. The gold standard therefore serves primarily for understanding the differences between the data, and the underlying principles of the different measurement systems. Validation is still possible, if differences are known in the first place or at least expected, and subsequently confirmed through a validation study. This issue poses a new challenge for wearable technology not experienced before, specifically when dealing with lateral innovation [Fuss 2017]. Finding a suitable gold standard could then become a problem.

6.5 Summary

This chapter details the first half of the exploration of muscle activation and fatigue measurement using smart apparel. Specifically it documents the experimental methodology and data collection approach taken in an effort to enforce a fatigue condition upon a participants lower limbs. A total of seven individuals completed both testing sessions, allowing for the detailed capture of musculoskeletal activity in the quadricep and hamstring muscle groups. All measured muscle FMG pressures, and all but one single EMG measurement were successfully recorded for later analysis.

The smart compression garment based on force myography with pressure sensors returned performance parameters (muscle activity and fatigue) comparable to the surface EMG, used as gold standard for validation. The major differences were that the EMG measured the electrical activity whereas the FMG pressure sensor measured the mechanical activity. As such, there was a phase shift between electrical and mechanical signals, with the electrical ones preceding the mechanical ones in most cases. This is specifically important in high speed cycling, the activity investigated in this study. Using the activity sectors on the polar diagrams, obtained from EMG, for biomechanical models, could result in incorrect outcomes, compared to using the activity data obtained from force myography. The latter are considered more appropriate as input for biomechanical modelling.

The results from this chapter also begin to highlight the role that specific muscles undertake within given activities and the impact that fatigue has on their performance. The quadriceps responsible for the power generation while cycling are more prone to earlier peak activation as a consequence of fatigue to that of the hamstrings muscles providing stability. The importance of conditioning of these muscles was also highlighted, where the dominant activity of participants, and the muscle fibre distribution required that supports high performance in this activity, played a role in the direction and magnitude of the phase shift in peak activation of the muscles.

7. Measurement and Analysis of Muscle Fatigue

Published Research

The following chapter contains work published within:

- Belbasis, A. & Fuss, F. K. Muscle performance investigated with a novel smart compression garment based on pressure sensor force myography and its validation against emg. *Frontiers in Physiology* **9** [2018]
- Fuss, F. K., Belbasis, A., Sidhu, J., *et al. Fractal dimension analysis of muscle fatigue with muscle surface pressure measured via compression garments* in *Proceedings of ICSST 2016, 2nd International Conference in Sports Science and Technology* [Nanyang Technological University, Singapore, 2016]

Continuing from the outcomes of the last chapter, we now focus upon on a more detailed analysis into the behaviour of the muscles monitored, with specific relation to the transitioning fatigue condition. The collected muscle data from the cycling fatigue tests was processed into a Raw and Conditioned dataset utilising the techniques highlighted within Chapter 3, differing only in the conditioning of the EMG signal in the latter. These datasets were utilised for the specific analysis of the fatiguing condition on the muscle through three analyses;

- The Median Frequency shift in the EMG signal (gold standard)
- The Fractal Dimension of the EMG signal
- The Fractal Dimension of the FMG signal

The discrete comparison of two different fatigue states, as shown in Chapter 6, is useful in identifying the effects that fatigue activity has on active muscles. It is however also important to explore the transitional change the muscles undergo as the body moves between these two fatigue states. This is the focus of the work that follows within this chapter.

Foundational works by De Luca (1997; 2003) has shown that the median frequency (MDF) of the Fast Fourier Transform (FFT) of an EMG signal shifts towards lower frequencies as fatigue sets in. This has become the industry-accepted method for the reliable indication of muscular fatigue (EMG-MDF). Whilst widespread, this method relies on significant implementation expertise and a

high entry cost for equipment and consumables. The aim of this work is to explore the utilisation of Force Myography and the pressure sensor garment [Belbasis & Fuss 2015; Belbasis, Fuss & Sidhu 2015a,b] as a suitable performance analysis alternative. Specifically measuring muscle activation and fatigue, with validation of the prototype against EMG, used as the gold standard for muscle performance assessment.

The method selected for this task had to comprise of a standardised repeatable activity and a defined fatigue protocol. The research used a cycling activity on a stationary power-controlled bicycle as the method of choice. Fatigue was assessed through the FFT (Fast Fourier Transform, gold standard) of the EMG signal, as well as with fractal dimension signal processing. For the latter, the Higuchi method ([Higuchi 1988]) is considered the gold standard method, however a new customisable fractal dimension method (Fuss' method; Fuss, 2013) was selected that offers advantages over Higuchi's method.

7.1 Measurement of Fatigue: Median EMG Frequency

The use of EMG has long been relied upon as a gold-standard tool in measuring muscular fatigue. De Luca (1997) established that the median frequency of an EMG signal (MDF) over a set time period shifted towards lower frequencies as a result of increasing muscular fatigue (Figure 7.1). The negative trend of the plotted MDF provided an understanding of the performance decrease in the muscle under investigation. Through the increase of both the measured time window, and the frequency of the analysis, a more comprehensive understanding of the fatigue trend is observed [Luca 2003]. More specific to cycling, Dingwell *et al.*(2008) built on this approach further by utilising a Short-time Fourier Transform (STFT) technique, where the calculation of the MDF was performed over individual time segments attributed to each crank cycle revolution.

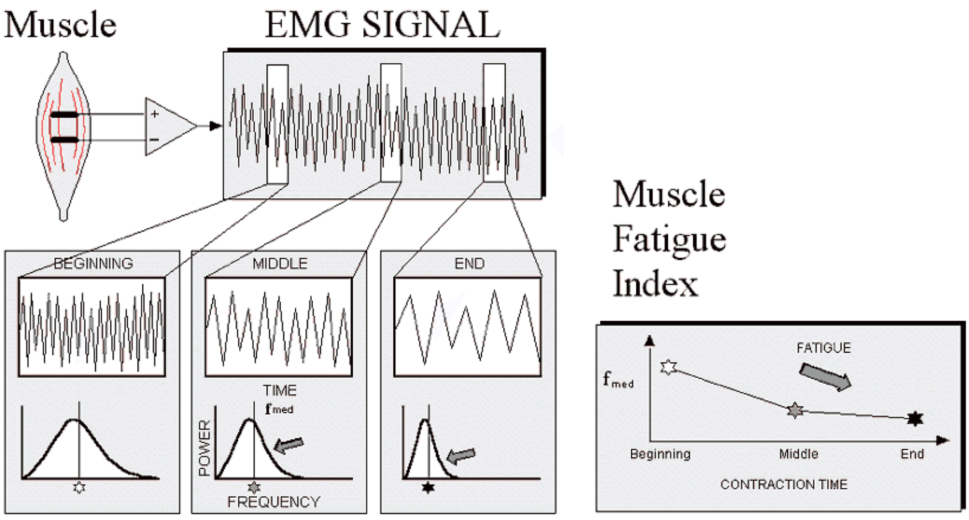

Figure 7.1: Influence of fatigue on median frequency of the EMG signal [De Luca 1997]

7.1.1 Calculating the Median FFT signal

For the fatigue analysis of the EMG muscle data each of the tests was processed as detailed within Section 3.4.4. The raw signal amplitude was expressed as a time series with a 4th order Butterworth bandpass filter (10-350Hz) applied to the EMG dataset to remove unwanted noise. Sampling frequency was downsampled to 80Hz to accommodate better comparisons to the FMG pressure measurement datasets.

The negative trend of the median frequency over time provides an understanding of the performance decrease in the muscle under investigation. Following work from Dingwell *et al.* (2008) a Short-time Fourier Transform (STFT) technique was applied, whereas the calculation of the power spectrum, and the resultant median frequency, is performed over individual time segments attributed to each crank cycle revolution. This allows for the distinct observation of temporal muscular performance changes over each rotation of the bicycle crank, rather than the utilisation of sliding FFT window, to observe median frequency changes.

A directional trend is fitted using a linear regression model indicative of the presence and rate of fatigue. All calculation was made using the FFT function within MATLAB (The MathWorks, Inc., Massachusetts, USA) and a sliding average window of 1-minute width to define the averaged trend of the data. The resultant signals were normalised for both amplitude and time to allow for consistent comparison amongst each other.

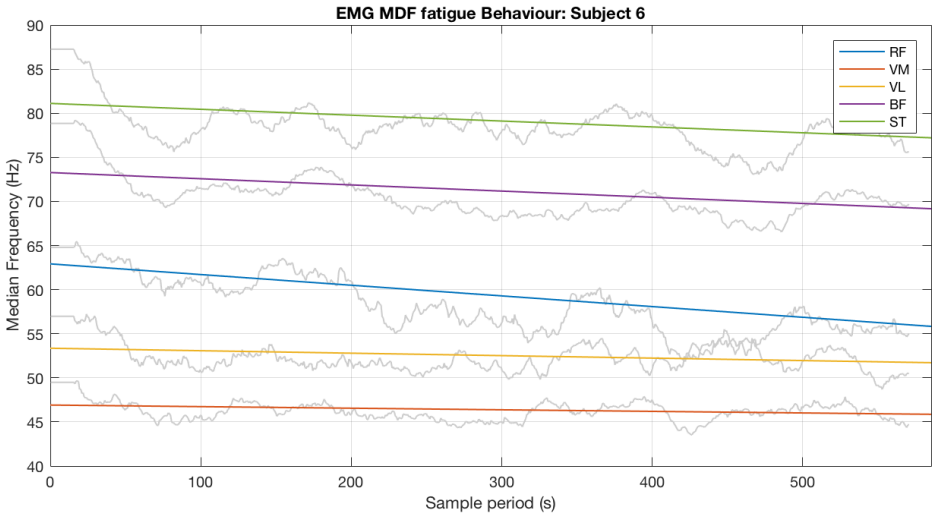

Figure 7.2: Averaged Median EMG frequency over each crank cycle for all five measured muscles of participant 6 showing the linear trend. Observing comparatively smaller Vasti muscle fatigue

7.1.2 Summary of results

As was anticipated through the application of both the gold-standard EMG-MDF technique [De Luca 1997] and Dorel's (2009) fatigue-inducing regiment, the results conclusively show evidence that all measured muscles experienced a transient or continuing fatigue state during testing. The majority of muscles (31/34, 91%) experienced a global decrease (negative trend) in the median frequency, reflective of a continuing fatigue state.

Where the results were indicative of shallow gradients or positive trends, discretion of the fatigue condition is needed as the use of a linear fit assists in capturing the trend over the entire period of the test, which does not truly represent transient positive/negative slopes within segments of the test. Muscles that are prone to transient fatigue-recovery cyclic behaviour resulted in lower gradient results (discussed further in Section 7.3.2). These muscular efforts, although impinged by the onset of fatiguing elements, demonstrate the ability to forestall the effects through bouts of recovery, where grouped muscles cooperate in fatigue load sharing to allow for individual muscle recovery periods whilst not sacrificing the power generation required throughout the task.

Summarised in Table 7.1 and visualised in Figure 7.3 are the normalised gradient values for the linear fit for all muscles. Additionally all values were averaged (median, $\tilde{x}$) and results were conclusive of the existence of a median negative trend, thus a fatigued condition, for each muscle and participant. Weakest average participant performance, thus highest fatigue was observed in participant 2 ($\tilde{x} = -0.6438$). The strongest performance was from participant 4 ($\tilde{x} = -0.2598$).

For all subjects the RF ($\tilde{x} = -0.5826$), BF ($\tilde{x} = -0.4919$) and ST ($\tilde{x} = -0.553$) experienced significant negative slopes. Whereas the conditioned Vasti muscles (VM, VL) showed higher ability in forestalling the onset of fatigue within the VM ($\tilde{x} = -0.4168$) and VL ($\tilde{x} = -0.4047$). A possible explanation for this behaviour is the higher level of conditioning of the Vasti for cycling, thus slower fatigue onset. The example can be seen in Subject 6's Vasti muscle performance (Figure 7.2) where the Vasti muscles exhibit a lower gradient (fatigue decline) to that of the other measured muscles.

Table 7.1: Normalised fatigue gradient for all EMG-MDF values

Subject	RF	VM	VL	BF	ST	median
1	-0.4711	-0.7969	-0.6303	0.2554	-	-0.5507
2	-0.6438	-0.853	-0.4047	-0.605	-0.7031	-0.6438
3	-0.5826	-0.5394	-0.0628	-0.6013	-0.5441	-0.5441
4	-0.2598	-0.1992	-0.1188	-0.4408	-0.5618	-0.2598
5	0.1038	-0.3137	-0.5763	-0.4919	-0.5436	-0.4919
6	-0.7615	-0.1798	-0.2844	-0.5138	-0.4208	-0.4208
7	-0.6939	-0.4168	-0.5056	0.1192	-0.5955	-0.5056
median	-0.5826	-0.4168	-0.4047	-0.4919	-0.553	

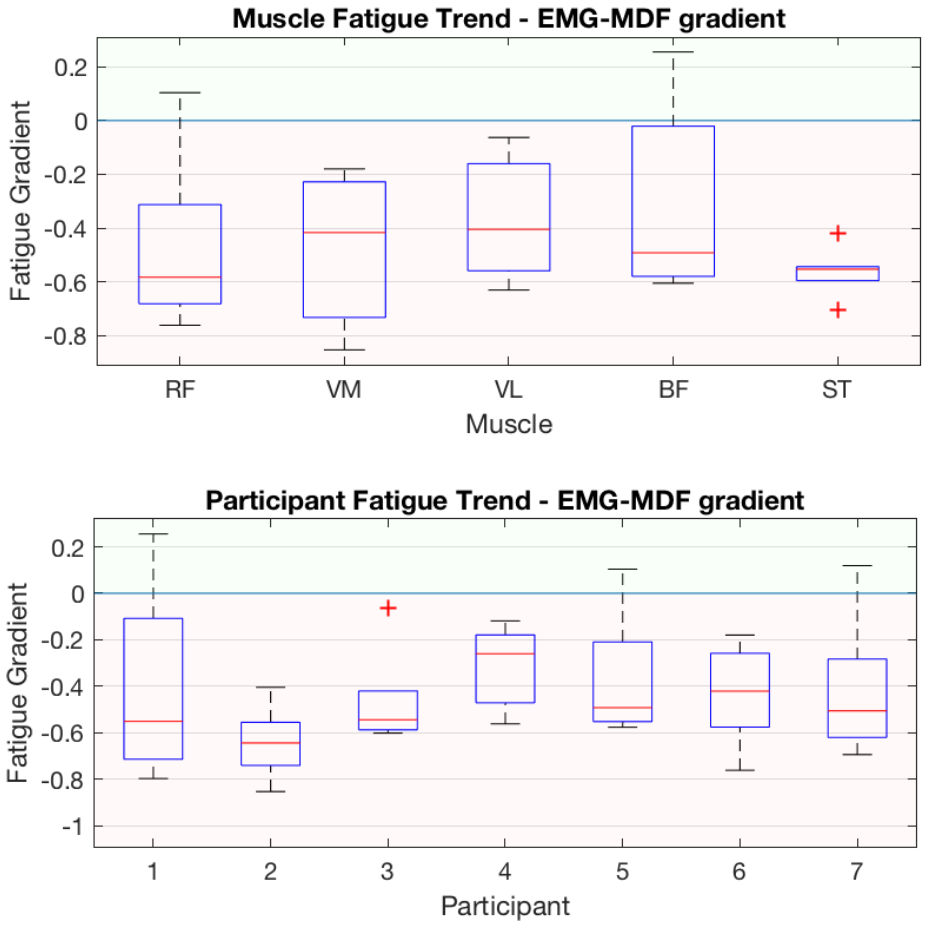

Figure 7.3: Boxplot of fatigue gradient trend for EMG-MDF of Muscles and Participants. Red shaded area denotes negative gradient and thus fatigue.

7.2 Measurement of Fatigue: Fractal Dimension Analysis

With increased frequency, non-traditional data analysis methods are becoming more commonly used within physiological monitoring; of particular interest to the research was the potential of a Fractal Dimension Analysis (FD) in the providing an alternate measurement of a fatigued condition. Traditionally an FD analysis provides a measurement of a signal's instability, quantifying the level of chaotic behaviour it experiences. Research [Chua 2013; Fuss 2013] has indicated that the use of this technique can provide significant advantages and insight into a measured dynamic signal when compared to traditional signal processing techniques.

The research follows an investigative path into whether quantification of a fatigue state is achievable through the measurement of chaotic muscle behaviour. Whereas it is anticipated that muscles succumbing to fatigue increasingly exhibit discontinuity in their activation pattern during a continuously rhythmic activity. As such an analysis was undertaken to investigate the effect fatigue has on the FD analysis of the recorded muscular activity, with a goal of evaluating whether physiological effects of muscle fatigue produce a greater fractal dimension in the corresponding signal being measured.

A robust analysis technique

Whilst the correct placement and calibration of a sensor is good-practice, limitations in the implementation of wearable technology can result in non-optimal measurement conditions, often to the detriment of the resulting analysis. A key benefit in the analytical use of the FD analysis is its higher independency on sensor placement and calibration when compared to traditional techniques (i.e. EMG). The analysis utilises the relative chaos within the signal itself, providing a normalised amplification of the signal's chaotic behaviour between two known extremes within the signal, namely a non-fatigued and fatigued state. Provided the sensor itself has not been adversely affected by the conditions of the test, a resultant FD analysis provides an accurate understanding to the chaotic behaviour within the muscle. Furthermore, as the nature of electro-mechanical sensor drift is a low frequency change in the signal output, the use of an FD analysis discounts effects attributed to drift present within the sensor due to the lower effect it has on influencing chaotic behaviour.

7.2.1 Calculating the Fractal Dimension signal

The fractal dimension of EMG and pressure signals was calculated with the FD analysis method developed by Fuss (2013). The Modified Amplitude Fractal Dimension Method (MAFDM) was utilised based on previous development work showing robustness and functionality by the research team (see appendix A.1). To improve the efficiency and maintain consistency of testing, a computational Matlab program was written to automate the FD analysis for all measured signals. The MAFDM method allows for maximal separation of two conditions (e.g. fresh and fatigued muscle states) by means of adjusting and optimising the signal amplitude multiplier. If this multiplier is set to high values (infinity in theory), then Fuss' method is identical to that of Higuchi's (1988) method.

The analysis relies upon identification of ranges within the signal where minimal and maximal

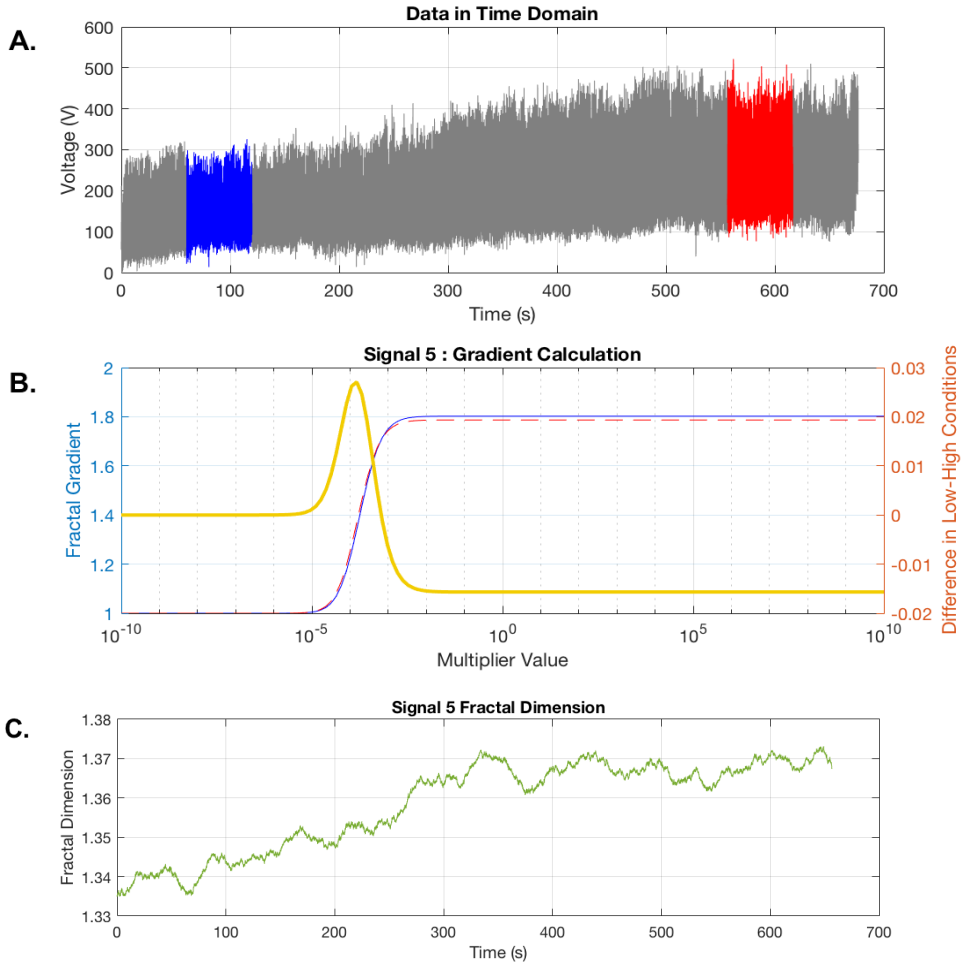

Figure 7.4: Fractal Calculator Analysis output. (A) Original signal with extrema selected, (B) Calculation of optimal multiplier, and (C) Result amplified Fractal Signal.

chaos is expected. In order to identify the optimal amplitude multiplier the extrema conditions are utilised to identify the optimal multiplier (M-value) where amplification yields the best distinction in the FD signal. From the recorded signals, the non-fatigued and fatigued states were the necessary selection for these extrema ranges. A range of 60 seconds (120K samples) was taken for each extrema where the non-fatigued state was selected as the second full minute and the fatigue state the second last minute. The bounding first and last full minute of the test were omitted as extrema (though included in the analysis) to ensure the signal reflected activity periods were the participant was completing the task as assigned and not influenced by the artefacts introduced by the start or end of the test. The differential of the fractal dimensions of fatigued and fresh states (Figure 7.4.B) was plotted against the decadic logarithm of the multiplier [Fuss 2013] and the optimal multiplier was identified at the maximum differential (see technique in Appendix A.2). This amplitude multiplier was then used to calculate the fractal dimensions continuously through the signals with a running window width of 1 minute.

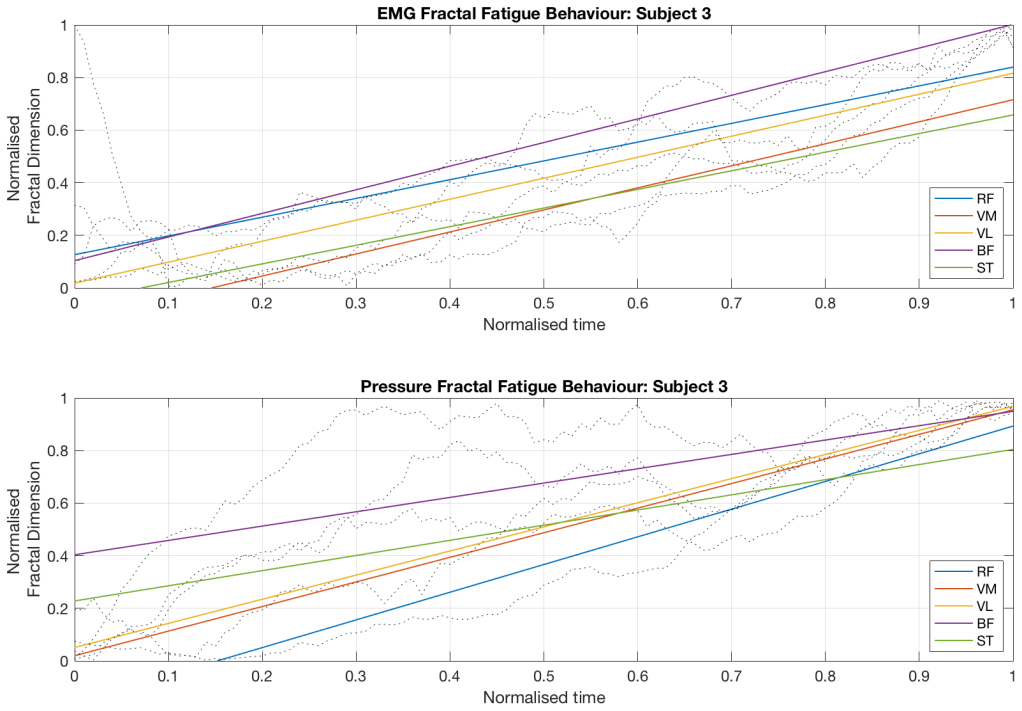

Figure 7.5: Example of linear trend for Fractal Dimension response of normalised (Top) EMG and (Bottom) FMG sensor signals for all five measured muscles of Participant 3.

7.2.2 Summary of results

As was applied to the EMG-MDF data, a linear regression fit was applied to the resultant fractals to determine the gradient of the fractal signal. However, unlike the EMG-MDF plots which trended downward to reflect the influence of fatigue, the proposed hypothesis was the expectation of a positive gradient reflecting an increased chaotic fractal behaviour influenced by the presence of fatigue. The resultant gradient of the fit for each signal is summarised within Tables 7.2 and 7.3 for the fractal EMG (EMG-FD) and FMG pressure (PRS-FD) signals respectively, with presentation of these results within Figures 7.6 and 7.7.

Following a linear trend fit to the both FD signal groups, all EMG-FD muscles (34/34, 100%) exhibited a positive linear gradient, while for PRS-FD 94% (33/35) of the muscles were reflective of a positive (fatiguing) gradient. These results, supported by a uniform positive gradient in the grouped average of the muscles, furthers evidence that the FD analysis of both the EMG and FMG sensor signals were indeed influenced via muscular fatigue.

For the EMG-FD results the highest gradients observed within the dominant power generating quadricep muscles, highest average in the RF ($\tilde{x} = 0.8025$). The median FD gradient of the hamstring muscles was similar to quadriceps, however with a wider overall spread of results toward the lower end. This could be due to the reduced usage of these muscles during the cycling activity (stability-support role) as well as evidence of transient fatigue within the FD signals for the BF and

ST muscles not being captured via a linear regression fit. The highest individual EMG-FD gradient was participant 2's RF ($\tilde{x} = 1.0118$), however the highest median gradient was by participant 5 ($\tilde{x} = 0.8296$). Noting that the unequal distribution of effort for participant 5 was distinct through some of the highest quadricep gradients and lowest hamstring gradients, possible indicators of poor technique or conditioning.

As with the EMG-FD gradients for the PRS-FD all muscles exhibited a high median average gradient of fatigue. The RF ($\tilde{x} = 0.8296$) and VL ($\tilde{x} = 0.8296$) power generating muscles ranked highest in the averaged results. Highest overall positive PRS-FD gradient was participant 3 ($\tilde{x} = 0.9174$), however much like participant 5's EMG-FD results (above), the hamstring gradients were nearly half that of the quadriceps, though still high ($\tilde{x} > 0.5$). The lowest individual gradients were highly negative with participant 1's RF ($\tilde{x} = -0.8384$) and participant 2's ST ($\tilde{x} = -1.004$), likely indicators of poor technique or conscious discontinued use of the muscle due to poor endurance capability.

Table 7.2: Normalised fatigue gradient for all EMG-Fractal values

Subject	RF	VM	VL	BF	ST	median
1	0.7711	0.648	0.6368	0.6814	-	0.6647
2	1.0118	0.9388	0.7818	0.6276	0.7176	0.7818
3	0.7134	0.838	0.7984	0.8982	0.708	0.7984
4	0.0374	0.6483	0.5542	0.7939	0.7864	0.6483
5	0.9434	0.8296	1.0112	0.0404	0.0536	0.8296
6	0.8368	0.358	0.6683	0.4684	0.6029	0.6029
7	0.8025	0.5647	0.7189	0.0649	0.2812	0.5647
median	0.8025	0.6483	0.7189	0.6276	0.6554	

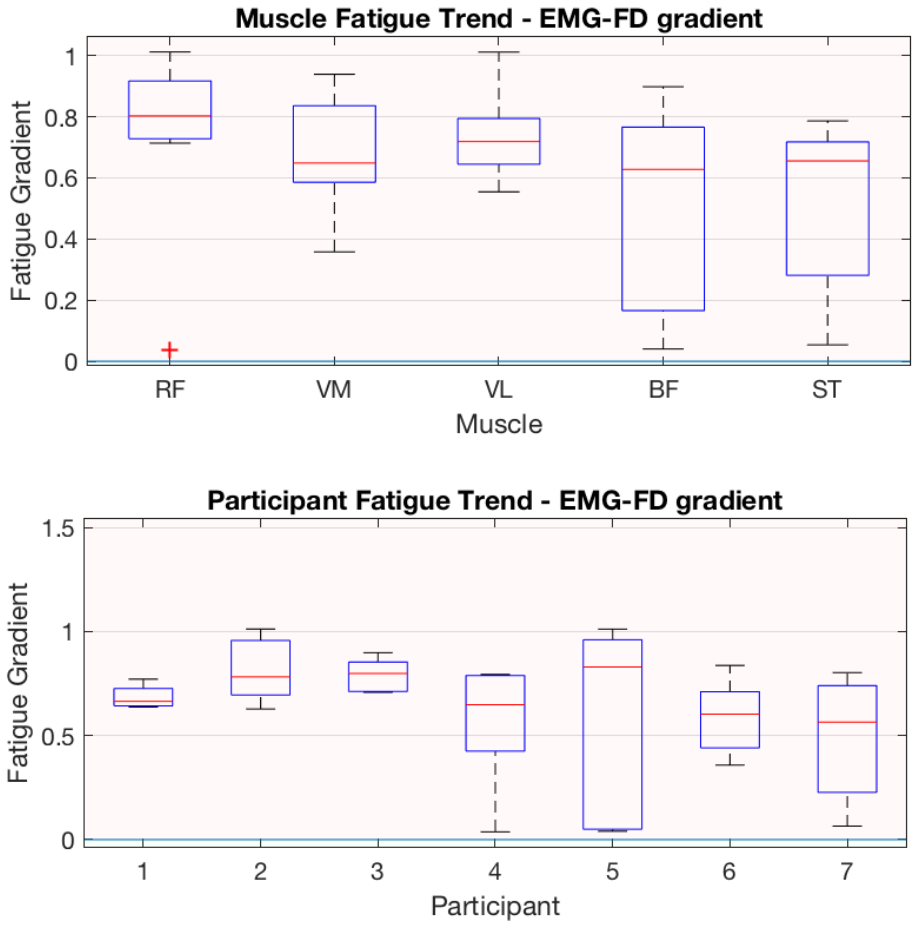

Figure 7.6: Boxplot of fatigue gradient trend for EMG-Fractal of Muscles and Participants. Red shaded area denotes positive gradient and thus fatigue.

Table 7.3: Normalised fatigue gradient for all FMG-Fractal values

Subject	RF	VM	VL	BF	ST	median
1	0.3051	0.5994	0.3971	0.6006	-0.8384	0.3971
2	-1.004	0.7652	0.2315	0.8485	1.0529	0.7652
3	1.0529	0.9353	0.9174	0.5454	0.5764	0.9174
4	0.9278	0.4665	0.7496	0.6644	0.5309	0.6644
5	0.7243	0.55	0.5538	0.5336	0.9785	0.5538
6	0.6373	0.6452	0.7078	0.7066	0.5642	0.6452
7	0.7702	0.6624	0.7944	0.6642	0.5703	0.6642
median	0.7243	0.6452	0.7078	0.6642	0.5703	

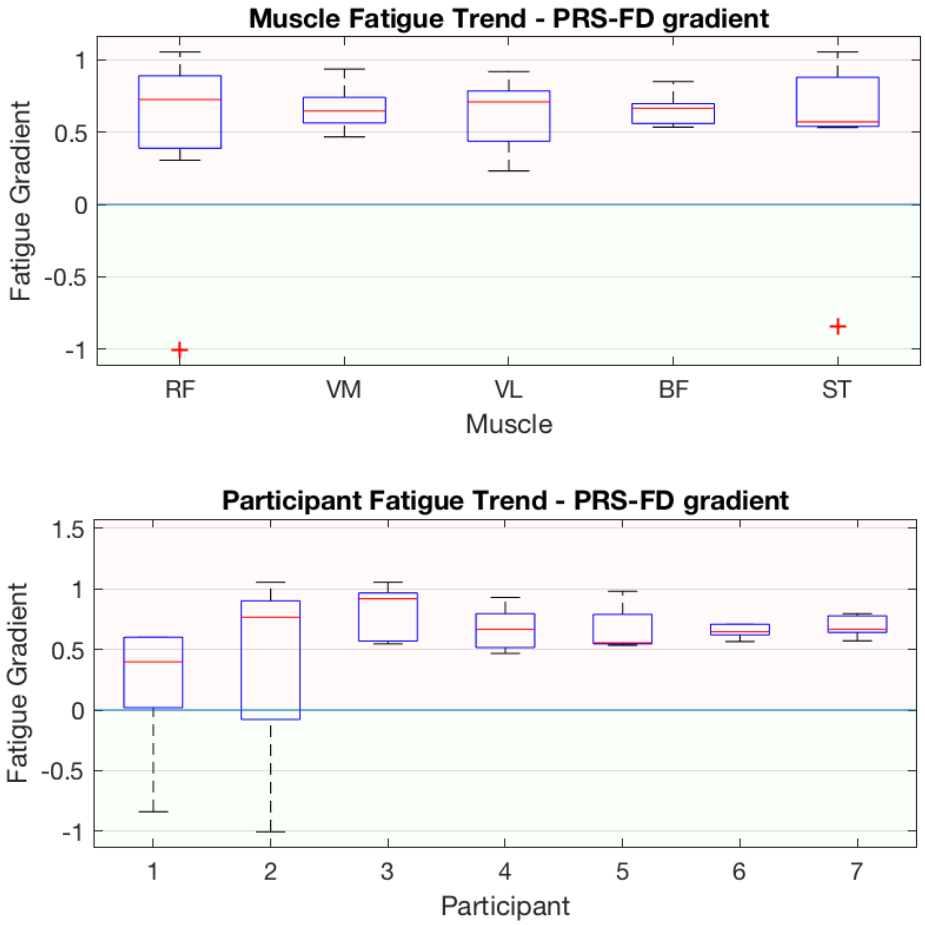

Figure 7.7: Boxplot of fatigue gradient trend for FMG-Fractal of Muscles and Participants. Red shaded area denotes positive gradient and thus fatigue.

7.3 Discussion

7.3.1 Fatigue testing using fractal dimensions

Assessment of the fatigue performance over the entirety of the cycling fatigue test was made through two different measurement methods and two different algorithms resulting in the need to compare by correlation three different fatigue signals; namely the Fast Fourier Transform (FFT median frequency of an EMG signal; EMG-MDF) and the fractal dimension for the EMG signal (EMG-FD) and FMG signal (PRS-FD).

As was confirmed through the EMG-MDF analysis, at one time throughout the testing all muscles for EMG-FD and PRS-FD exhibited a transient fatigued state. However all measured signals (EMG and FMG) revealed a near-global increase in their respective fractal dimension, corresponding to the increases in fatigue enforced by the testing. Statistically significant change in the FD signals showed that the increasing presence of fatigue within the muscle drove higher instability within the measured signal, increasing the observed fractal dimension. In general, when considering the overall behaviour of each participant across all three fatigue assessment methods (see Figure 7.8), the overall fatigue trend is clearly seen in all signals, with increasing (Fractals) and decreasing (FFT) trends.

Key Research Discovery

During a fixed-cyclic activity, increases in the presence of muscular fatigue is reflective in the increased signal instability, thus establishing a causal relationship between Muscular Fatigue and the Fractal Dimension of the measured signal.

The results also highlight that the use of a linear regression fit leads to non-optimal representation of the gradient the fractal signal exhibits, where low or negative gradients do not truly capture the muscles that experienced a transient fatigue state. This raises a need to explore the time dependency of the results. As at present transient fatigue conditions either, consciously or sub-consciously, are actively modulated muscle activity to aid in forestalling the effects of fatigue. The cyclic behaviour by muscles to prevent fatigue through load sharing is evident within the fractal signals for both the recorded EMG and FMG sensor data. The results relay evidence of the quadriceps as primary muscles to complete the knee-extensor role during the cycling task, where they experienced the greatest increases in fatigue-induced instability. Where the hamstrings, traditionally weaker and under-utilised within cycling, show lower fatigue and function as primarily stability-support muscles leading to the modulated cyclic fatigue they experience.

To assess time dependency, both median frequency data and fractal dimensions data were normalised. For comparing the fatigue development across all participants, the time was normalised as well (due to different experiment durations). The median frequency data and fractal dimensions data were linearly correlated to the normalised time to assess the percentage of the time dependence by means of R^2 correlation. The R^2 values were compared as to their significant difference with Fisher's Z-test for comparing correlations from independent samples.

The normalised FMG pressure fractals correlate with the normalised cycling time in 84% of the results ($R^2 = 0.8405$, linear fit; 84% of the fatigue level is explained from the time progression of the exercise). The normalised EMG fractals and median frequencies correlate with the normalised cycling time in 51% ($R^2 = 0.5081$) and 71% ($R^2 = 0.7092$) of the results respectively.

The R^2 value expresses merely that, for the FFT method, 71% of the fatigue level are time-dependent whereas 29% are not time dependent. Time-independent fatigue would be if a fatigue level or the average fatigue were kept relatively constant over a longer time. Furthermore, the different performance levels of the subjects could also contribute to the time-independent fatigue; for example, more experienced athletes are more skilled in fatigue management over time. FD-EMG reflects more time independent fatigue (49%) compared to PRS-FD (16%), i.e. approximately three times as much. When comparing EMG-FD and PRS-FD to EMG-MDF, all three variables correlated to the normalised time of the experiments, PRS-FD showed highest time dependent correlation (84%), and EMG-FD the highest time-independent component (41%). These differences come from the fact that PRS-FD, a measurement of mechanical instability, is more related to mechanical fatigue, whereas EMG-FD and EMG-MDF are related to central and peripheral fatigue, respectively.

There is indication [Mesin *et al.* 2009] that shift of the median frequency of the EMG signal is related to peripheral muscle fatigue (decrease in conduction velocity) whereas the fractal dimension of the EMG signal is related to central fatigue (increase in motor unit synchronisation). This seems illogical at first sight, as the higher the amplitude of higher frequencies is, the greater is the fractal dimension, and therefore any reduction of median frequencies is coupled to a smaller fractal dimension. This principle can be easily verified when using synthetic fractal signals, such as Knopp/Takagi function, Weierstrass cosine and Weierstrass-Mandelbrot functions, and stochastic Brownian Motion function [Fuss 2013]. However, EMG data are not based on functions that generate signals with predefined fractal dimensions. As such, low median frequencies and small fractal dimension do not necessarily exhibit a parallel trend. This possibility is also affected by the method used for calculating fractal dimensions.

Additionally there is indication that a power-trained subject is more affected by peripheral fatigue whereas an endurance trained subject was more prone to central fatigue [Mesin *et al.* 2009]. It is therefore expected that the correlation of fatigue parameters that measure different components of fatigue is not necessarily high. This correlation is not just affected by the fatigue component, but also by the distribution of training type across the participants of a study. For example, participant 3 identifies as a long-distance cyclist and therefore endurance trained, whereas participant 4 is a soccer player and thus power-trained.

If EMG-MDF and EMG-FD are related to central and peripheral fatigue, respectively, then PRS-FD could be related to mechanical fatigue. Mechanical fatigue is actually defined as the failure of the muscle system, i.e. that the force level cannot be maintained anymore [Basmajian & De Luca 1985]. Nevertheless, metabolic fatigue (measured with EMG) becomes apparent even before system failure [Basmajian & De Luca 1985]. As such, the term mechanical fatigue is probable not appropriate, and should be replaced by mechanical pre-fatigue.

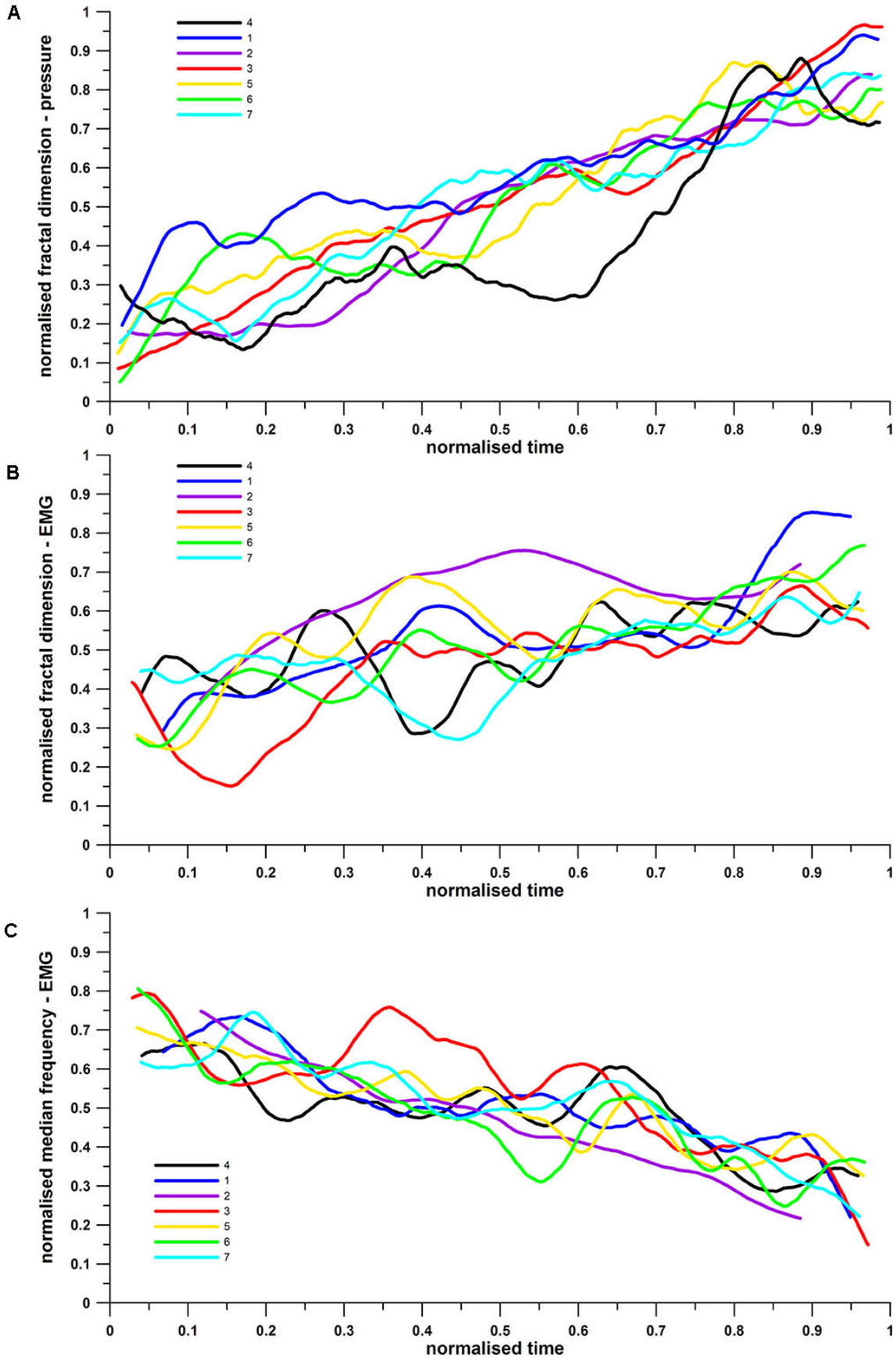

Figure 7.8: Normalised average fatigue (fractal dimensions and median frequency) vs. normalised time: (A) FMG fractal, (B) EMG fractal, and (C) EMG median frequency for all participants.

This chapter explores a range of key muscular measurement and analytical techniques, but focus is placed on the exploration of measuring muscle fatigue through a novel fractal dimension analysis technique using both electrical and mechanical (pressure) measurement techniques. Evaluation was based on the calculation of the fractal dimensions of FMG and EMG signals. For calculating these fractal dimensions, Fuss' method was used as it maximally separates the fractal dimensions FD of a normal and an abnormal signal, by finding the maximum differential of FD-abnormal minus FD-normal, when subjecting both signals to the same amplitude multiplier. Normal and abnormal signals could be physiological/pathological ones, less/more chaotic ones, signals from fresh and fatigued states, low/high activity signals, etc.

From common sense, the abnormal signal is expected to have a higher fractal dimension. Common sense is confirmed if there is a maximum differential and the two asymptotic fractal differentials at multipliers of close to 0 or to infinity are smaller than the maximum. It has been seen on numerous occasions, that Higuchi's method, corresponding to Fuss' method with an infinite multiplier, returns higher FD for normal signals [Fuss 2013, 2016], compared to abnormal ones. This problem is seen here as well, more pronounced in the EMG-FD data, though. This behaviour is not unexpected in the EMG signal, as the decreased amplitude of high frequencies in the power spectrum (typically seen in fatigued muscles) leads to a decrease of FD. The increase in EMG amplitude, also typical for fatigue, increases the FD. If the cadence drops, so does the FD. Even if there are multiple influences that affect the FD, it would be more logical to assume that the FD of a fatigued muscle's signal is smaller than the one of a fresh muscle, if the principle of left-shift of the median frequency is known.

Irrespective of logical assumptions, all three methods applied, EMG-MDF, EMG-FD and PRS-FD, showed the same clear trend, namely that fatigue increases with time, with some individual differences between participants. Over the duration of the cycling exercise this deterioration in the ability to produce consistent power was clearly reflected in the fatigue parameters (fractal dimensions and median frequency) obtained from the surface electrical (EMG) and mechanical (FMG) activity.

7.3.2 Muscle Fatigue Affect: Power-Stability relationship

Introduced within Section 6.4 and further discussed throughout this chapter is the power-stability relationship observed between the muscle groups. Within Figure 7.9 we see the fatigue distribution of the muscular efforts for two participants, using the PRS-FD method. Whilst the singular task set for the test was to maintain a constant power output, no restrictions were placed on which muscles could be used to achieve this goal. Due to this participants presented unique muscle usage profiles throughout the tests, yet a distinct pattern was observant within the muscular behaviour across all participants. That was that loading-recovery cycles were evident (see sinusoidal behaviour in VM, VL & BF of Figure 7.9B) throughout the duration of the test when stability-support muscles were unable to provide the consistent power generation needed throughout the activity.

Muscular conditioning plays a significant driving role for this behaviour and thus becomes further apparent when you explore the PRS-FD response for two of the more experienced participants

within the test. Both participant 3 and 6 are accomplished cyclists yet in distinctly different exertion training areas. Where one participant (3, Figure 7.9A) focuses largely on long distance endurance training, the other (6, Figure 7.9B) maintains shorter duration track sprint training and performance.

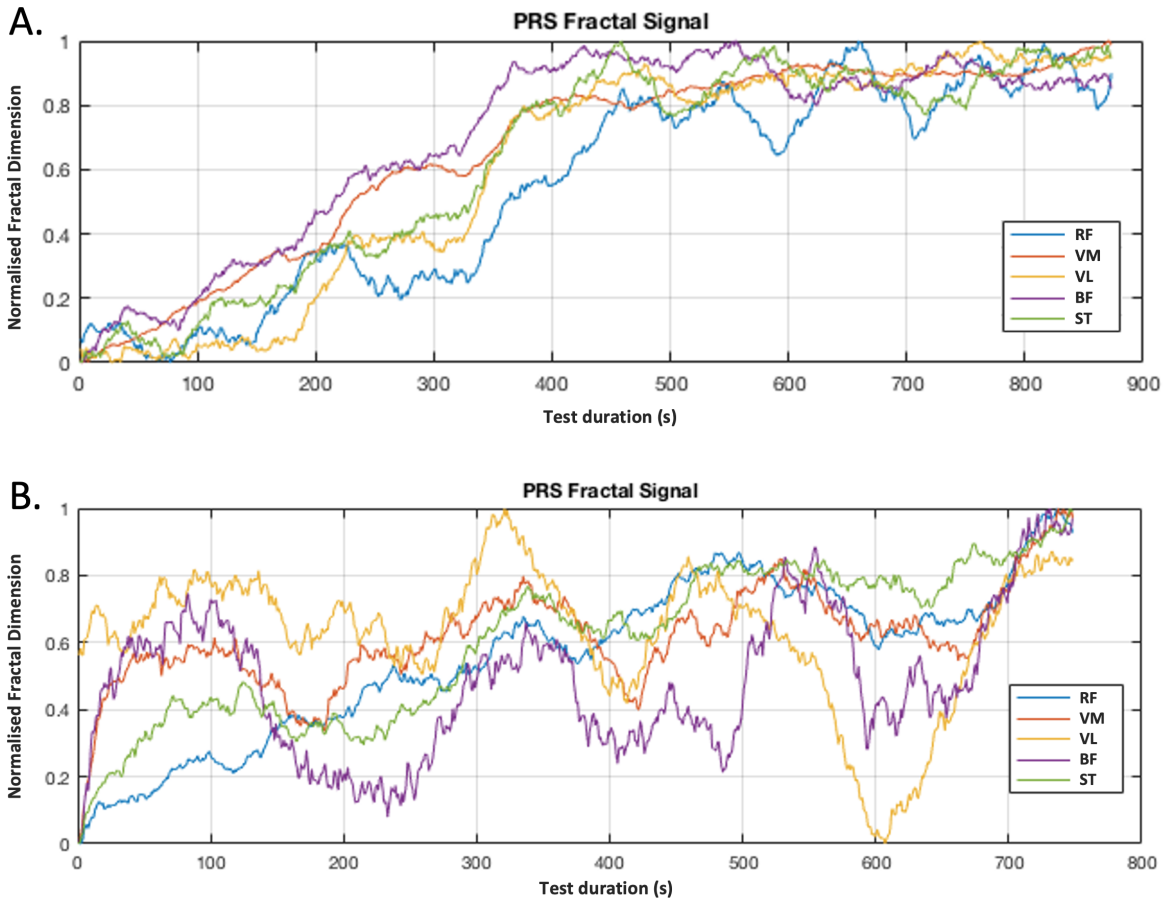

Figure 7.9: Normalised PRS-FD fractal fatigue response for A) endurance conditioned participant 3, and B) power conditioned participant 6.

Conditioned to duration-based fatigue training, participant 3 clearly drives all five muscles almost equally throughout the test, presenting a similar fatigue curve across all 5 muscles. Whilst some muscles perform more consistently with less fluctuation in the fractal curve, in essence each muscle has not been tasked with an activity it alone cannot sustain. Participant 6 however trains specifically in cycling sprint and power events. Although possessing conditioned muscles, the long-term fatigue exposure of the test is not complementary to the standard training regiment. As a result both the Vasti (VM, VL) and Biceps Femoris (BF) muscles exhibit greater cyclic load-recovery behaviour (approximately 3.5 cycles lasting 2-3 minutes each) consistent with that of stability-support muscles. The participant's main power-generation muscles however the Rectus Femoris and Semitendinosus (RF, ST) exhibit the constantly increasing fatigue curve similar to that of participant 3.

The exploration of this Power-Stability relationship is critical in the evaluative understanding of performance and the development of an athlete. It provides clear evidence of recovery behaviour

of muscles during a fatigue-dominant training test. Importantly it provides a method in which to isolate performance traits between athletes to better assign or develop athletes to appropriate competitive activity based on their unique muscular response to a fatigue inducing condition.

7.3.3 Muscle Fatigue Affect: Antagonist load sharing

The analytical techniques employed above all showed evidence of transient fatigue behaviour within the activity. This behaviour hinted at muscle load-sharing to the effect of forestalling the influence of fatigue, largely present within the less conditioned muscles. Observation of this behaviour with respect to the antagonistic pairing of the Quadricep and Hamstring muscles yields a unique distinction in the FD signal behaviour - namely muscle pairs work together to alleviate fatigue through overwork-underwork cycles. This behaviour is clearly demonstrated between the RF and BF antagonistic muscles within Figure 7.10. Specifically in Figure 7.10A we see that over the full (macro) duration of the test, both muscles experience increases in their FD signal (dotted line), yet interestingly when observing the micro-fluctuations during the test it becomes evident that the signals of the RF (blue) and BF (green) behave as almost mirrored signals to one-another.

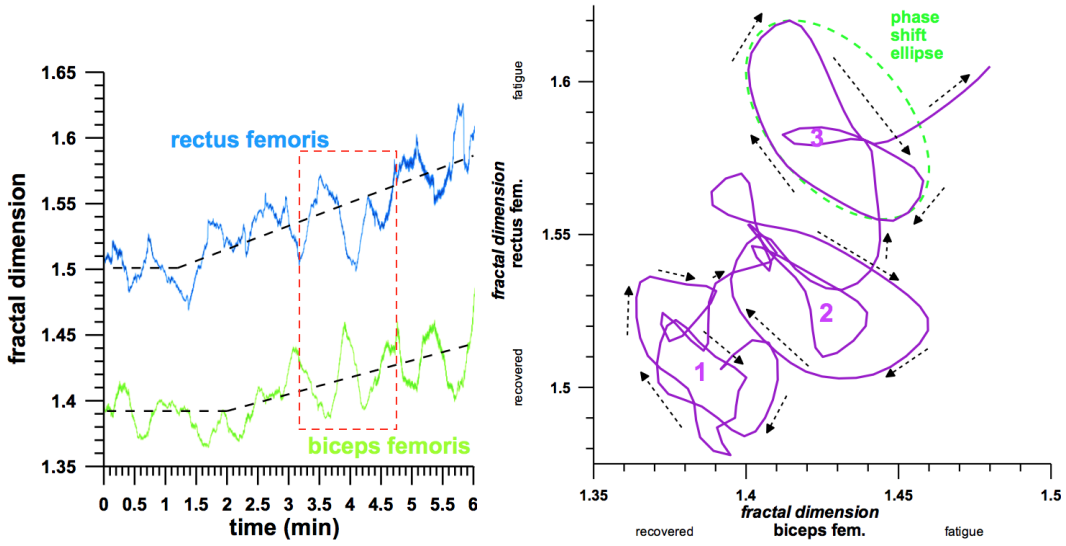

Figure 7.10: (A) Load-sharing between antagonistic RF and BF muscles. (B) Phase shift of the load-sharing cycle

These mirrored signals reveal that whilst a positive trend in the FD is concurrent with the global increase in fatigue across all muscles, transient fatigue cycles reveal significantly higher rates of fatigue (beyond one order of magnitude larger). The mirrored nature of the paired signals indicates that this transient fatigue process is the result of one muscle working harder, thus inducing a higher fatigue rate penalty, whilst the paired muscle is given suitable time to rest and reduce the impact of fatigue it has sustained in the previous cycle. Once a threshold of limitation is reached by either the Fatiguing or Recovery muscle, this process is reversed producing the elliptical phase shift behaviour shown in Figure 7.10B.

Key Research Discovery

The Fractal Dimension of fatiguing antagonistic muscles exhibit a mirrored signal relationship that is evidence of load-sharing behaviour. This allows for transient periods of alternating fatigue-recovery cycles that assist in forestalling ultimate fatigue-induced muscular failure.

The significance of this discovery lies in the ability to now observe and quantify a traditionally subjective (somewhat subconscious) decision made by an athlete during an activity as to how they utilise fatiguing muscle groups. Where data-driven performance and endurance focused training can implement knowledge of these load-sharing cycles to monitor and/or control the threshold at which the cycles occur, increasing an individual's fatigue tolerance and overall athletic performance.

An important remark on the mirrored behaviour is that the recorded signals demonstrate only the muscular behaviour of a single leg. Wherein, as the bicycle crank enforces an 180 degree offset in left-right muscle use, we are only observing half of the relationship. Thus further testing utilising both legs is necessary to improve the understanding the antagonistic pairs across both legs have on the load-sharing relationship. However, Antagonistic pairs may not always work against one another to balance fatigue onset, where results from testing are indicative that between particular muscle groups (i.e. Quadriceps) the muscles will share fatigue-recovery loading behaviour between each other to alleviate fatigue affects without compromising the performance of the muscle group as a whole. Figure 7.11 shows this behaviour, where the two Vasti muscle begin the activity in a load sharing behaviour, but mid-activity (∼325 seconds) begin working in sync to one-another.

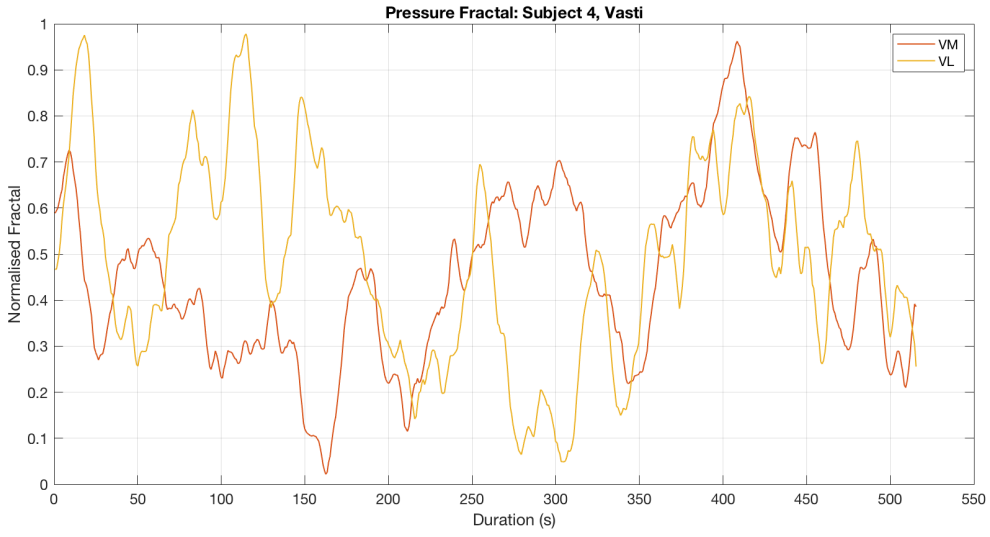

Figure 7.11: Antagonistic load-sharing between the VM and VL muscles for participant 4 (PRS-FD)

7.4 Summary

Muscle activity and fatigue performance parameters were obtained and compared from a smart compression garment measuring force myography (FMG) activity and the gold-standard, a surface electromyography (EMG) system during high speed cycling in seven participants. The muscle activity was assessed by means of crank cycle diagrams (polar plots) that displayed the muscle activity relative to the crank cycle. The muscle fatigue was assessed by means of the median frequency of the power spectrum of the EMG signal; the fractal dimension of the EMG signal; and the fractal dimension of the FMG pressure signal.

The smart compression garment returned performance parameters (muscle activity and fatigue) comparable to the surface EMG. The major differences were that the EMG measured the electrical activity, whereas the FMG pressure sensor measured the mechanical activity. As such, there was a phase shift between electrical and mechanical signals, with the electrical signals preceding the mechanical counterparts in most cases. This is specifically pronounced in high speed cycling.

The fatigue trend over the duration of the cycling exercises was clearly reflected in the fatigue parameters (fractal dimensions and median frequency) obtained from FMG and EMG signals. The fatigue parameter of the FMG signal (fractal dimension) showed a higher time dependency compared to the EMG signal. This reflects that the FMG pressure signal puts more emphasis on the fatigue as a function of time rather than on the origin of fatigue (e.g. peripheral or central fatigue).

Key observations were identified from the analysis of works within this chapter:

- Increasing influence of Muscular fatigue has a direct affect on the instability of a muscle's contractile behaviour. Measuring instability through a Fractal Dimension analysis allows for a new, near real-time analytical technique evaluating muscle fatigue behaviour through either electrical or mechanical behaviour.
- The fatigue parameter of the FMG signal (fractal dimension) showed a higher time dependency ($R2 = 0.84$) compared to the EMG signal. This reflects that the FMG signal puts more emphasis on the fatigue as a function of time rather than on the origin of fatigue (peripheral or central).
- Muscle conditioning and training plays a strong role in the behaviour of the leg muscles throughout the test. Power generating and stability muscles are clearly identified by their fatigue performance.
- Load-sharing between muscles can be further explored to show the balancing of load to alleviate/induce periods of fatigue beyond the continuing trend of the overall fatigue growth. This suggests muscles are capable of sustaining significantly higher fatigue levels for finite periods of time to allow supporting paired muscles time to recover without reducing overall power output from the muscle system as a whole.

III

Conclusions

8. Conclusions and Recommendations

The work of this thesis explored a key research gap surrounding monitoring muscular performance using surface pressure variations across the body. While significant existing works had been established looking at such performance using muscular electrical behaviours through surface Electromyography (EMG), alternate exploration of the mechanical changes to the body have been largely untouched in comparison.

This work undertook portions of this exploration, building upon work by others in the research field of Force Myography and muscular performance monitoring. The work utilised gold standard methods employed within research, namely Electromyography and video-based Motion Capture, to assist in understanding advantages and limitations of monitoring mechanical surface pressure. Importantly this is from an Engineering lens (over a more traditional biological one), exploring the human body as an unstable and dynamic mechanical system, one that requires the exploration of both significant robustness and flexibility for any performance monitoring solution.

The establishing body of work surrounding FMG monitoring is still in early stage development, yet has become increasingly popular as researchers and practitioners look to alternative monitoring techniques to overcome the limitations and challenges within the established gold standard methods. As a result of an exhaustive literature search a defined gap within the field was identified and the following research questions posited as a means to explore and build upon the body of literature.

Q1 How can deformation changes in the physical surface of a limb during activity be utilised for quantification of muscular activity levels?

Q2 With an understanding of the muscle loads associated with a set activity, how can we further determine the non-measurable loads (i.e. knee ligament loads, fatigue), that otherwise cannot, or have not been measured before within a real-time measurement capacity?

Q3 What insight can the analysis of temporal loading conditions on the muscle surface provide?

The research work contained explored these questions through a defined methodology of testing and evaluation, presenting a summary of the findings, limitations and conclusions of the work.

8.1 Conclusions

The thesis encompasses the research and development undertaken of a smart garment capable of monitoring muscle performance of the lower limbs. It explored the limitations of gold standard measurement techniques and introduced a novel monitoring technique as an additional tool in performance measurement. It addressed three general gaps in the knowledge base through the development of a wearable FMG measurement system, the application of FMG in muscular activity analysis, and the detailed Fatigue analysis of cyclists using an FMG system and a novel signal analysis approach.

Part One (Chapters 1-3) explored the need, gaps in knowledge and necessary research development of a muscular monitoring solution using Force Myography. This involved the design of a novel pressure sensors capable of unobtrusive pressure monitoring whilst underneath a compression garment. The design, calibration and deployment of the supporting system was paired with the understood gold standards of Surface Electromyography for electrical muscle activity, and video-based Motion Capture to determine relevant limb positioning. The completed 'Smart Apparel' system and calibration procedures are detailed for the exploration of key performance parameters, including muscular activity, loading, co-contraction, ligament force and muscle fatigue. This system bceame the foundational testing apparatus in exploring the three research questions.

Part Two (Chapters 4-7) explored the Research Implementation, namely the application of Smart Apparel to address the three research questions.

Chapter Four presented testing of muscular behaviour during knee extension and flexion activity, showing that muscular activity measured through FMG correlates to increases in the shank loading, the EMG measurement and the biomechanical loading model. This research demonstrated that Pressure-based FMG allows for the detection of separate muscular activation across 5 muscles, and determined that changes in limb loading conditions were correlated to muscle surface pressure. Limitations of the method however are raised in the need for baseline calibration procedures and sensor placement considerations throughout the limb range of motion to remove dynamic pressure changes introduced through muscle belly movement. This directly explored research question 1 and presents evidence that surface pressure activity is determinant of muscle activation and loading.

Chapter Five highlighted the exploration of the biomechanical link which the muscular activity of the upper leg has with the Cruciate Ligaments (CL) within the knee. The work approaches the connection of upper leg muscular activity and knee flexion angle to determine a novel analytical model to determining CL forces using the muscle activity outputs and knee flexion angle from the smart garment. This work directly addressed research question 2 and demonstrated that the real-time monitoring of ligament conditions within the encapsulated knee joint are possible through evaluation of muscle activation of the quadriceps and hamstrings, and the knee flexion angle.

Chapter Six explored the application of FMG monitoring on muscular activity performance during cycling. It demonstrated that pressure-based FMG is suitable for muscle activation and load monitoring of athlete cycling performance. The testing demonstrated the suitable use of FMG

alongside EMG to monitor the fatigue-induced changes in peak activation load and position of muscle during the crank cycle relative to a non-fatigued and fatigued condition. Furthermore, a key highlight of the work demonstrated the limitation in the gold standard method (EMG) to maintain reliability and accuracy with increasing high speed activity. The electromechanical delay present within this system is discussed and compared to the Pressure FMG technique demonstrating an advantage the mechanical technique has during high cadence cycling. This work directly addressed all three of the research questions.

Chapter Seven further explored the dynamics of fatigue throughout the duration of the cycling test activity performed in the previous chapter. A novel approach is introduced to calculating a fatigue index across the entirety of the tests using the analysis of the fractal dimension of both the electrical (EMG-FD) and mechanical (PRS-FD) signals. This technique is compared to the established gold-standard by which the median frequency of the EMG signal is monitored (EMG-MDF). The chapter presents findings that during a fixed-cyclic activity, increases in the presence of muscular fatigue is reflective in the increased signal instability, establishing a direct relationship between muscle fatigue and the fractal dimension of the signal. Furthermore, the technique also highlighted the unique partnership that paired muscles (particularly antagonistic pairs) employ to manage fatigue onset. Fractal analysis of the FMG pressure signal revealed the amplified fatigue-recovery load sharing behaviour muscles undergo to maximally extend the duration of an activity before the limitation of fatigue-induced failure occurs. This chapter directly addressed all three of the research questions.

In summary, the use of compression garments and pressure sensors based on Force Myography is a valid alternative to the established EMG-garments and provides an alternative method to capturing muscular activity as a means to represent loading and activation timing. Whilst the novel technique requires further work in on-body calibration, it proves to provide accurate results during high-speed activity (avoiding the electro-mechanical delay) in comparison to EMG. Furthermore, through the post-processing of pressure variations a clear observation and measurement of mechanical muscle fatigue is possible, with greater insights into muscular load-sharing during transitioning fatigue conditions and the subsequent involuntary muscle activation responses made to extend overall functional muscle output. As such, the work leads to the conclusion that utilising an instrumented compression garment with pressure sensors and Force Myography is a beneficial tool toward providing direct feedback to an athlete of their muscle and soft tissue behaviour, and ultimately provides an avenue to reduce the prevalence and likelihood of sports-related injuries.

8.2 Future work recommendations

The following recommendations for future work are made to address both limitations observed within the completed works and highlighted opportunities for further exploration:

- Custom garment design - Off-the-shelf compression garments were utilised and were limited in design of compression zones and siliconised areas. Development of a custom garment will aid in targeted sector compression, reducing the mechanical crosstalk from other muscles.
- Multiple position sensors - Positioning of additional sensors along the longitudinal line of the muscle belly movement to capture peak muscle pressure during full range of limb movement activities.
- Dynamic calibration - Utilisation of a digital dynamometer to capture force generation and angle to improve calibration of sensors to muscular force. Secondly this will aid in efficient capture of dynamic zero baseline pressures throughout full limb range of movement.
- Eccentric and concentric analysis - Leg extension and flexion only considered a single direction of movement during concentric muscle activation. Differing muscle performance was observed within the results of eccentric and concentric muscular behaviour but detailed exploration was not performed.
- Dual leg analysis - Further analysis of muscle fatigue monitoring on both legs during cycling fatigue tests. Current testing was restricted to only a participant's right leg, limiting the availability on insights into dominant leg usage and load-sharing across limbs. In addition, instrumentation of the crank arms with power meters would be beneficial.
- Hybrid system - Incorporate both the gold standard (EMG) and new (FMG) techniques to build upon limitations of each system using the strengths of the other.
- Portable system - Use of an integrated wiring and electronics solutions. Incorporating IMU-based positional trackers to determine limb angles over static motion-capture camera systems.

IV Appendices

A. Correlation of Muscle Fatigue Behaviour

A.1 Fractal Dimension: Method Selection

Works highlighted by Fuss (2013) show that the varied FD techniques within literature result in non-identical analytical outcomes. At times, the results produced can behave in contrary to one another, or in contrast to a confidently hypothesised outcome based upon literature. An example of this was shown within Tan, Fuss, Weizman & Azari (2015), where the stability of a participant was measured on a force plate whilst standing on a solid plate, or on a foam pad. The expected results (from literature and logical deduction) was to observe higher fractal behaviour whilst standing on foam due to increased instability in movement of the centre of pressure. However the results of the initial fractal analysis indicated this to be the more stable of the two measured conditions, an unexpected outcome of the work. This aligned with earlier work by Doyle *et al.* (2005) who determined a similar issue with the fractal technique in use, a method proposed by Higuchi (1988), was responsible for the difference in expected results to the hypothesised outcome of an eyes -open/-closed stability test. Adjustment of the FD technique utilised by both authors corrected the result to match that of literature and expected findings.

In the development of the presented work, determination of the correct FD techniques was also necessary. Fractal analysis of the observed signals through the Higuchi technique revealed an M-value tending towards infinity, or provided an M-value where the differential between the two extrema was negative (reversed). Whilst being unusable, this also leads to a counterintuitive response in the hypothesised fractal dimension response of fatigue; suggesting that at higher fatigue conditions, the behaviour of the muscle was less chaotic. As shown in Figure A.1 utilisation of the FD technique proposed by Fuss, provides a greater (positive) differential condition more appropriately useful to the FD analysis of the signal.

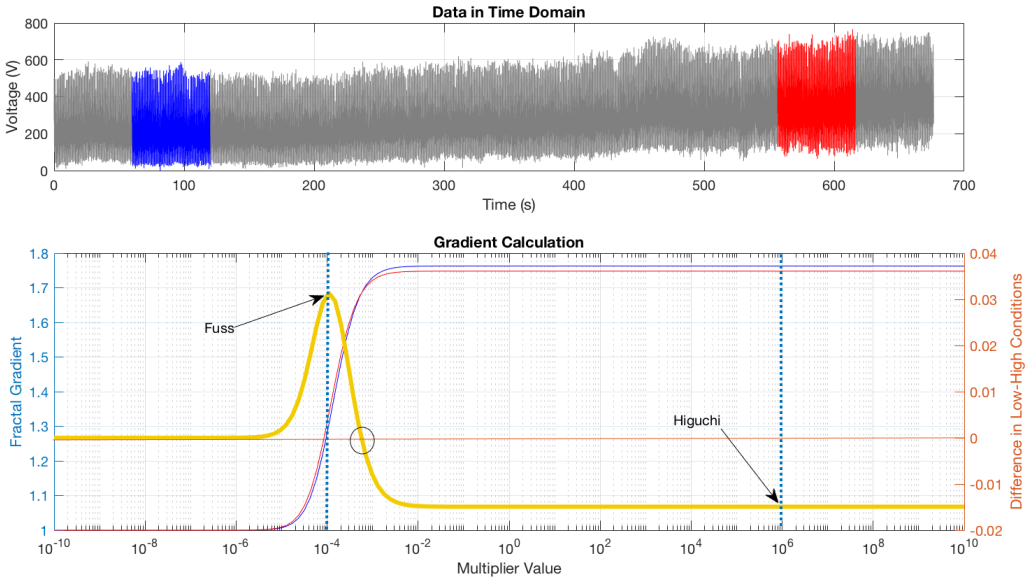

Figure A.1: Highlighted difference in Fractal method selection; Fuss's MAFDM and the Higuchi methods

A.2 Fractal Dimension: M-Value Selection

An optimal multiplier value is determined for each signal, however due to different muscle properties and loading conditions this multiplier is not always common between all muscles. To ensure suitable amplification of the fractal signal a common multiplier for all muscles must be calculated.

This was achieved by performing the following steps (shown in MATLAB pseudocode):

1. Calculation of the gradient for each signal and isolating only the positive component by taking the product of the gradient and the Heaviside function of the gradient and finally normalising each resultant signal to allow for summation with the other muscles.
   ```
   n = GRAD(:,2,i)-GRAD(:,1,i);
   B(:,i) = normalise(n .* Heaviside(n))
   ```
2. Determine the 'sign' of the number (neg or zero numbers = 0; pos =1)
   ```
   X = sign(B);
   ```
3. Calculate the product (later corrected to mode) across the array to determine the first signal that goes "negative" - this is the LIMIT point
   ```
   Y = mode(X,2);
   ```
4. Remove the summed values after the LIMIT point, this effectively stacks the graphs on top of each other by using sum(BB,2)
   ```
   Z = sum(B,2) .* Y;
   ```
5. Determine the max point (peak) in the summed signal; the index (x-axis) of which corresponds to the M-value of the multiplier
   ```
   [maxSum,indexSum] = max(Z);
   multiplier = M(indexSum);
   ```

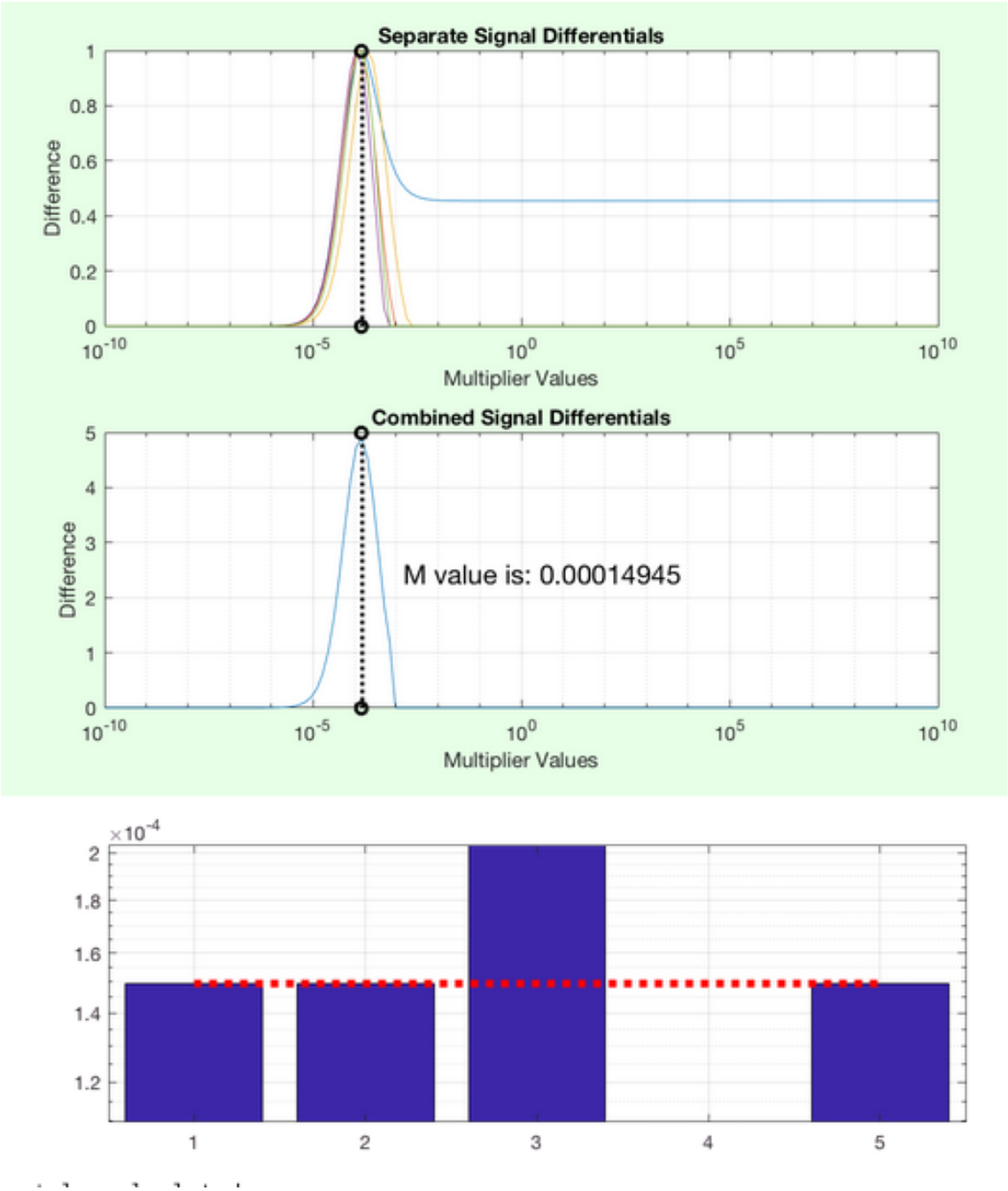

Figure A.2: Visual output of calculation process for the common multiplier

B. Ethics Approval Documentation

See next page for attached University Ethics Approval.

RMIT University

Science Engineering and Health

College Human Ethics Advisory Network (CHEAN)

Plenty Road
Bundoora VIC 3083

PO Box 71
Bundoora VIC 3083
Australia

Tel. +61 3 9925 7096
Fax +61 3 9925 6506
• www.rmit.edu.au

23rd September 2015

Franz Fuss
Building 251 Level, Room 60
School of Aerospace Mechanical &
Manufacturing Engineering
RMIT University

Dear Franz

ASEHAPP 45-15 FUSS-BELBASIS-SIDHU Evaluation of muscle fatigue and activity performance through smart compression apparel

Thank you for submitting your application for consideration by the Science, Engineering & Health College Human Ethics Advisory Network (CHEAN) of RMIT University.

Your application was considered at **meeting 07 – 15** on, **Wednesday 16th September 2015** and an extract of the minutes are attached for your information

4.1.2 ASEHAPP 45-15 FUSS-BELBASIS-SIDHU Evaluation of muscle fatigue and activity performance through smart compression apparel

The CHEAN noted the ethical issues as:

1. Interviews
2. Audio recording
3. Surveys (known respondents)
4. Confidentiality
5. Anonymity
6. Sub-maximal exercise testing

Pursuant to review the CHEAN noted:

1. Section 3 what type of sporting clubs are you approaching, as in the Participant Information Statement you refer to semi-elite cyclists as the target group but this is not mentioned in the application. Please provide copies of approval/agreement from sporting clubs to stating they are happy to distribute your advertisement to their members

2. Section 9. Please explain how the participants will be de-identified?

3. The Participant Information Statement is complex in description, the CHEAN suggest simplification for ease of understanding for participants. In particular, under 'If I agree to participate….' information on what participants are required to do requires simplification so that it can be easily understood by the lay person.

4. Participant Information Statement under 'What will happen to the information……' please remove statements: "Your participation in this study is anonymous. You will not be identified at any stage of the research, this is incorrect as you will have face to face contact with the participants and will know who they are. You should include that the data will be de-identified

and that no identifying data will be used in any publications etc. The description of data storage is not required in this section.

5. Participant Information Statement under 'Whom should I contact if I have any questions?' please include the names of researchers.

6. Participant Information Statement should include post-nominal for each of the researchers and their signatures.

7. Please clarify who the RMIT fist aider is and if they are a part of the research team and if their first aid certificate is current.

The CHEAN considers this to be a **Low Risk** proposal and that it is appropriate to be approved for a period of **6 Months from the date of final approval** subject to the above points being addressed to the satisfaction of one of the CHEAN members **Toh Yen Pang (99256128) tohyen.pang@rmit.edu.au Please liaise directly with the reviewer in the first instance**. To expedite the final review process the CHEAN recommend that you address each point raised by the CHEAN and place the point/s and the response/s into a table and highlight the changes / amendments throughout your document. This will enable the reviewer to quickly and easily check that all points have been satisfactorily addressed. Once the reviewer has approved the amendments they will direct you to submit one clean copy, to **Julie Barnett**, Secretary to the Science, Engineering & Health CHEAN **(202.04.72 X57096)** for a formal letter of approval.

A formal letter of approval will not be forwarded until the final amended clean copy has been received. Research may not begin until approval has been given.

Please note that if the CHEAN does not receive a response to this letter within six weeks from the date of the letter, it will be assumed that you are no longer seeking approval for your project and your application will be withdrawn.

For your information your application number is **ASEHAPP 45 – 15** please refer to this number in any future correspondence to the CHEAN.

Yours sincerely

Dr Linda Jones
Chair, Science Engineering & Health
College Human Ethics Advisory Network

Cc CHEAN Member: Toh Yen Pang School of Aerospace Mechanical & Manufacturing Engineering RMIT University
Student Investigator/s: Aaron Belbasis [redacted] School of Aerospace Mechanical & Manufacturing Engineering RMIT University
Jesper Sidhu [redacted] School of Aerospace Mechanical & Manufacturing Engineering RMIT University

Bibliography

1. Alentorn-Geli, E. *et al.* Prevention of non-contact anterior cruciate ligament injuries in soccer players. Part 1: Mechanisms of injury and underlying risk factors. *Knee Surgery, Sports Traumatology, Arthroscopy* **17,** 705–729. ISSN: 09422056. http://www.ncbi.nlm.nih.gov/pubmed/19452139 (July 2009).

2. Alentorn-Geli, E. *et al.* Prevention of non-contact anterior cruciate ligament injuries in soccer players. Part 2: A review of prevention programs aimed to modify risk factors and to reduce injury rates. *Knee Surgery, Sports Traumatology, Arthroscopy* **17,** 859–879. ISSN: 09422056. http://www.ncbi.nlm.nih.gov/pubmed/19506834 (Aug. 2009).

3. Asplund, C. & St Pierre, P. Knee pain and bicycling: fitting concepts for clinicians. *The Physician and sportsmedicine* **32,** 23–30. ISSN: 0091-3847 (2004).

4. Basmajian, J. & De Luca, C. J. *Muscles Alive 6* 168–186. ISBN: 068300414X. http://rheumatology.oxfordjournals.org/content/7/4/local/back-matter.pdf (1985).

5. Belbasis, A. & Fuss, F. K. Development of Next-generation Compression Apparel. *Procedia Technology* **20,** 85–90. ISSN: 22120173. http://linkinghub.elsevier.com/retrieve/pii/S2212017315001929 (2015).

6. Belbasis, A. & Fuss, F. K. Muscle performance investigated with a novel smart compression garment based on pressure sensor force myography and its validation against emg. *Frontiers in Physiology* **9** (2018).

7. Belbasis, A., Fuss, F. K. & Sidhu, J. Estimation of cruciate ligament forces via smart compression garments. *Procedia Engineering* **112,** 169–174. ISSN: 18777058 (2015).

8. Belbasis, A., Fuss, F. K. & Sidhu, J. Muscle activity analysis with a smart compression garment. *Procedia Engineering* **112,** 163–168. ISSN: 18777058 (2015).

9. Beretta-Piccoli, M. *et al.* Evaluation of central and peripheral fatigue in the quadriceps using fractal dimension and conduction velocity in young females. *PLoS ONE* **10.** ISSN: 19326203 (2015).

10. Beynnon, B., Howe, J. G., Pope, M. H., Johnson, R. J. & Fleming, B. C. The measurement of anterior cruciate ligament strain in vivo. *International Orthopaedics (SICOT)* **16.** https://journals.scholarsportal.info/pdf/03412695/v16i0001/1%7B%5C_%7Dtmoaclsiv.xml (1992).

11. Boccia, G. *et al.* Muscle fiber conduction velocity and fractal dimension of EMG during fatiguing contraction of young and elderly active men. *Physiological Measurement* **37,** 162–174. ISSN: 13616579 (2016).

12. Castellini, C. *et al. Proceedings of the first workshop on peripheral machine interfaces: Going beyond traditional surface electromyography* 2014.

13. Cavanagh, P. R. & Komi, P. V. Electromechanical delay in human skeletal muscle under concentric and eccentric contractions. *European Journal of Applied Physiology and Occupational Physiology* **42,** 159–163. ISSN: 03015548 (1979).

14. Cheng, J., Amft, O. & Lukowicz, P. *Active capacitive sensing: Exploring a new wearable sensing modality for activity recognition* in *Lecture Notes in Computer Science (including subseries Lecture Notes in Artificial Intelligence and Lecture Notes in Bioinformatics)* **6030 LNCS** (2010), 319–336. ISBN: 3642126537.

15. Chua, J. *A novel approach to identify and quantify activity and performance in wheelchair rugby* PhD Thesis (RMIT University, 2013).

16. Cifrek, M., Medved, V., Tonković, S. & Ostojić, S. *Surface EMG based muscle fatigue evaluation in biomechanics* 2009.

17. Colby, S. *et al.* The American Journal of Sports Medicine Electromyographic and Kinematic Analysis of Cutting Maneuvers Implications for Anterior Cruciate Ligament Injury. *The American Journal of Sports Medicine* **28,** 234–240. ISSN: 14402440. arXiv: 21. http://www.ncbi.nlm.nih.gov/pubmed/10751001 (2000).

18. Connan, M., Ramírez, E. R., Vodermayer, B. & Castellini, C. Assessment of a wearable forceand electromyography device and comparison of the related signals for myocontrol. *Frontiers in Neurorobotics* **10.** ISSN: 16625218 (2016).

19. Contini, R., Drillis, R. J. & Bluestein, M. Determination of Body Segment Parameters. *Human Factors: The Journal of Human Factors and Ergonomics Society* **5,** 493–504. ISSN: 15478181 (1963).

20. Crozara, L. F. *et al.* Utility of electromyographic fatigue threshold during treadmill running. *Muscle and Nerve* **52,** 1030–1039. ISSN: 10974598 (2015).

21. De Luca, C. J. Myoelectrical manifestations of localized muscular fatigue in humans. *Critical reviews in biomedical engineering* **11,** 251–279. ISSN: 0278-940X. arXiv: arXiv:1011.1669v3 (1984).

22. De Luca, C. J. The use of surface electromyography in biomechanics. *Journal of Applied Biomechanics* **13,** 135–163. ISSN: 10658483. arXiv: arXiv:1011.1669v3 (1997).

23. DeMorat, G., Weinhold, P., Blackbur, T., Chudik, S. & Garrett, W. Aggressive Quadriceps Loading Can Induce Noncontact Anterior Cruciate Ligament Injury. *The American Journal of Sports Medicine* **32,** 477–483. ISSN: 0363-5465. http://journal.ajsm.org/cgi/doi/10.1177/0363546503258928%7B%5C%%7D5Cnpapers3://publication/doi/10.1177/0363546503258928 (Mar. 2004).

24. Dingwell, J. B., Joubert, J. E., Diefenthaeler, F. & Trinity, J. D. Changes in muscle activity and kinematics of highly trained cyclists during fatigue. *IEEE Transactions on Biomedical Engineering* **55,** 2666–2674. ISSN: 00189294 (2008).

25. Dordevic, S., Tomazic, S., Narici, M., Pisot, R. & Meglic, A. In-vivo measurement of muscle tension: Dynamic properties of the MC sensor during isometric muscle contraction. *Sensors (Switzerland)* **14,** 17848–17863. ISSN: 14248220 (2014).

26. Dorel, S., Drouet, J. M., Couturier, A., Champoux, Y. & Hug, F. Changes of pedaling technique and muscle coordination during an exhaustive exercise. *Medicine and Science in Sports and Exercise* **41,** 1277–1286. ISSN: 15300315 (2009).

27. Dowling, A. V., Favre, J. & Andriacchi, T. P. A Wearable System to Assess Risk for Anterior Cruciate Ligament Injury During Jump Landing: Measurements of Temporal Events, Jump Height, and Sagittal Plane Kinematics. *Journal of Biomechanical Engineering* **133,** 071008. ISSN: 01480731 (2011).

28. Dowling, A. V., Favre, J. & Andriacchi, T. P. Inertial sensor-based feedback can reduce key risk metrics for anterior cruciate ligament injury during jump landings. *American Journal of Sports Medicine* **40,** 1075–1083. ISSN: 03635465 (2012).

29. Doyle, T. L., Newton, R. U. & Burnett, A. F. Reliability of traditional and fractal dimension measures of quiet stance center of pressure in young, healthy people. *Archives of Physical Medicine and Rehabilitation* **86,** 2034–2040. ISSN: 00039993 (2005).

30. Drillis, R., Contini, R. & Bluestein, M. *Body segment parameters* 1964. http://oandplibrary.com/al/pdf%7B%5C_%7Draw/1964%7B%5C_%7D01%7B%5C_%7Draw.pdf%7B%5C#%7Dpage=48.

31. Düking, P., Hotho, A., Holmberg, H. C., Fuss, F. K. & Sperlich, B. *Comparison of non-invasive individual monitoring of the training and health of athletes with commercially available wearable technologies* 2016.

32. Early, J. W. *Business Opportunity Analysis of Wearable and Wireless Electromyography Sensors in Athletics* 2016.

33. Esposito, D. *et al.* A piezoresistive sensor to measure muscle contraction and mechanomyography. *Sensors (Switzerland)* **18,** 1–12. ISSN: 14248220 (2018).

34. EU DG Connect. Smart Wearables : Reflection and Orientation Paper, 31 (2016).

35. Fang, Y., Hettiarachchi, N., Zhou, D. & Liu, H. Multi-modal sensing techniques for interfacing hand prostheses: A review. *IEEE Sensors Journal* **15,** 6065–6076. ISSN: 1530437X (2015).

36. Finni, T., Hu, M., Kettunen, P., Vilavuo, T. & Cheng, S. Measurement of EMG activity with textile electrodes embedded into clothing. *Physiological Measurement* **28,** 1405–1419. ISSN: 09673334 (2007).

37. Fleming, B. C. *et al.* The strain behavior of the anterior cruciate ligament during bicycling: an in vivo study. *Arthroscopy : the journal of arthroscopic & related surgery : official publication of the Arthroscopy Association of North America and the International Arthroscopy Association* **15,** 185–91. ISSN: 0749-8063. http://www.ncbi.nlm.nih.gov/pubmed/10210077 (1999).

38. Fregly, B. J. *et al.* Grand challenge competition to predict in vivo knee loads. *Journal of Orthopaedic Research* **30,** 503–513. ISSN: 07360266. arXiv: NIHMS150003 (2012).

39. Fu, W., Liu, Y. & Fang, Y. Research advancements in humanoid compression garments in sports. *International Journal of Advanced Robotic Systems* **10.** ISSN: 17298806 (2013).

40. Fuss, F. K. Anatomy of the cruciate ligaments and their function in extension and flexion of the human knee joint. *American Journal of Anatomy* **184,** 165–176. ISSN: 15530795. file:///Users/TyBrown/Documents/Papers2/Articles/1989/Fuss/Am%20J%20Anat%201989%20Fuss.pdf%7B%5C%%7D5Cnpapers2://publication/doi/10.1002/aja.1001840208 (1989).

41. Fuss, F. K. Biomechanics of the child's knee joint. *Acta Chirurgica Austriaca* **28,** 7–10 (1996).

42. Fuss, F. K. A robust algorithm for optimisation and customisation of fractal dimensions of time series modified by nonlinearly scaling their time derivatives: Mathematical theory and practical applications. *Computational and Mathematical Methods in Medicine* **2013.** ISSN: 1748670X (2013).

43. Fuss, F. K. A Method for Quantifying the Emotional Intensity and Duration of a Startle Reaction with Customized Fractal Dimensions of EEG Signals. *Applied Mathematics* **7,** 355 (2016).

44. Fuss, F. K. *Smart equipment and wearable technology: pushing the boundaries of lateral innovation. Keynote* in *8th APCST. Asia-Pacific Conference on Sports Technology, Tel Aviv* (2017).

45. Fuss, F. K. & Belbasis, A. Soft tissue management method and system. *WIPO PCT Patent (filed)* **WO2016065404A1** (May 2016).

46. Fuss, F. K., Belbasis, A., Sidhu, J. & Mueller, F. *Fractal dimension analysis of muscle fatigue with muscle surface pressure measured via compression garments* in *Proceedings of ICSST 2016, 2nd International Conference in Sports Science and Technology* (Nanyang Technological University, Singapore, 2016).

47. Fuss, F. K., Belbasis, A., van den Hazel, B. & Ketabi, A. Design Strategy For Selecting Appropriate Energy Absorbing Materials and Structures: Data Library and Customised Selection Criteria. *Procedia Technology* **20,** 98–103. ISSN: 22120173. http://linkinghub.elsevier.com/retrieve/pii/S2212017315001942 (2015).

48. González-Izal, M., Malanda, A., Gorostiaga, E. & Izquierdo, M. *Electromyographic models to assess muscle fatigue* 2012.

49. Hermens, H. J., Frericks, B., Disselhorst-Klug, C. & Rau, G. Recommendations for sensor locations on individual muscles. *Journal of Electromyography and Kinesiology* **10,** 361–374 (2000).

50. Higuchi, T. Approach to an irregular time series on the basis of the fractal theory. *Physica D: Nonlinear Phenomena* **31,** 277–283. ISSN: 01672789. arXiv: 0002046 [nlin.CD] (1988).

51. Hill, J. A., Howatson, G., van Someren, K. A., Davidson, S. & Pedlar, C. R. The variation in pressures exerted by commercially available compression garments. *Sports Engineering* **18,** 115–121. ISSN: 14602687 (2015).

52. Holmes, J. C., Pruitt, A. L. & Whalen, N. J. Lower extremity overuse in bicycling. *Clinics In Sports Medicine* **13,** 187–205. ISSN: 0278-5919. http://search.ebscohost.com/login.aspx?direct=true%7B%5C&%7Ddb=cmedm%7B%5C&%7DAN=8111852%7B%5C&%7Dsite=ehost-live (1994).

53. Hug, F., Turpin, N. A., Guevel, A. & Dorel, S. Is interindividual variability of EMG patterns in trained cyclists related to different muscle synergies? *Journal of Applied Physiology* **108,** 1727–1736. ISSN: 8750-7587. http://jap.physiology.org/cgi/doi/10.1152/japplphysiol.01305.2009 (2010).

54. Hug, F. Can muscle coordination be precisely studied by surface electromyography? *Journal of Electromyography and Kinesiology* **21,** 1–12. ISSN: 10506411 (2011).

55. Interlink Electronics. *FSR 400 Series Data Sheet* tech. rep. (2016). http://www.interlinkelectronics.com/datasheets/Datasheet%7B%5C_%7DFSR.pdf.

56. Islam, M. A., Sundaraj, K., Ahmad, R. B., Ahamed, N. U. & Ali, M. A. Mechanomyography sensor development, related signal processing, and applications: A systematic review. *IEEE Sensors Journal* **13,** 2499–2516. ISSN: 1530437X (2013).

57. James, D. A. & Petrone, N. *Sensors and wearable technologies in sport : technologies, trends and approaches for implementation* 49. ISBN: 9789811009914 (2016).

58. Jorge, M. & Hull, M. L. Analysis of EMG measurements during bicycle pedalling. *Journal of Biomechanics* **19,** 683–694. ISSN: 00219290 (1986).

59. Jung, P. G., Lim, G., Kim, S. & Kong, K. A Wearable Gesture Recognition Device for Detecting Muscular Activities Based on Air-Pressure Sensors. *IEEE Transactions on Industrial Informatics* **11,** 485–494. ISSN: 15513203 (2015).

60. Kim, P. T. *et al.* Mountain biking injuries requiring trauma center admission: A 10-year regional trauma system experience. *Journal of Trauma - Injury, Infection and Critical Care* **60,** 312–318. ISSN: 00225282 (2006).

61. Kinney, A. L., Besier, T. F., D'Lima, D. D. & Fregly, B. J. Update on Grand Challenge Competition to Predictn in vivo Knee Loads. *Journal of Biomechanical Engineering* **135,** 021012. ISSN: 0148-0731. arXiv: NIHMS150003. http://biomechanical.asmedigitalcollection.asme.org/article.aspx?doi=10.1115/1.4023255 (2013).

62. LeRouge, C. & Wickramasinghe, N. A review of user-centered design for diabetes-related consumer health informatics technologies. *Journal of Diabetes Science and Technology* **7,** 1039–1056. ISSN: 19322968 (2013).

63. Li, L. & Baum, B. S. Electromechanical delay estimated by using electromyography during cycling at different pedaling frequencies. *Journal of Electromyography and Kinesiology* **14,** 647–652. ISSN: 10506411 (2004).

64. Li, N., Yang, D., Jiang, L., Liu, H. & Cai, H. Combined Use of FSR Sensor Array and SVM Classifier for Finger Motion Recognition Based on Pressure Distribution Map. *Journal of Bionic Engineering* **9,** 39–47. ISSN: 16726529 (2012).

65. Lin, C. F. *et al.* Biomechanical risk factors of non-contact ACL injuries: A stochastic biomechanical modeling study. *Journal of Sport and Health Science* **1,** 36–42. ISSN: 20952546. http://dx.doi.org/10.1016/j.jshs.2012.01.001 (2012).

66. Liu, J. Z., Brown, R. W. & Yue, G. H. A dynamical model of muscle activation, fatigue, and recovery. *Biophysical Journal* **82,** 2344–2359. ISSN: 00063495 (2002).

67. Lorussi, F., Galatolo, S., Bartalesi, R. & De Rossi, D. Modeling and characterization of extensible wearable textile-based electrogoniometers. *IEEE Sensors Journal* **13,** 217–228. ISSN: 1530437X. http://ieeexplore.ieee.org/lpdocs/epic03/wrapper.htm?arnumber=6257412 (Jan. 2013).

68. Lorussi, F., Galatolo, S. & De Rossi, D. E. Textile-based electrogoniometers for wearable posture and gesture capture systems. *IEEE Sensors Journal* **9,** 1014–1024. ISSN: 1530437X (2009).

69. Luca, G. D. Fundamental Concepts in EMG Signal Acquisition Table of Contents. *Delsys,* 1–31 (2003).

70. Lucia, A., Sánchez, O., Carvajal, A. & Chicharro, J. L. Analysis of the aerobic-anaerobic transition in elite cyclists during incremental exercise with the use of electromyography. *British Journal of Sports Medicine* **33,** 178–185. ISSN: 03063674 (1999).

71. Lukowicz, P., Hanser, F., Szubski, C. & Sehobersberger, W. *Detecting and interpreting muscle activity with wearable force sensors* in *Lecture Notes in Computer Science (including subseries Lecture Notes in Artificial Intelligence and Lecture Notes in Bioinformatics)* **3968 LNCS** (2006), 101–116. ISBN: 3540338942.

72. Lynn, S. K., Watkins, C. M., Wong, M. A., Balfany, K. & Feeney, D. F. Validity and reliability of surface electromyography measurements from a wearable athlete performance system. *Journal of Sports Science and Medicine* **17,** 205–215. ISSN: 13032968 (2018).

73. Manero, R. B. *et al. Wearable embroidered muscle activity sensing device for the human upper leg* in *Proceedings of the Annual International Conference of the IEEE Engineering in Medicine and Biology Society, EMBS* **2016-Octob** (2016), 6062–6065. ISBN: 9781457702204. arXiv: 1602.04841.

74. Marri, K. & Swaminathan, R. *Classification of muscular nonfatigue and fatigue conditions using surface EMG signals and fractal algorithms* in *ASME 2016 Dynamic Systems and Control Conference, DSCC 2016* **1** (2016). ISBN: 9780791850695.

75. McLaren, J., Helmer, R. J., Horne, S. L. & Blanchonette, I. Preliminary development of a wearable device for dynamic pressure measurement in garments. *Procedia Engineering* **2,** 3041–3046. ISSN: 18777058. http://linkinghub.elsevier.com/retrieve/pii/S1877705810003620%20http://www.sciencedirect.com/science/article/pii/S1877705810003620 (June 2010).

76. McLean, S. G., Mallett, K. F. & Arruda, E. M. Deconstructing the Anterior Cruciate Ligament: What We Know and Do Not Know About Function, Material Properties, and Injury Mechanics. *Journal of Biomechanical Engineering* **137,** 020906. ISSN: 0148-0731. http://biomechanical.asmedigitalcollection.asme.org/article.aspx?doi=10.1115/1.4029278 (2015).

77. Merletti, R., Afsharipour, B., Dideriksen, J. & Farina, D. in *Surface Electromyography: Physiology, Engineering and Applications* 273–310 (2016). ISBN: 9781119082934.

78. Merletti, R., Knaflitz, M. & De Luca, C. J. Myoelectric manifestations of fatigue in voluntary and electrically elicited contractions. *Journal of applied physiology,* 1810–1820. ISSN: 01617567. http://jap.physiology.org/content/69/5/1810.short (1990).

79. Mesin, L., Cescon, C., Gazzoni, M., Merletti, R. & Rainoldi, A. A bi-dimensional index for the selective assessment of myoelectric manifestations of peripheral and central muscle fatigue. *Journal of Electromyography and Kinesiology* **19,** 851–863. ISSN: 10506411 (2009).

80. Meyer, J., Lukowicz, P. & Tröster, G. *Textile pressure sensor for muscle activity and motion detection* in *Proceedings - International Symposium on Wearable Computers, ISWC* (2007), 69–74. ISBN: 1424405971.

81. Moustafa, H., Kenn, H., Sayrafian, K., Scanlon, W. & Zhang, Y. Mobile wearable communications [Guest Editorial]. *IEEE Wireless Communications* **22,** 10–11. ISSN: 15361284 (2015).

82. Myer, G. D., Ford, K. R. & Hewett, T. E. The effects of gender on quadriceps muscle activation strategies during a maneuver that mimics a high ACL injury risk position. *Journal of Electromyography and Kinesiology* **15,** 181–189. ISSN: 10506411. http://www.ncbi.nlm.nih.gov/pubmed/15664147 (Apr. 2005).

83. Ogris, G., Kreil, M. & Lukowicz, P. *Using FSR based muscule activity monitoring to recognize manipulative arm gestures* in *Proceedings - International Symposium on Wearable Computers, ISWC* (2007), 45–48. ISBN: 9781424414536.

84. Raasch, C. C., Zajac, F. E., Ma, B. & Levine, W. S. Muscle coordination of maximum-speed pedaling. *Journal of Biomechanics* **30,** 595–602. ISSN: 00219290 (1997).

85. Salim, F., Belbasis, A., Prohasky, D., Houshyar, S. & Fuss, F. K. *Design and evaluation of smart wearable undergarment for monitoring physiological extremes in firefighting* in *Proceedings of the 2014 ACM International Symposium on Wearable Computers Adjunct Program - ISWC '14 Adjunct* (2014), 249–254. ISBN: 9781450330480.

86. Sanderson, D. J. & Black, A. The effect of prolonged cycling on pedal forces. *Journal of Sports Sciences* **21,** 191–199. ISSN: 02640414 (2003).

87. SENIAM. *Recommendations for Sensor Locations on Individual Muscles* 1999. `http://seniam.org/sensor%7B%5C_%7Dlocation.htm` (2017).

88. Shafti, A., Ribas Manero, R. B., Borg, A. M., Althoefer, K. & Howard, M. J. Embroidered Electromyography: A Systematic Design Guide. *IEEE Transactions on Neural Systems and Rehabilitation Engineering* **25,** 1472–1480. ISSN: 15344320 (2017).

89. Sports Medicine Australia, (Program), A. S. & Coaching Council, A. *Safety guidelines for children in sport and recreation.* tech. rep. (Sports Medicine Australia, 1997).

90. Taelman, J., Adriaensen, T., Van Der Horst, C., Linz, T. & Spaepen, A. *Textile integrated contactless EMG sensing for stress analysis* in *Annual International Conference of the IEEE Engineering in Medicine and Biology - Proceedings* (2007), 3966–3969. ISBN: 1424407885.

91. Tan, A. M., Fuss, F. K., Weizman, Y. & Azari, M. F. *Centre of pressure detection and analysis with a high-resolution and low-cost smart insole* in *Procedia Engineering* **112** (2015), 146–151.

92. Tan, A. M., Fuss, F. K., Weizman, Y., Woudstra, Y. & Troynikov, O. Design of Low Cost Smart Insole for Real Time Measurement of Plantar Pressure. *Procedia Technology* **20,** 117–122. ISSN: 22120173. `http://linkinghub.elsevier.com/retrieve/pii/S2212017315001978` (2015).

93. Taylor, K. A. *et al.* Measurement of in vivo anterior cruciate ligament strain during dynamic jump landing. *Journal of Biomechanics* **44,** 365–371. ISSN: 00219290. `http://dx.doi.org/10.1016/j.jbiomech.2010.10.028` (2011).

94. Thelen, D. G., Anderson, F. C. & Delp, S. L. Generating dynamic simulations of movement using computed muscle control. *Journal of Biomechanics* **36,** 321–328. ISSN: 00219290. arXiv: `S0021-9290(02)00432-3 [10.1016]` (2003).

95. Thompson, W. R. Worldwide Survey of Fitness Trends for 2016. *ACSM's Health & Fitness Trends* **19,** 9–18 (2015).

96. Thompson, W. R. Worldwide Survey of Fitness Trends for 2017. *ACSM's Health & Fitness Trends* **20,** 8–17. http://journals.lww.com/acsm-healthfitness/Fulltext/2016/11000/WORLDWIDE%7B%5C_%7DSURVEY%7B%5C_%7DOF%7B%5C_%7DFITNESS%7B%5C_%7DTRENDS%7B%5C_%7DFOR%7B%5C_%7D2017.6.aspx (2016).

97. Thompson, W. R. Worldwide Survey of Fitness Trends for 2018. *ACSM's Health & Fitness Trends* **21,** 10–19. http://journals.lww.com/acsm-healthfitness/Fulltext/2016/11000/WORLDWIDE%7B%5C_%7DSURVEY%7B%5C_%7DOF%7B%5C_%7DFITNESS%7B%5C_%7DTRENDS%7B%5C_%7DFOR%7B%5C_%7D2017.6.aspx (2017).

98. Thompson, W. R. Worldwide Survey of Fitness Trends for 2019. *ACSM's Health & Fitness Trends* **22,** 10–17. http://journals.lww.com/acsm-healthfitness/Fulltext/2016/11000/WORLDWIDE%7B%5C_%7DSURVEY%7B%5C_%7DOF%7B%5C_%7DFITNESS%7B%5C_%7DTRENDS%7B%5C_%7DFOR%7B%5C_%7D2017.6.aspx (2018).

99. Troiano, A. *et al.* Assessment of force and fatigue in isometric contractions of the upper trapezius muscle by surface EMG signal and perceived exertion scale. *Gait and Posture* **28,** 179–186. ISSN: 09666362 (2008).

100. Troynikov, O. *et al. Factors influencing the effectiveness of compression garments used in sports* in *Procedia Engineering* **2** (2010), 2823–2829. ISBN: 18777058.

101. Wilber, C. A., Holland, G. J., Madison, R. E. & Loy, S. F. An epidemiological analysis of overuse injuries among recreational cyclists. *International Journal of Sports Medicine* **16,** 201–206. ISSN: 01724622 (1995).

102. Wininger, M. Pressure signature of forearm as predictor of grip force. *The Journal of Rehabilitation Research and Development* **45,** 883–892. ISSN: 07487711. http://www.rehab.research.va.gov/jour/08/45/6/pdf/winninger.pdf (2008).

103. Withrow, T. J., Huston, L. J., Wojtys, E. M. & Ashton-Miller, J. A. Effect of varying hamstring tension on anterior cruciate ligament strain during in vitro impulsive knee flexion and compression loading. *The Journal of Bone and Joint Surgery* **90,** 815–823. ISSN: 1535-1386. http://eutils.ncbi.nlm.nih.gov/entrez/eutils/elink.fcgi?dbfrom=pubmed%7B%5C&%7Did=18381320%7B%5C&%7Dretmode=ref%7B%5C&%7Dcmd=prlinks%7B%5C%%7D5Cnpapers3://publication/doi/10.2106/JBJS.F.01352 (Apr. 2008).

104. Xsens Technologies. *Gait Analysis - Xsens Motion Tracking* 2019. https://www.xsens.com/tags/gait-analysis/ (2019).

105. Yungher, D. A., Wininger, M. T., Barr, J. B., Craelius, W. & Threlkeld, A. J. Surface muscle pressure as a measure of active and passive behavior of muscles during gait. *Medical Engineering and Physics* **33,** 464–471. ISSN: 13504533. http://dx.doi.org/10.1016/j.medengphy.2010.11.012 (2011).

106. Zajac, F. E. Understanding muscle coordination of the human leg with dynamical simulations. *Journal of Biomechanics* **35,** 1011–1018. ISSN: 00219290. arXiv: 168 (2002).

107. Zhang, Y., Liu, G. & Xie, S. Q. Biomechanical simulation of anterior cruciate ligament strain for sports injury prevention. *Computers in Biology and Medicine* **41,** 159–163. ISSN: 00104825. http://dx.doi.org/10.1016/j.compbiomed.2011.01.006 (2011).

108. Zhou, B., Sundholm, M., Cheng, J., Cruz, H. & Lukowicz, P. Measuring muscle activities during gym exercises with textile pressure mapping sensors. *Pervasive and Mobile Computing*. ISSN: 15741192 (2017).